FREE ZONE ELECTROPHORESIS

BY

STELLAN HJERTÉN

UPPSALA 1967
ALMQVIST & WIKSELLS BOKTRYCKERI AB

FREE ZONE ELECTROPHORESIS

INAUGURAL DISSERTATION

By

STELLAN HJERTÉN
Fil. lic., Vg

By due permission of the Faculty of Science
of the University of Uppsala,
to be publicly discussed in the lecture hall of
the Institute of Chemistry
on May 19, 1967, at 10 a.m.,
for the degree of Doctor of Philosophy

UPPSALA 1967
ALMQVIST & WIKSELLS BOKTRYCKERI AB

FREE ZONE ELECTROPHORESIS

BY

STELLAN HJERTÉN

UPPSALA 1967
ALMQVIST & WIKSELLS BOKTRYCKERI AB

UNIVERSITEITSBIBLIOTHEEK - LEIDEN

To my Parents

CONTENTS

Preface 7

I. *Introduction* 9

II. *The method* 13

II:1. Theory of Zone Stabilization by Rotation of the Electrophoresis Tube 13

A. Qualitative Considerations 13

B. Quantitative Considerations 14

B:1. The Equations of Motion for an Applied Liquid Element in a Fixed Coordinate System 14

a. Derivation of the Differential Equations 14

b. Determination of C in Eqn. (4) 15

c. Determination of λ_1 and λ_2 in Eqn. (4) 15

d. Interpretation of the Equations of Motion 17

e. Minimizing γ_1 18

f. Minimizing $\sqrt{k^2+l^2}$ and Calculation of a Working Value of ω 21

g. The Decrease of γ_1 and $\sqrt{k^2+l^2}$ during a Run 23

B:2. The Equations of Motion for an Applied Liquid Element in a Rotating Coordinate System 24

a. Derivation of the Equations 24

b. Interpretation of the Equations of Motion (32) and (33) . . . 25

c. The Distance L from the Liquid Element to the Axis of the Electrophoresis Tube as a Function of Time 26

C. Experimental Demonstrations of Zone Stability in the Revolving Electrophoresis Tube 29

II:2. Design and Function of the Equipment 31

A. Over-All Description 31

B. The Separate Units 35

B:1. The Carriage Bearing the Electrophoresis Tube and the Electrode Vessels 35

a. General Description 35

b. Leakage-Free Sealing of the Electrophoresis Tube 35

c. The Coupling between the Belt Pulley and the Electrophoresis Tube 37

B:2. The Quartz Electrophoresis Tube 38

B:3. The Carriage-Positioning Arm 38

B:4. The Cooling Reservoir and the Immersion Bath 38

B:5. The Scanning Device 39

a. The Need for a Scanning Device 39

b. The Earliest Version of the Scanning Device 40

b:1. The Principle 40

b:2. The Disadvantages 40

c. The New Version of the Scanning Device 40
c:1. The Principle and Its Advantages 40
c:2. The Optics 41
1. General Description 41. 2. The Light Filter Units 42. 3. Filter Combination for Samples with Absorption Maxima Near 280 mμ 43. 4. Filter Combination for Samples with Absorption Maxima Near 260 mμ 44. 5. The Width of the Aperture 44. 6. The Height of the Aperture 44.
c:3. The Photo Multiplier 44
c:4. The Ratio Recording System 45
1. The Principle 45. 2. The Advantages 46.
c:5. The Pulse Comparator 46
c:6. The Recorder 46
B:6. High Voltage Source with Stabilizer for the Electrode Current 47
B:7. Current Stabilizer for the Hydrogen Lamp 47
B:8. Automation Devices 47
a. Programing Unit for Scanning 47
b. Zone-Position Indicator Unit 48

II:3. Experimental Procedure 51
A. Coating the Electrophoresis Tube with Methyl Cellulose to Eliminate Electroendosmosis 51
A:1. The Coating Solution 51
A:2. The Coating Procedure 51
B. Preparation of the Gel Plug (GP in Fig. 8) 51
C. Application of the Sample 52
C:1. General 52
C:2. Application by Injection 54
C:3. Application by Layering 54
D. Condensed Instructions for the Performance of a Run 55

II:4. Electroendosmosis 55
A. General 55
B. Deformation of a Zone by Electroendosmosis 56
C. Hydrodynamic Compensation of the Electroendosmotic Reflow 58
D. Reduction of Electroendosmosis by Reducing the ζ-potential . . 60
E. Reduction of Electroendosmosis by Increasing the Resistance to Flow in the Diffuse Double Layer 61

II:5. The Electrophoretic Migration Velocity Profile 64
A. The Migration Velocity as a Function of the Distance from the Axis of the Electrophoresis Tube 64
B. The Effect of Coolant Temperature on the Migration Velocity at Constant Current 69

II:6. Analytical Runs 73
A. Quantitative Analysis 73
A:1. Changes in the Intensity and Direction of the Scanning Beam Caused by the Electrophoresis Tube 73
A:2. The Relationship between Transmission and Sample Concentration (Calibration Curve) 75

a. The Theoretical Curve 75
b. The Empirical Curve 77
A:3. The Accuracy of Quantitative Determinations 79
A:4. Approximation of Eqn. (85) 81
B. Mobility Determinations 82
B:1. The Moving Boundary Method 82
B:2. Zone Electrophoresis in a Supporting Medium 84
B:3. Free Zone Electrophoresis 84
a. The Range of Application 85
b. Construction Details Affecting the Accuracy of Mobility Determinations 85
c. The Influence of the Composition of Sample Solution on the Accuracy of a Mobility Determination 86
d. Performance of Mobility Determinations 87
d:1. The Mobility Equation 87
d:2. Determination of C in Eqn. (87) 87
d:3. Determination of v_{app} in Eqn. (87) 87
d:4. Determination of q in Eqn. (87) 88
d:5. Determination of $\varkappa$ and I in Eqn. (87) 88
e. A Comparison of Mobility Values Determined by Moving Boundary Electrophoresis and Free Zone Electrophoresis . . 88
e:1. The Moving Boundary Experiment 88
e:2. The Free Zone Electrophoresis Experiment 90
f. Interpretation of Electropherograms 90
II:7. Preparative Runs 91
A. The Capacity 91
B. Recovery of Zones from the Electrophoresis Tube 93
III. *Applications* 95
III:1. Low Molecular Weight Substances 95
A. Inorganic Ions 95
B. Hydrolysis Products of Nucleic Acids 95
B:1. Purine and Pyrimidine Bases 97
B:2. Nucleosides 97
B:3. Nucleotides 98
III:2. Proteins 99
A. Normal Human Serum 99
B. Some Other Proteins 102
III:3. Nucleic Acids 103
A. The Mobility of Free-Draining Molecules 103
B. Separation of Native and Thermally Denatured T2 DNA 103
III:4. Viruses 106
III:5. Subcellular Particles 106
III:6. Cells 109

IV. *Modification of the Method for Special Applications* 111

IV:1. Detection of Substances which have no UV Absorption 111
A. Detection by Analysis of Withdrawn Fractions 111
B. Detection by Recording the Boundary Anomalies 111

IV:2. Electrophoresis in a Medium Consisting of Buffer and an Additive 112
A. The Use of Additives to Increase the Capacity 112
B. The Use of Additives to Create Isoelectric Spectra 113

V. *Summary* 114

VI. *References* 115

PREFACE

I wish to express my deep appreciation to Professor Arne Tiselius for his advice and for the many ideas that have arisen from stimulating discussions with him during the years he has been my teacher.

I am also much indebted to all members of the scientific staff of the Institute of Biochemistry at Uppsala for valuable help in different forms. In this connection I will particularly mention fil. lic. Paul Roos.

Many persons have been involved in the design and the construction of the free zone electrophoresis equipment. I want to thank all of them, especially Messrs Tore Dahm and Göran Eriksson, electronic engineers, Göte Eriksson and Arne Jansson, instrument makers, Lars Mattsson, head of the workshop, Karl-Erik Oscarsson, mechanical engineer, and Göran Rosén, electronic engineer.

For skilful technical assistance in many free zone electrophoresis experiments I want to thank Mrs Irja Blomqvist and Mrs Elsy Johnsen.

I am very grateful to Messrs Gösta Forsling, laboratory engineer, and Kjell Larsson, photographer, for assistance with the illustrations and to Mrs Lotten Borgman, Mrs Maj Rudberg, and Mrs Christina Sjöholm for typing the manuscript.

My thanks are extended to my co-authors in previous publications (see refs. 82, 83, 88 and 92) for advice on the application of the free zone electrophoresis technique to particular problems.

I am also indebted to the following persons outside the Institute for valuable discussions: fil. mag. Ingvar Blomgren, Professor Hilding Faxén, fil. lic. Sten Herlitz, fil. lic. Ragnar Westberg, and fil. mag. Assar Westin.

I also wish to emphasize the very great value of the examination of the theoretical sections, kindly undertaken by fil. dr Fredrik Eriksson, AB Astra, Södertälje and fil. dr Per-Olof Schörling, Regionala Tekniska Magisterutbildningen, Örebro.

The computer calculations have been performed at Uppsala Data Center by fil. lic. Göran Pettersson, whose help is gratefully acknowledged.

Figs. 33, 36*a*, 36*b*, and 37 have been published previously. Therefore, I am grateful to the copyright owners for their permission to reproduce these figures.

All patent applications and negotiations for commercial development of

the free zone electrophoresis equipment have been handled by Mr Nils Berling, director of EFOR, Stockholm, and his collaborator, Mr Ulf Hallne, electrical engineer. I am very much obliged for their kindness in undertaking this task.

The linguistic revision of this monograph and of several other of my scientific articles to which I refer, has been performed by Dr David Eaker, to whom I want to address my sincere thanks. In connection with the linguistic revision he has also contributed valuable criticism of the scientific contents of this monograph.

I. INTRODUCTION

Tiselius's refinement of moving boundary electrophoresis and his application of the technique to the study of biological molecules were immensely important to the development of biochemistry as an exact science. The soundness of his original apparatus is evidenced by the fact that only a few modifications in design have been made since the apparatus was first described more than 35 years ago [1]. With the introduction of schlieren optics to detect the boundaries [2, 3], the resolution was increased and the apparatus became easier to handle. This improvement favored its wider use.

Moving boundary electrophoresis, along with a contemporary innovation, analytical ultracentrifugation, allowed for the first time accurate qualitative and quantitative analyses of the complex solutions encountered in biochemistry. Serum, for example, could be resolved into many components, each of which was associated with a mobility value or a sedimentation coefficient.

When studying macromolecules it is often of great value to be able to identify them in a simple way. Determination of the primary structure would be very informative for this aim, but presents great practical difficulties. In such cases one can with advantage determine the values of a few physical parameters and use these for identification (characterization). Methods that provide rapid means of characterization are thus essential tools in most studies of natural products. Among such methods, electrophoresis and ultracentrifugation hold unique positions historically. They also provided firm physical evidence for the existence of macromolecules as discrete entities and were the first methods used for assessing homogeneity of a population of macromolecules. Even today it would be futile to initiate such an investigation as a structural analysis of a complicated substance without first establishing its purity by these techniques.

Moving boundary electrophoresis can also be used for preparative work [2, 3]. However, the method is not very efficient in this application, since only a part of the fastest-migrating and a part of the slowest-migrating substance can be withdrawn in pure form. Any attempt to achieve zone separation by this electrophoresis technique will be confounded by the onset of convection. Theoretically, moving boundary electrophoresis can be transformed to zone electrophoresis simply by including an anticonvec-

tion agent in the separation cell. In isolation work, especially, a complete separation into zones is extremely valuable. According to Poiseuille's law, the pressure required to force a liquid through a capillary tube at a given velocity increases greatly as the radius of the tube decreases. Therefore, it is not surprising that convection can be suppressed by the inclusion of substances which confer a capillary structure on the system. Cellulose in the form of powder or filter paper, grains of starch or plastic, etc., and coherent gels of substances such as agar, agarose, starch, and polyacrylamide have been used successfully for this purpose. (For a review of stabilizing media see refs. 4–6.)

The above distinction between "boundary" separations and "zone" separations was introduced by Tiselius as early as 1950 in order to classify the various electrophoresis methods in a rational way [7, 8]. This terminology is applicable also to other fractionation methods, e.g., chromatography and centrifugation.

However effective the use of stabilizing media might be in many applications of zone electrophoresis, it has several inherent disadvantages, both theoretical and practical. The main problem is interaction between the solutes of interest and the support. Although such interactions might appear to be helpful in many cases, they are certainly undesirable in general. Adsorptive and steric interactions preclude any possibility of obtaining accurate electrophoretic parameters and often cause partial or complete losses of sensitive substances. Furthermore, the capillaries of any effective anticonvection medium are too small to allow the passage of large particles and cells. An important technical disadvantage associated with zone electrophoresis in stabilized media is that migrating substances usually cannot be observed during the course of a run unless they are colored.

The free zone electrophoresis apparatus described in this monograph was constructed in an attempt to combine the advantages of carrier-free moving boundary electrophoresis with those of zone electrophoresis in anticonvection media.

There are at least two obvious alternative approaches to the problem of eliminating convection in free solution. One alternative involves the use of a cell of very narrow cross-section, wherein stabilization depends on the principle involved in the capillary systems described above. This approach is the basis of the continuous preparative "flowing film" electrophoresis method developed by Barrolier, Watzke and Gibian [9] and by Hannig [10].

In the other alternative, the convective movement of a liquid element is not suppressed, but is instead directed into a *periodic* orbit. In a horizontal electrophoresis tube such stabilization can be achieved by rotating the tube about its longitudinal axis. (For details see section II : 1, p. 13 ff.) The car-

rier-free zone electrophoresis method described in this monograph is based upon this principle of stabilization.

Apparently, the use of rotation to eliminate the disturbing influence of convection in a liquid was first considered by Kolin [11]. He produced temperature gradients in a rectangular cell ($16 \times 18 \times 41$ mm) by passing alternating current through it. No motion of the liquid was observed when the cell was rotated slowly.

To my knowledge, however, no electrophoresis experiments utilizing this means of stabilization were performed until I constructed my first free zone electrophoresis apparatus in 1958 [12]. (At that time I was not aware of Kolin's work.) Although the prototype apparatus was rather simple and crude the results obtained with it demonstrated clearly that the method was worth developing further. However, I soon found that several difficult technical problems had to be solved before the potential value of the method could be realized fully.

The problems were as follows:

1. Electroendosmosis had to be eliminated or compensated for. The method could have no practical value at all unless this could be done.

2. A scanning system for the detection of the migrating zones had to be constructed. Since a short optical path was mandatory and only dilute zones could be stabilized, the scanning system had to be very sensitive, but it ought not to record irregularities in the electrophoresis tube.

3. A simple means for introducing the sample in a sharp starting zone had to be devised.

4. The revolving electrophoresis tube would have to be immersed in a UV-transmitting liquid (water) in order to control the temperature, and to avoid excessive deflection of the scanning beam.

5. The revolving electrophoresis tube had to be sealed off from the surrounding coolant in order to avoid current leakage.

6. The electrophoresis tube should have the same inner diameter throughout its length. Otherwise no accurate mobility determinations could be performed. A method for making such electrophoresis tubes (of quartz) had to be developed, as commercially available quartz tubes are not manufactured to the tolerances required.

All of these technical problems have been overcome to the extent that free zone electrophoresis can now be regarded as a routine method for the study of low molecular weight substances (e.g., inorganic and organic ions, amino acids, purine and pyrimidine bases, nucleosides, nucleotides, etc.) as well as large structures such as proteins, nucleic acids, viruses, subcellular particles, and even whole cells. The method requires only very small amounts of material. For example, zones representing 20 μg of a protein or

3 μg of a virus can be detected readily. The electrophoretic mobility of each substance can be determined easily. Since the individual zones can be withdrawn at the end of a run, free zone electrophoresis is useful for both analysis and isolation on a micro scale.

II. THE METHOD

II:1. *Theory of Zone Stabilization by Rotation of the Electrophoresis Tube*

A. Qualitative Considerations

Assume that the density for one reason or another varies over the cross-section of a zone in a rotating, horizontal electrophoresis tube. Assume further that a liquid element A in this cross-section has a higher density than the surrounding medium. Under the influence of gravity the liquid element in the position shown in Fig. 1*a* thus moves *from* the tube wall (the rotational speed is sufficiently low that the centrifugal force can be neglected). After half a revolution the liquid element has arrived at the position indicated in Fig. 1*b*, where gravity pulls it *toward* the tube wall. Obviously, the liquid element will move away from the wall when it is in the upper half of the cross-section and toward the wall when in the lower

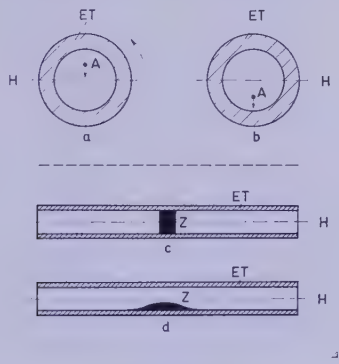

Fig. 1. Drawings illustrating the principle involved in the stabilization of zones by rotation of the horizontal electrophoresis tube ET around its long axis. H represents the horizontal plane. A is a liquid element which has a higher density than the surrounding buffer solution. If we assume that gravity and frictional forces are the only forces acting upon the liquid element, the direction of its movement must always be downward. Therefore, the liquid element moves away from the tube wall when it is in the upper half of the cross-section (a) and toward the wall when in the lower half (b). According to these simplified diagrams the liquid element is forced by the rotation of the tube to move to-and-fro relative to the tube wall, which is equivalent to zone stabilization. If rotation is stopped the sharp zone Z in (c) will spread rapidly as shown in (d).

half. When the tube is rotated, the liqiud element will thus perform a periodic back-and-forth movement relative to the tube wall. The net movement of the liquid element relative to the wall is thus approximately zero, which amounts to zone stabilization. When rotation is stopped, the initially sharp zone Z (Fig. 1*c*) will begin to spread as indicated in Fig. 1*d*.

B. Quantitative Considerations

B:1. The Equations of Motion for an Applied Liquid Element in a Fixed Coordinate System

a. Derivation of the Differential Equations

The derivation given below was performed with the assumption that the liquid element A considered in the previous section is non-diffusable and thus behaves as a rigid particle. This assumption was made to simplify the mathematical treatment but does not affect the validity of the general conclusion drawn from the equations derived.

We first introduce the horizontal revolving electrophoresis tube into a fixed right-angled coordinate system whose x-axis is horizontal and y-axis vertical. If the long axis of the tube is perpendicular to the x, y-plane and the axis of the tube is at the origin, the differential equations governing the motion of a liquid element of a zone take the following form:

$$V_p \varrho_p \frac{d^2x}{dt^2} = - V_p \varrho_m \omega^2 x - F\left(\frac{dx}{dt} + \omega y\right) \tag{1}$$

$$V_p \varrho_p \frac{d^2y}{dt^2} = - V_p \varrho_m \omega^2 y + V_p \varrho_m g - V_p \varrho_p g - F\left(\frac{dy}{dt} - \omega x\right) \tag{2}$$

where V_p = the volume of the liquid element, which is regarded as a rigid particle

ϱ_p = the density of the liquid element A

ϱ_m = the density of the surrounding medium (the buffer)

t = time

ω = the angular velocity of the revolving electrophoresis tube

F = a constant

g = the gravitational acceleration.

The term to the left of the equality sign in eqn. (1) [eqn. (2)] represents the x-component [y-component] of the inertial force. The term $-V_p\varrho_m\omega^2 x$ is the x-component and the term $-V_p\varrho_m\omega^2 y$ is the y-component of the force that the surrounding medium exerts upon the liquid element as a consequence of the rotation of the electrophoresis tube ("centrifugal pressure

force"). The influence of gravity produces the force $-V_p\varrho_p g$. $V_p\varrho_m g$ represents the buoyancy force. The last term in eqn. (1) and eqn. (2) refers to the frictional force, which is assumed to be proportional to the difference in velocity between the medium and the liquid element.

In order to express x and y as explicit functions of t we multiply eqn. (2) by i, (i.e., $\sqrt{-1}$), and add eqn. (1). The result is the following relation:

$$\frac{d^2Z}{dt^2}+\frac{F}{V_p\varrho_p}\cdot\frac{dZ}{dt}+Z\cdot\left(\frac{\varrho_m}{\varrho_p}\cdot\omega^2-\frac{F\omega}{V_p\varrho_p}\cdot i\right)=-\frac{\varrho_p-\varrho_m}{\varrho_p}\cdot g\cdot i \tag{3}$$

where $Z=x+i\cdot y$.

The general solution of this equation is

$$Z=U_1\cdot e^{\lambda_1 t}+U_2\cdot e^{\lambda_2 t}+C \tag{4}$$

where U_1, U_2, λ_1, λ_2 and C are complex numbers.

b. Determination of C in Eqn. (4)

Assume that $Z(=C)=k+i\cdot l$ is a particular solution of eqn. (3). Inserting this expression for Z in that equation and equating the real and imaginary parts, respectively, gives

$$k=\frac{(\varrho_p-\varrho_m)gV_pF}{\omega(V_p^2\varrho_m^2\omega^2+F^2)} \tag{5}$$

$$l=-\frac{(\varrho_p-\varrho_m)gV_p^2\varrho_m}{V_p^2\varrho_m^2\omega^2+F^2} \tag{6}$$

c. Determination of λ_1 and λ_2 in Eqn. (4)

The homogeneous equation corresponding to the linear differential eqn. (3) gives

$$\lambda_{1,2}=-\frac{F}{2V_p\varrho_p}\pm\frac{F}{2V_p\varrho_p}\sqrt{1-\frac{\varrho_m\omega^2}{\varrho_p}\cdot\left(\frac{2V_p\varrho_p}{F}\right)^2+\frac{4V_p\varrho_p\omega}{F}\cdot i}$$

Expressing the square root factor as $a+i\cdot b$ and making the substitution

$$\frac{F}{2V_p\varrho_p}=f \tag{7}$$

we get

$$\lambda_1=f(-1+a+i\cdot b) \tag{8}$$

$$\lambda_2=f(-1-a-i\cdot b) \tag{9}$$

Then,

$$a=\sqrt{\tfrac{1}{2}\left(1-\frac{\varrho_m\omega^2}{\varrho_p f^2}\right)+\sqrt{\tfrac{1}{4}\left(1-\frac{\varrho_m\omega^2}{\varrho_p f^2}\right)^2+\frac{\omega^2}{f^2}}} \tag{10}$$

and

$$b=\frac{\omega}{af} \tag{11}$$

As $(\varrho_m/\varrho_p)<1$ in most electrophoresis experiments,

$$\sqrt{\tfrac{1}{4}\left(1-\frac{\varrho_m\omega^2}{\varrho_p f^2}\right)^2+\frac{\omega^2}{f^2}}>\tfrac{1}{2}\left(1+\frac{\varrho_m\omega^2}{\varrho_p f^2}\right)$$

Insertion of this inequality into eqn. (10) gives $a>1$. For the limiting case $\varrho_m=\varrho_p$, eqn. (10) yields $a=1$.

As ϱ_m differs very little from ϱ_p in an electrophoresis experiment (see Table 1, p. 23) a will be only slightly greater than 1. Therefore, $a=1+\varepsilon$, where $1\geqslant\varepsilon>0$. Then, ε can be approximated by the relation

$$\varepsilon=\frac{\omega^2(1-(\varrho_m/\varrho_p))}{2f^2[1+(\varrho_m/\varrho_p)\cdot(\omega^2/f^2)]}$$

Insertion of eqn. (7) gives

$$\varepsilon=\frac{2V_p^2(\varrho_p-\varrho_m)\omega^2\varrho_p}{F^2+4\omega^2V_p^2\varrho_m\varrho_p} \tag{12}$$

Eqns. (8) and (9) can therefore be written:

$$\lambda_1=\frac{F}{2V_p\varrho_p}\cdot\varepsilon+i\frac{\omega}{1+\varepsilon}$$

$$\lambda_2=\frac{F}{2V_p\varrho_p}(-2-\varepsilon)-i\cdot\frac{\omega}{1+\varepsilon}$$

or

$$\lambda_1=\gamma_1+i\cdot\delta \tag{13}$$

$$\lambda_2=\gamma_2-i\cdot\delta \tag{14}$$

where

$$\gamma_1=\frac{(\varrho_p-\varrho_m)V_p}{F\left(\frac{1}{\omega^2}+\varrho_m\varrho_p\left(\frac{2V_p}{F}\right)^2\right)} \tag{15}$$

$$\gamma_2=\frac{F}{2V_p\varrho_p}(-2-\varepsilon) \tag{16}$$

$$\delta=\frac{\omega}{1+\varepsilon} \tag{17}$$

If the applied liquid element is spherical ($V_p=\frac{4}{3}\pi R_p^3$, where R_p is the radius of the sphere) and if Stokes law is valid ($F=6\pi\eta R_p$, where η is the viscosity constant), eqns. (12), (15) and (16) can be written as follows:

$$\varepsilon=\frac{2(\varrho_p-\varrho_m)\omega^2\varrho_p}{(9\eta/2R_p^2)^2+4\omega^2\varrho_m\varrho_p} \tag{18}$$

$$\gamma_1 = \frac{\varrho_p - \varrho_m}{9\eta/(2R_p^2\omega^2) + (8R_p^2\varrho_m\varrho_p)/9\eta} \tag{19}$$

$$\gamma_2 = -\frac{9\eta}{2R_p^2\varrho_p} \tag{20}$$

Eqn. (20) is obtained upon assuming that $\varepsilon = 0$. That this is a reasonable assumption is evident from Table 1.

d. Interpretation of the Equations of Motion

We now rewrite eqn. (4) in the form

$$x + i\cdot y = (u_1 + i\cdot v_1)e^{(\gamma_1 + i\cdot\delta)t} + (u_2 + i\cdot v_2)e^{(\gamma_2\ \ i\cdot\delta)t} + k + i\cdot l$$

Using the Euler formula ($e^{i\cdot x} = \cos x + i\cdot\sin x$) the equation can be transformed to

$$x + i\cdot y = (u_1 + i\cdot v_1)e^{\gamma_1 t}(\cos\delta t + i\cdot\sin\delta t) + (u_2 + i\cdot v_2)e^{\gamma_2 t}(\cos\delta t - i\cdot\sin\delta t) + k + i\cdot l.$$

Consequently,

$$x - k = e^{\gamma_1 t}(u_1\cos\delta t - v_1\sin\delta t) + e^{\gamma_2 t}(u_2\cos\delta t + v_2\sin\delta t) \tag{21}$$

and

$$y - l = e^{\gamma_1 t}(u_1\sin\delta t + v_1\cos\delta t) + e^{\gamma_2 t}(v_2\cos\delta t - u_2\sin\delta t) \tag{22}$$

If these equations of motion are squared and then added, one obtains

$$(x-k)^2 + (y-l)^2 = e^{2\gamma_1 t}(u_1^2 + v_1^2) + e^{2\gamma_2 t}(u_2^2 + v_2^2) + 2e^{(\gamma_1+\gamma_2)t}[(u_1u_2 + v_1v_2)\cos 2\delta t + (u_1v_2 - v_1u_2)\sin 2\delta t] \tag{23}$$

This is the equation of a spiral with the center coordinates $(k; l)$ and a radius vector whose square is the expression to the right of the equality

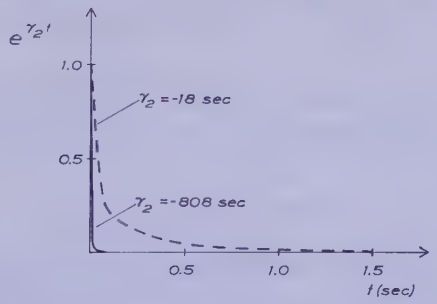

Fig. 2a. Plots of $e^{\gamma_2 t}$ as a function of time, t, for two different values of γ_2 both calculated from eqn. (20). The diagram shows that $e^{\gamma_2 t}$ approaches zero very rapidly even when $\gamma_2 = -18$ sec^{-1}, a value that is never exceeded in practice (see Table 1, p. 23). Consequently, all terms containing $e^{\gamma_2 t}$ can be dropped when the equations of motion (eqns. (21), (22), (32) and (33)) are applied to real experimental situations.

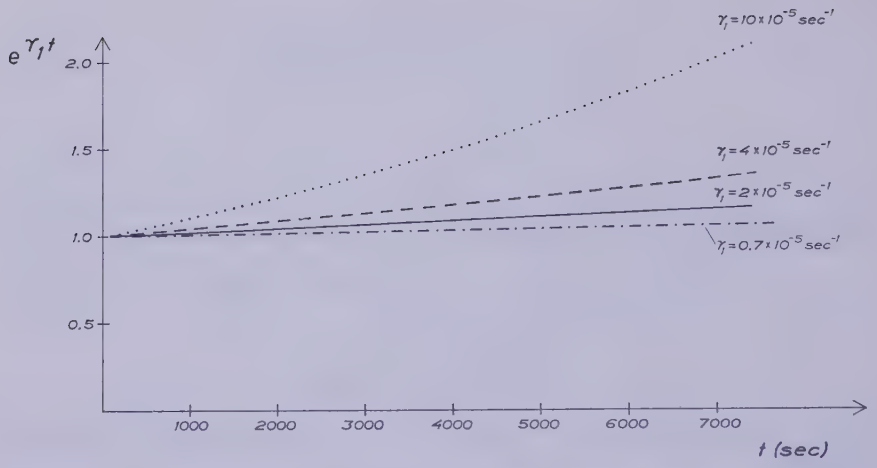

Fig. 2b. Plots of $e^{\gamma_1 t}$ as a function of time, t, for four different values of γ_1. Eqn. (19) has been used for the calculation of γ_1. Table 1 provides an idea of how the experimental conditions should be chosen in order to give these and other γ_1-values (cf. Figs. 3*a* and 3*b*). $e^{\gamma_1 t}$ determines the rate at which a liquid element of the applied sample moves toward the wall of the revolving electrophoresis tube (see eqns. (21), (22), (24), (32), (33), and (38)). Therefore, experimental conditions should be chosen such that γ_1 is close to zero.

sign. Because $\gamma_2 \ll 0$ (see Table 1), $e^{2\gamma_2 t}$ approaches zero after a very short time (Fig. 2*a*). The same is true for $e^{(\gamma_1+\gamma_2)t}$, as γ_1 is close to zero (see below and Table 1). Following this initial step of a run the liquid element moves on the spiral

$$(x-k)^2+(y-l)^2=e^{2\gamma_1 t}(u_1^2+v_1^2) \tag{24}$$

This motion has no component in the direction of the long axis of the tube. The observed migration velocity of a zone is therefore due only to the applied electric field.

As shown in the next section it is possible to choose the experimental conditions such that γ_1 is approximately zero. In practice therefore, one can often write eqn. (24) as

$$(x-k)^2+(y-l)^2=u_1^2+v_1^2 \tag{25}$$

As u_1 and v_1 are constants the liquid element describes a circle (Fig. 4*a*) and consequently undergoes no net displacement toward the tube wall.

e. Minimizing γ_1

Eqn. (24) represents a spiral, which, for convenience, we will regard as a circle whose radius increases with time. This increase is extremely

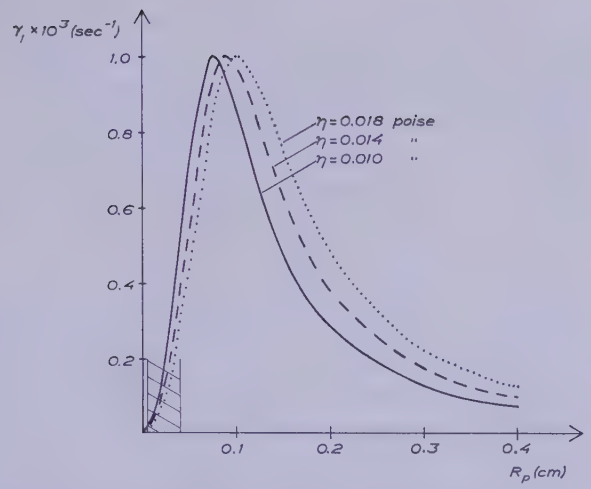

Fig. 3a. Plots of γ_1 as a function of R_p for three different values of the coefficient of viscosity, η. R_p is the radius of a spherical sample element. γ_1 was calculated from eqn. (19) for the case where $\varrho_p - \varrho_m = 0.001$ g cm^{-3}, $\varrho_m \varrho_p = 1.000$ g^2 cm^{-6}, and $\omega = 4$ sec^{-1}. The hatched area represents the practical operating range.

slow if γ_1 is close to zero (see Fig. 2*b*). We shall therefore consider how the variables involved in the expression for γ_1 (eqns. (15) and (19)) should be chosen in order to keep γ_1 close to the ideal zero.

(1) First, we should determine how the magnitude of γ_1 is influenced by the size of the applied liquid element. Therefore we take the derivative of the denominator of eqn. (19) with respect to R_p. This operation shows that γ_1 is devoid of a minimum, but has a maximum =

$$\frac{(\varrho_p - \varrho_m)}{4\sqrt{\varrho_p \varrho_m}} \quad \text{for} \quad R_p = \tfrac{3}{2}\sqrt[4]{\frac{\eta^2}{\omega^2 \varrho_p \varrho_m}}$$

The curve γ_1 as a function of R_p (eqn. (19)) is outlined in Fig. 3*a*. According to this diagram, one ought to choose either small values ($\ll$0.1 cm) or large values ($\gg$0.1 cm) for the radius of the applied liquid element in order to obtain low values of γ_1. As the radius of the electrophoresis tube should not be much greater than 0.15 cm (see section A, p. 91 ff.), only the first alternative is practicable. Therefore, the syringe (Fig. 14) employed for the application of the sample should have a very narrow orifice.

(2) If we next consider γ_1 as a function of η, we see that γ_1 lacks a minimum but has a maximum =

$$\frac{(\varrho_p - \varrho_m)\omega}{4\sqrt{\varrho_p \varrho_m}} \quad \text{for} \quad \eta = \frac{4 R_p^2 \omega \sqrt{\varrho_m \varrho_p}}{9}$$

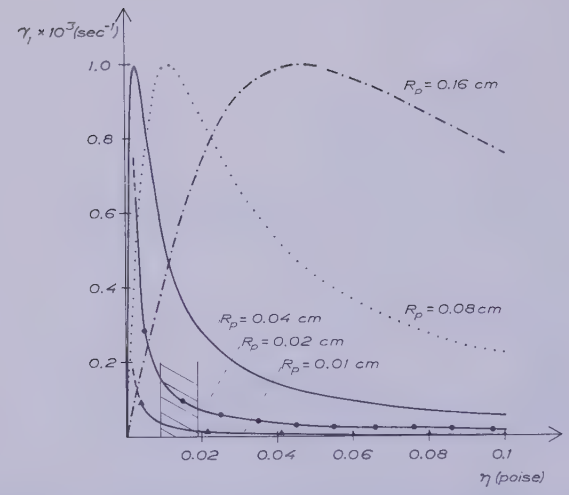

Fig. 3b. Plots of γ_1 as a function of the coefficient of viscosity, η, (eqn. (19)) for five different values of R_p, the radius of a spherical sample element. For these plots, $\varrho_p - \varrho_m = 0.001$ g cm^{-3}, $\varrho_m \varrho_p = 1.000$ g^2 cm^{-6}, and $\omega = 4$ sec^{-1}. The hatched area represents the practical operating range.

(see Fig. 3*b*). As most electrophoresis experiments are performed at temperatures between 0 and +20°, the viscosity of the buffer will vary between 0.018 and 0.010 poise. This viscosity range corresponds to the shaded area of the diagram in Fig. 3*b*. To minimize γ_1 then, according to this figure, one should perform an experiment at the lowest temperature possible, provided that the radius R_p of the liquid element is smaller than about 0.1 cm. For larger radii the reverse is true as evidenced by the curve for $R_p = 0.16$ cm. However, as was stressed under point (1) in the discussion of the influence of R_p upon γ_1, liquid elements of the smallest possible radius should be applied. Therefore, the curve drawn for $R_p = 0.16$ cm, as well as those for $R_p = 0.08$ and 0.04 cm, does not represent useful experimental conditions. Fig. 3*b* also shows that a great increase in the viscosity of the buffer decreases γ_1 considerably, even if R_p has a relatively large value. This has been verified experimentally by adding substances such as methyl cellulose to the buffer. Such very viscous buffers provide stabilization even at high sample concentrations (see section A, p. 91 ff.).

(3) Eqn. (15) shows that a decrease in the concentration of the sample applied, i.e., in $\varrho_p \quad \varrho_m$, causes γ_1 to decrease. The minimum concentration that can be applied is determined by the sensitivity of the scanning system (see section A, p. 91 ff.).

(4) From eqn. (15) one can also conclude that low rotational speeds of the electrophoresis tube (small values of ω) should be used to obtain small

γ_1-values. However, a decrease in ω increases the parameter $\sqrt{k^2+l^2}$ (eqn. (27)), which is unfavorable as discussed in the next section. Therefore, the speed of rotation must be chosen such that neither γ_1 nor $\sqrt{k^2+l^2}$ have large values. The optimum speed was found empirically to be about 40 rev./min ($\omega \sim 4$ sec^{-1}) as mentioned in the next section. Eqn. (19) shows that γ_1 is essentially independent of ω when

$$\frac{9\eta}{2R_p^2\omega^2} \ll \frac{8R_p^2\varrho_m\varrho_p}{9\eta}$$

Insertion of typical values of the parameters in this inequality ($\eta = 0.015$ poise, $R_p = 0.01$ cm, $\varrho_m\varrho_p = 1.00$ g^2 cm^{-6}) shows that ω must be several orders of magnitude larger than 4 sec^{-1} before γ_1 becomes independent of ω. Furthermore, for these parameter values, $\gamma_1 = (\varrho_p - \varrho_m) \cdot 170$ sec^{-1}, which, according to Fig. 2*b*, is far above acceptable values. It is therefore not possible to find such a working value of ω that γ_1 is independent of ω.

f. Minimizing $\sqrt{k^2+l^2}$ and Calculation of a Working Value of ω

The parameter $\sqrt{k^2+l^2}$ represents the distance between the center of the circle C_A (Fig. 4*a*) and the axis of the electrophoresis tube ET. If this distance is comparatively large the circle C_A will cut the electrophoresis tube, which means that the liquid element will come into contact with the wall of the tube and spread out along it. Therefore, $\sqrt{k^2+l^2}$ must be kept small. The experimental conditions required for small values of this parameter can be determined from the expression for $\sqrt{k^2+l^2}$ that is obtained by squaring and adding eqns. (5) and (6). This gives

$$\sqrt{k^2+l^2} = \frac{(\varrho_p - \varrho_m)g}{\omega\sqrt{\varrho_m^2\omega^2 + (F/V)^2}} \tag{26}$$

Making the substitution $V_p = \frac{4}{3}\pi R_p^3$ and $F = 6\pi\eta R_p$ we arrive at

$$\sqrt{k^2+l^2} = \frac{(\varrho_p - \varrho_m)g}{\omega\sqrt{\omega^2\varrho_m^2 + (9\eta/2R_p^2)^2}} \tag{27}$$

From this expression one can conclude that $\sqrt{k^2+l^2}$ decreases when ϱ_p and R_p decrease or when η, ω and ϱ_m increase. As shown in the preceding section, all of these variables except ω affect the parameter γ_1 in the same direction. Since efficient zone stabilization is attained only when both γ_1 and $\sqrt{k^2+l^2}$ are small, a compromise value for ω must be used. To calculate a good working value for ω we assume that the rotation of the electrophoresis tube provides acceptable zone stabilization only if $\sqrt{k^2+l^2} \leqslant 1.0 \times 10^{-2}$ cm (which corresponds to 7 per cent of the tube radius, which is about 0.15 cm) and if $\gamma_1 \leqslant 5 \times 10^{-5}$ sec^{-1} (Fig. 2*b*). The maximum value (ω_{max}) and

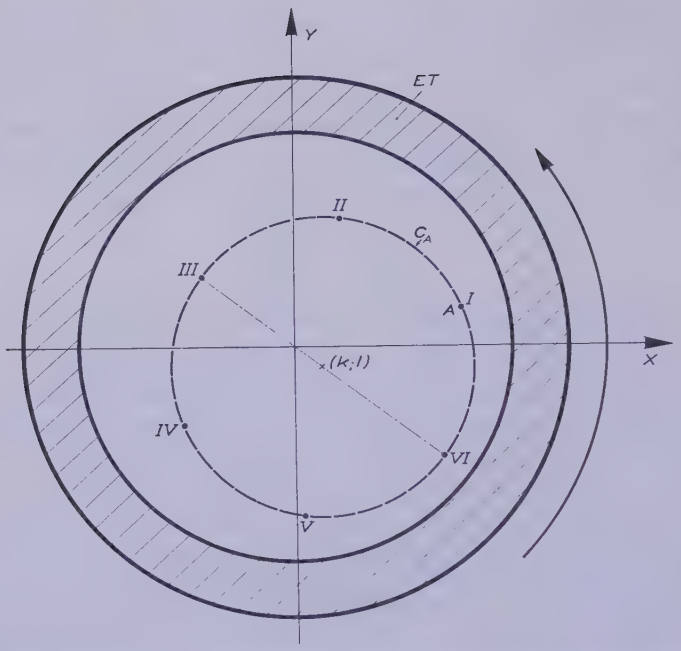

Fig. 4a. The motion of a liquid element A of the sample during the rotation of the electrophoresis tube ET as depicted in a fixed coordinate system (cf. Fig. 4*b*). This figure gives a more detailed description of the effect illustrated in Figs. 1*a* and 1*b*. I, II, etc., denote successive positions of the liquid element during one revolution of the tube. The liquid element moves along the circle C_A defined by eqn. (25). The motion is described more precisely by eqn. (24). The center coordinates of C_A are $(k; l)$. The distance between the center of C_A and the axis of ET is $\sqrt{k^2+l^2}$.

minimum value ($\omega_{\min}$) of ω can then be calculated from eqns. (19) and (27), respectively. This calculation will be made for the case that the run is performed under unfavorable conditions, i.e., at high sample concentrations ($\varrho_p - \varrho_m = 0.003$ g cm $^{-3}$).[a] Using for the sample application a syringe with such a narrow orifice that R_p is about 0.01 cm, we get, with the above figures and with $g = 980$ cm sec $^{-2}$ and $\eta = 0.015$ poise, $\omega_{\max} = 3.4$ sec^{-1} and $\omega_{\min} = 0.44$ sec $^{-1}$. If we use a mean (~ 2) of these extreme values of ω, both $\sqrt{k^2+l^2}$ and γ_1 will be less than the above values of 1×10^{-2} and 5×10^{-5}, respectively, and they will be still less if we use a lower sample concentration than was assumed for the calculation of ω.

This estimation of ω is very rough and should be considered only as an attempt to arrive at a suitable order of magnitude. In all experiments described in this monograph a rotational speed of the electrophoresis tube

[a] In the case of proteins, this value of $\varrho_p - \varrho_m$ represents a concentration of approximately 1.2 per cent (see footnote, p. 23).

of 40 rev./min ($\omega \sim 4$ sec^{-1}) has been used. This value was obtained empirically several years ago and long before the above theoretical study was started. Only by extremely thorough examinations of the distortion of a zone at various angular velocities can it be decided whether it is advantageous to reduce ω.

g. The Decrease of γ_1 and $\sqrt{k^2+l^2}$ during a Run

So far we have assumed that the liquid element behaves as a rigid body. In reality it will expand with time due to diffusion and to motions relative to the tube wall. This expansion of the applied liquid element causes γ_1 and $\sqrt{k^2+l^2}$ to decrease continuously during a run. To prove this statement we multiply eqns. (19) and (27) by $V_p/(\frac{4}{3}\pi R_p^3)$ [$=1$], which gives

$$\gamma_1 = \frac{V_p(\varrho_p - \varrho_m)}{(6\pi\eta R_p)/\omega^2 + (32\pi R_p^5 \varrho_m \varrho_p)/27\eta} \tag{28}$$

$$\sqrt{k^2+l^2} = \frac{V_p(\varrho_p - \varrho_m)g}{\omega\sqrt{(\frac{4}{3}\pi R_p^3)^2\omega^2\varrho_m^2 + (6\pi\eta R_p)^2}} \tag{29}$$

Table 1. Calculated values of the parameters ε (eqn. (18)), γ_1 (eqn. (19)), γ_2 (eqn. (20)), k (eqn. (5)), l (eqn. (6)) and $\sqrt{k^2+l^2}$ (eqn. (27)) for some different values of ω, ϱ_p, R_p and η; g is considered to be 980 cm sec^{-2} and $\varrho_m = 1.0000$ g cm^{-3}.

ω sec^{-1}	ϱ_p [f] g cm^{-3}	R cm	η poise	$\varepsilon \times 10^6$	$\gamma_1 \times 10^5$ sec^{-1}	γ_2 sec^{-1}	$k \times 10^3$ cm	$l \times 10^5$ cm	$\sqrt{k^2+l^2} \times 10^3$ cm
4	1.0003	0.01	0.018	0.015	0.60	−810	0.091	0.045	0.091
4	1.0010	0.01	0.018	0.049	2.0	−809	0.30	0.15	0.30
4	1.0030	0.01	0.018	0.15	6.0	−808	0.91	0.45	0.91
4	1.0100	0.01	0.018	0.49	20	−802	3.0	1.5	3.0
4	1.0010	0.02	0.018	0.78	8.0	−202	1.2	2.4	1.2
4	1.0010	0.04	0.018	12	30	− 50.6	4.8	38	4.8
4	1.0010	0.08	0.018	140	90	− 12.6	18	570	19
4	1.0010	0.01	0.010	16	3.6	−450	0.54	0.50	0.54
4	1.0010	0.01	0.014	0.080	2.5	−626	0.39	0.25	0.39
1	1.0010	0.02	0.018	0.049	0.49	−202	4.8	2.4	4.8
16	1.0010	0.02	0.018	12	120	−202	0.30	2.4	0.30
1	1.0010	0.01	0.018	0.0030	0.12	−809	1.2	0.15	1.2
16	1.0010	0.01	0.018	0.78	31	−809	0.076	0.0093	0.076

[f] The density is related to the concentration by eqn. (88). For proteins with $\bar{v} = 0.74$ cm^3 g^{-1}, a density difference $\varrho_p - \varrho_m = 0.0010$ g cm^{-3} thus corresponds to a 0.4 % solution.

As $V_p(\varrho_p - \varrho_m)$ is proportional to the mass of sample solute in the applied liquid element, the numerators in both equations are independent of the duration of the experiment.[b] Therefore, γ_1 and $\sqrt{k^2+l^2}$ must decrease as R_p increases. The fact that these parameters decrease as the applied element expands allows experiments to be prolonged far beyond the times indicated by the curves of Fig. 2*b*.[c] In the electrophoresis experiment illustrated in Fig. 33, little zone spreading is observed over a period of 4 hours (see also Fig. 5). Therefore, the approximate eqn. (25) often gives an adequate description of the real experimental situation.

In practice the liquid element is seldom spherical as assumed above: it is usually elongated. The relationship between form and frictional force then becomes more complicated than Stokes law. However, the general conclusions drawn from the equations derived for a spherical liquid element are valid also for other shapes.

B:2. The Equations of Motion for an Applied Liquid Element in a Rotating Coordinate System

a. Derivation of the Equations

The motion of a liquid element of the sample can be described in a somewhat different way by using the differential equations of motion in a rotating coordinate system. In this system, the coordinates x' and y' differ from those of the stationary $x-y$ system only by rotating with the same angular velocity ω as the electrophoresis tube. If the x'-axis is assumed to lie in the horizontal plane at the time $t=0$, the differential equations governing the motion in this x', y'-system are as follows:

$$V_p\varrho_p\frac{d^2x'}{dt^2} = V_p\varrho_p\omega^2x' - V_p\varrho_m\omega^2x' - V_p\varrho_p g\sin\omega t + V_p\varrho_m g\sin\omega t - F\frac{dx'}{dt} + 2V_p\varrho_p\omega\frac{dy'}{dt} \tag{30}$$

$$V_p\varrho_p\frac{d^2y'}{dt^2} = V_p\varrho_p\omega^2y' - V_p\varrho_m\omega^2y' - V_p\varrho_p g\cos\omega t + V_p\varrho_m g\cos\omega t - F\frac{dy'}{dt} - 2V_p\varrho_p\omega\frac{dx'}{dt} \tag{31}$$

[b] From eqn. (88) one gets

$$V_p(\varrho_p - \varrho_m) = c\cdot V_p(1-\bar{v}\cdot\varrho_m).$$

As $c\cdot V_p$ is the mass of sample substance in a liquid element, the product $V_p(\varrho_p-\varrho_m)$ is constant throughout the run.

[c] In other words: Although the experimental conditions at the start of a run might correspond to the curve for $\gamma_1 = 10\times10^{-5}$ sec^{-1} in Fig. 2*b*, they will gradually change during the electrophoresis such that the curves for $\gamma_1 = 4\times10^{-5}$, 2×10^{-5}, and 0.7×10^{-5} sec^{-1} will obtain successively as the experiment proceeds.

The term to the left of the equality sign in eqn. (30) represents the x'-component of the inertial force, whereas the terms to the right represent the x'-components of the following forces: the centrifugal force, the "centrifugal pressure force", the gravity, the buoyancy force, the frictional force, and the Coriolis force [13], respectively. The angle ωt is the angle between the horizontal plane and the x'-axis. Eqn. (31) is the analogous expression for the corresponding y'-components.[d]

If eqns. (30) and (31) are transformed similarly to eqns. (1) and (2) one obtains:

$$x' = e^{\gamma_1 t}(u_1 \cos \theta t - v_1 \sin \theta t) + e^{\gamma_2 t}(u_2 \cos \phi t - v_2 \sin \phi t) + k \cos \omega t + l \sin \omega t \tag{32}$$

$$y' = e^{\gamma_1 t}(u_1 \sin \theta t + v_1 \cos \theta t) + e^{\gamma_2 t}(u_2 \sin \phi t + v_2 \cos \phi t) - k \sin \omega t + l \cos \omega t \tag{33}$$

γ_1, γ_2, k and l are defined by the relations (15), (16), (5), and (6). Furthermore:

$$\theta = \omega\left(-1 + \frac{1}{1+\varepsilon}\right) \tag{34}$$

$$\phi = \omega\left(-1 - \frac{1}{1+\varepsilon}\right) \tag{35}$$

where the value of ε is calculated using relation (12).

b. Interpretation of the Equations of Motion (32) and (33)

Since ε (eqn. 12) is close to zero (see Table 1), θ (eqn. (34)) and ϕ (eqn. (35)) are approximately 0 and -2ω, respectively. Moreover, $\gamma_2 \leqslant 0$ (Fig. 2*a*). When these values are substituted into eqns. (32) and (33) we see that a liquid element of the sample will after a short time enter an orbit described by the equations

$$x' - u_1 \cdot e^{\gamma_1 t} = k \cos \omega t + l \sin \omega t \tag{36}$$

$$y' - v_1 \cdot e^{\gamma_1 t} = -k \sin \omega t + l \cos \omega t \tag{37}$$

Accordingly,

$$(x' - u_1 \cdot e^{\gamma_1 t})^2 + (y' - v_1 \cdot e^{\gamma_1 t})^2 = k^2 + l^2 \tag{38}$$

This equation represents a circle with the radius $\sqrt{k^2 + l^2}$ and the center coordinates $(u_1 \cdot e^{\gamma_1 t};\ v_1 \cdot e^{\gamma_1 t})$. The liquid element thus describes a small

[d] Eqns. (30) and (31) can also be derived from eqns. (1) and (2) by the use of the following transformations $x = x' \cos \omega t - y' \sin \omega t$, $y = x' \sin \omega t + y' \cos \omega t$. Many of the conclusions that will be drawn from differential equations (30) and (31) can also be reached by vector algebra on the basis of the information already provided by eqns. (1) and (2).

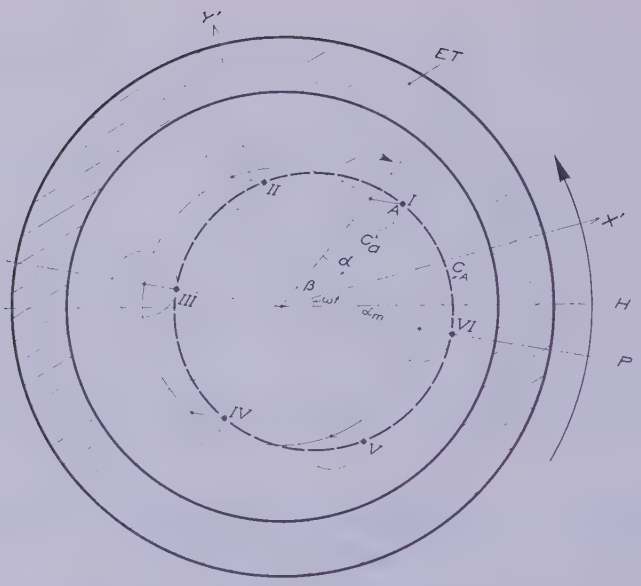

Fig. 4b. The motion of a liquid element A of the sample during the rotation of the electrophoresis tube ET as described in terms of a rotating coordinate system (cf. Fig. 4*a*). The small circle C_a is a graphic representation of eqn. (39). The angular velocity of the liquid element when moving along the small circles C_a is equal to the angular velocity of the revolving electrophoresis tube. The angle α_m between the horizontal plane H and the plane P is actually very small, as is the radius of the circle C_a. The circle C_A (shown also in Fig. 4*a*) refers to eqn. (25). The radius of the circle C_a is $\sqrt{k^2+l^2}$.

circle whose center continuously moves away from the axis of the electrophoresis tube. However, in many experiments γ_1 is very close to zero, as was mentioned above in section c, p. 18 ff. (see also Table 1 and Fig. 2*b*). In such cases eqn. (38) can be approximated by

$$(x'-u_1)^2+(y'-v_1)^2=k^2+l^2 \tag{39}$$

which implies that the liquid element shows no net displacement relative to the tube wall. The situation is depicted in Fig. 4*b*. The relative size of the small circles C_a is greatly exaggerated in the figure. The liquid element describes the small circle C_a during each revolution of the electrophoresis tube. This is proved in the next section along with several other things.

c. The Distance L from the Liquid Element to the Axis of the Electrophoresis Tube as a Function of Time

As $L^2=x'^2+y'^2$, then according to eqns. (36) and (37)

$$L^2=u_1^2\cdot e^{2\gamma_1 t}+v_1^2\cdot e^{2\gamma_1 t}+k^2+l^2+2\cdot e^{\gamma_1 t}(u_1 l-v_1 k)\sin\omega t$$
$$+2\cdot e^{\gamma_1 t}(u_1 k+v_1 l)\cos\omega t$$

For the reasons discussed in connection with the treatment of the motion of a liquid element in a fixed coordinate system, we set $e^{2\gamma_1 t} = 1$ (cf. Fig. 2*b*). Then,

$$L^2 = u_1^2 + v_1^2 + k^2 + l^2 + 2(u_1 l - v_1 k) \sin \omega t + 2(u_1 k + v_1 l) \cos \omega t \tag{40}$$

Making the substitutions

$$2(u_1 l - v_1 k) = A \cos \varphi \tag{41}$$

and

$$2(u_1 k + v_1 l) = A \sin \varphi \tag{42}$$

expression (40) can be transformed to

$$L^2 = u_1^2 + v_1^2 + k^2 + l^2 + A \sin (\omega t + \varphi) \tag{43}$$

Thus, the distance from the liquid element to the origin varies periodically with a frequency equal to the rotational frequency of the electrophoresis tube. In other words: the liquid element moves on the circle C_a (Fig. 4*b*) with an angular velocity equal to that of the rotating electrophoresis tube. Eqn. (43) also shows that L has a maximum at the angle

$$\omega t = -\varphi + \frac{\pi}{2} + n \cdot 2\pi \tag{44}$$

and a minimum at the angle

$$\omega t = -\varphi + \frac{3\pi}{2} + n \cdot 2\pi \quad (n = 0, 1, 2 \ldots) \tag{45}$$

Since the phase displacement, φ, is determined by the relation

$$\tan \varphi = \frac{u_1 k + v_1 l}{u_1 l - v_1 k} \tag{46}$$

obtained from eqns. (41) and (42), these special values of ωt depend on u_1 and v_1, which are related in a complicated way to the coordinates for the application of the liquid element. Therefore, we define an angle α as the angle between the horizontal plane H and a line passing from the origin to the center of the circle C_a (Fig. 4*b*). This angle is independent of u_1 and v_1, as is shown below.

By definition,

$$\alpha = \omega t + \beta \tag{47}$$

Since $(u_1; v_1)$ are the coordinates of the center of circle C_a

$$\tan \beta = \frac{v_1}{u_1} \tag{48}$$

Eqn. (47) can be transformed to

$$\tan \alpha = \frac{\tan \omega t + \tan \beta}{1 - \tan \omega t \cdot \tan \beta} \tag{49}$$

If the relations (44), (45) and (48) are substituted into eqn. (49) and relation (46) is used, we obtain

$$\alpha_m = \text{arc tan} \frac{l}{k} + n \cdot \pi \tag{50}$$

This equation thus gives the angles at which the liquid element is furthest from ($n = 0, 2, 4 \ldots$) and closest to ($n = 1, 3, 5 \ldots$) the axis of the electrophoresis tube.[e] Since $k > 0$ (eqn. (5)) and $l < 0$ (eqn. (6)) for $\omega > 0$ the liquid element attains these maximum and minimum positions in the fourth and second quadrants, respectively, if we think in terms of a fixed coordinate system and the direction of rotation of the tube is as indicated in Fig. 4*b*. The experimental conditions are usually chosen so that $|k| \gg |l|$ (see Table 1). In such cases, $\alpha_m = \varepsilon_0 + n \cdot \pi$, where ε_0 is a very small angle ($\varepsilon_0 < 0$ when $\omega > 0$).

The positions at which the liquid element is nearest to and farthest from the wall of the electrophoresis tube are thus known (positions VI and III in Fig. 4*b*). For the construction of other positions (I, II, IV, V) the following facts have been utilized:

(1) the liquid element moves on a small circle C_a, whose center is, to a good approximation, stationary with respect to the tube wall (eqn. (39)).

(2) The angular velocity of the liquid element on this small circle is equal to the angular velocity of the rotating electrophoresis tube (eqn. (43)).

(3) The rotational direction of the liquid element on this circle is opposite to that of the electrophoresis tube. Of these three statements, only (3) remains to be proved. To do this we proceed as follows:

The slope ($= \tan \Omega$) of a tangent to a circle at the point (x'; y') is determined by the relation $\tan \Omega = -(x' - x_0')/(y' - y_0')$, where x_0' and y_0' are the center coordinates of the circle. Insertion of eqns. (36) and (37) gives

$$\tan \Omega = -\frac{k \cos \omega t + l \sin \omega t}{-k \sin \omega t + l \cos \omega t}$$

By taking the derivative, we get

$$\frac{l}{\cos^2 \Omega} \cdot \frac{d\Omega}{d(\omega t)} = -\frac{k^2 + l^2}{(-k \sin \Omega + l \cos \Omega)^2}$$

[e] The finding that extreme values of L occur for angles satisfying relation (50) is in accordance with the fact that the center coordinates of the circle C_A in Fig. 4*a* are (k; l).

Accordingly, $d\Omega/d(\omega t) < 0$, (i.e., the angle Ω decreases when ωt increases). From this finding one can conclude that the direction of rotation of the liquid element along the circle C_a is as indicated in Fig. 4*b*.

Like those derived with the stationary coordinate system the equations of motion based on the rotating coordinate system also make apparent the importance of minimizing the parameters γ_1 and $\sqrt{k^2+l^2}$ (see eqn. (38)). The various means by which these parameters can be minimized were discussed in the treatment involving the stationary coordinate system. Perhaps I should mention here that $\sqrt{k^2+l^2}$ has different physical meanings in the two coordinate systems (see the legends to Figs. 4*a* and 4*b*).

C. Experimental Demonstrations of Zone Stability in the Revolving Electrophoresis Tube

The experiments a–c described below illustrate the extent to which zones can be stabilized by rotating the electrophoresis tube. Although some of the manipulations involved in the performance of these experiments might not be understood before reading section II:3, p. 51 ff., the principles should be clear. Therefore, it seems appropriate to discuss these experiments here in connection with the theoretical treatment of zone stabilization developed above.

(a) The electrophoresis tube was filled with 0.03 *M* sodium phosphate buffer, pH 7.3. About 0.5 mg of α-chymotrypsin was dissolved in 1 ml of the same buffer and a 10 μl aliquot of the solution was introduced into the revolving electrophoresis tube. Electrophoresis was carried out for 70 minutes in order to move the zone of chymotrypsin away from the starting position. Then, the electrode voltage was switched off and a scan (the zero time scan in Fig. 5) was made immediately. The electrophoresis tube was left rotating for nearly two days with no voltage applied to the electrodes and additional scans were made at the times indicated in the figure. The gradual, symmetrical spreading observed in the patterns is due almost entirely to diffusion and to the movement of liquid elements in the manner described in the preceding sections. The fact that the width of the zone increases by less than a factor of three over a period of 44 hours demonstrates clearly that rotation can provide satisfactory zone stabilization when no current is passed through the electrophoresis tube.

Another experiment was then performed as described above, but after the DC electrophoresis current was switched off, an alternating current (1500 V, 12 mA, 50 cycles) was applied to the electrodes in order to create in the electrophoresis tube a parabolic temperature gradient similar in shape to those which arise during electrophoresis. With joule heat generated

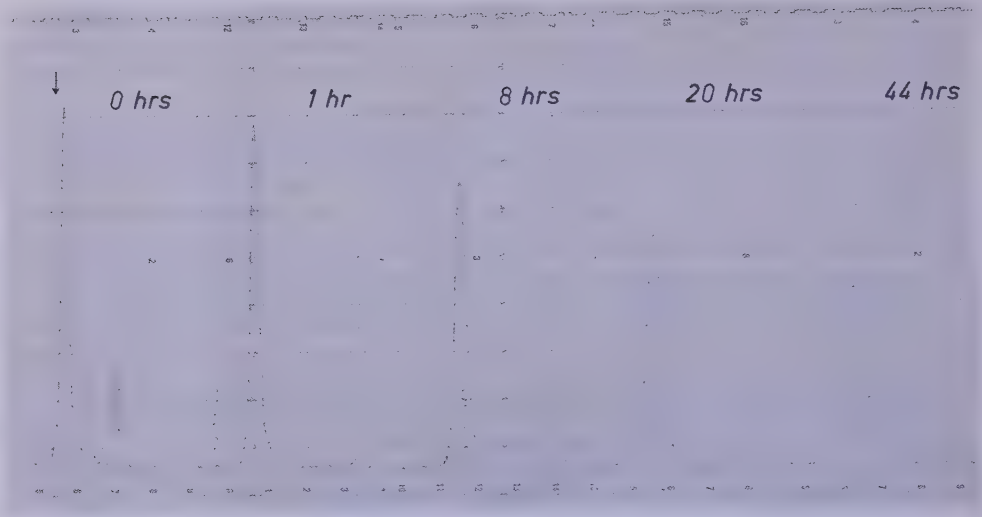

Fig. 5. Diagrams showing the gradual broadening of a zone in the rotating electrophoresis tube in the absence of an applied voltage. Sample: 10 μl of a 0.5 % solution of α-chymotrypsin (electrophoretically heterogeneous). Inner diameter of electrophoresis tube: 3 mm. Temperature of cooling water: ca. 16°. After the zone had migrated electrophoretically out of the starting position, the current was switched off and the rotating tube was scanned at the times indicated. The zero time scan was made immediately after the current was switched off. Only slightly broader peaks were obtained when alternating current was applied to the electrodes after completion of the electrophoresis. Obviously, very little zone broadening occurs during the 10–100 min required for most free zone electrophoresis runs.

at a rate of 18 watts, the temperature difference between the inner wall and the axis of the electrophoresis tube was 6° (as calculated by eqn. (74)) when the gradient was fully developed (i.e., in the steady state). In the absence of rotation, the radial variations in density caused by such a temperature gradient would give rise to convective disturbances. However, the peaks observed in the recorder chart during the alternating current experiment were only about 20 per cent broader than those shown in Fig. 5 for the companion experiment performed in the absence of a temperature gradient.

Although rotation can suppress convection adequately even in the presence of temperature gradients considerably steeper than that just mentioned, such a gradient cannot be tolerated in an actual electrophoresis experiment for another reason. Since a temperature difference of 6° corresponds to a difference of about 18 per cent in migration velocity (eqn. (70)), any zone that migrates in such a gradient will rapidly become parabolic. (Ob-

viously, this type of broadening cannot be suppressed by rotation.) This does not prohibit the use of 18 or more watts of power, however, when the time required to develop the steady-state temperature gradient is long compared with the duration of a free zone electrophoresis experiment. In the case of low molecular weight solutes, the separation desired can often be achieved in a few minutes. In such cases, currents corresponding to 30 watts or more can be used without significant zone broadening (see Fig. 29). In general, however, more moderate currents should be used, particularly when the solutes migrate slowly (as is often true of high molecular weight substances) or when accurate mobility measurements are to be made.

On the basis of the results obtained in the pair of experiments described above, one can conclude that very little zone-broadening occurs in most free zone electrophoresis runs with homogeneous substances, since the time of electrophoresis is usually less than 100 minutes and steep temperature gradients are almost always avoided.

(b) A small aliquot of serum was subjected to electrophoresis for 36 minutes. The electrodes were then reversed, causing the various components to migrate back toward the starting position. After 36 minutes of "reverse" electrophoresis only a single well defined zone was present, indicating that very little zone distortion had occurred despite the high protein concentration used (2.2 per cent). The experiment is illustrated in Fig. 31 and is discussed further in section A, p. 99 ff.

(c) A highly purified proteinase was subjected to free zone electrophoresis at a pH near its isoelectric point. The low mobility of the enzyme allowed the run to be continued for 4 hours. The zone remained very sharp throughout the experiment (see Fig. 33 and section B, p. 102 ff.). Therefore, if a zone increases appreciably in width during runs performed under moderate conditions the material is probably heterogeneous (see section f, p. 90 ff.).

II:2. *Design and Function of the Equipment*

A. Over-All Description

The design of the original version of the free zone electrophoresis apparatus had to be improved considerably before the potential advantages could be realized. Many construction problems had to be tackled and solved. However, technical problems will be discussed only in cases where such discussion facilitates description of the construction of particular units of the present equipment. In this section only a general over-all description of the equipment will be given.

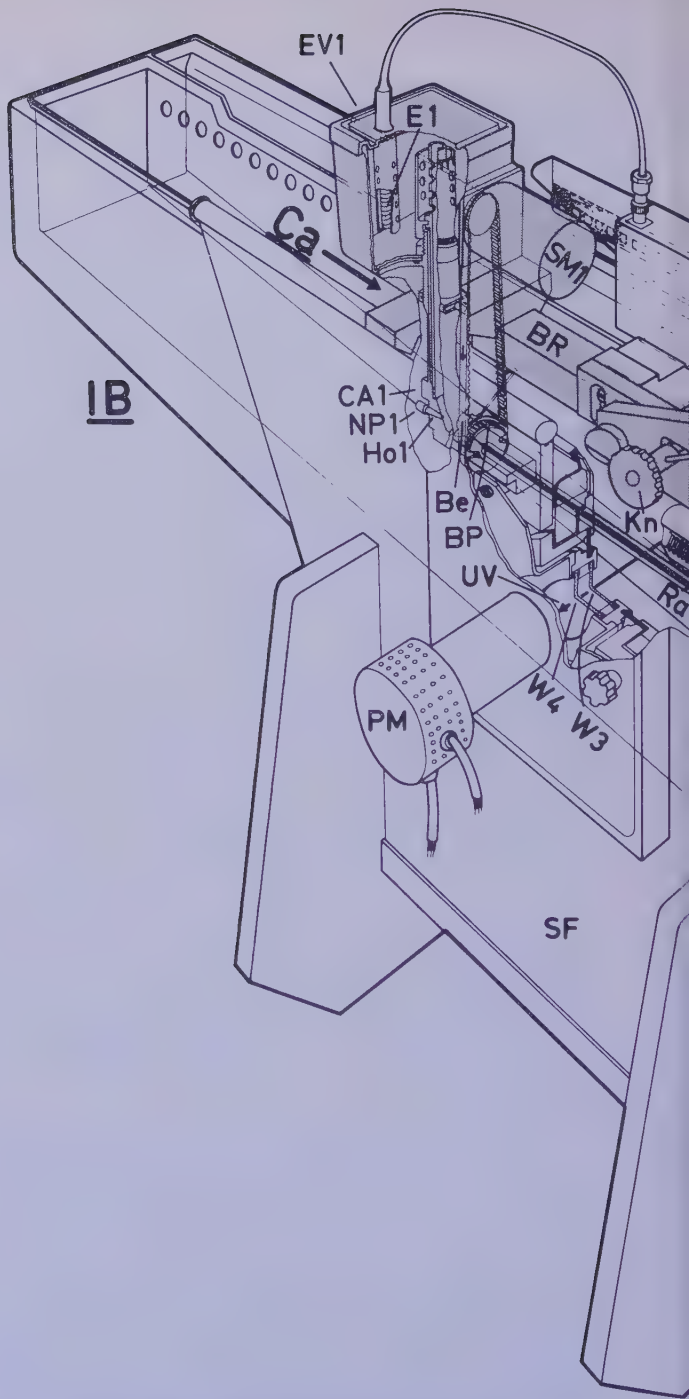

Fig. 6. Perspective drawing of the carriage Ca and the immersion bath IB (cf. Fig. 7). BR: CA2: connecting arms; Be: cogged belt; BP: cogged belt pulley; Ho1: hole through which reflow; Ho2: hole for introduction of sample; NP1, NP2: nylon plugs; SR1, SR2: steel rods; to drive carriage Ca; PG: pinion gear; Ra: rack; Kn: knob for raising and lowering motor zone position indicator unit in Fig. 13*a*); I: inlet for cooling water; O: outlet for cooling

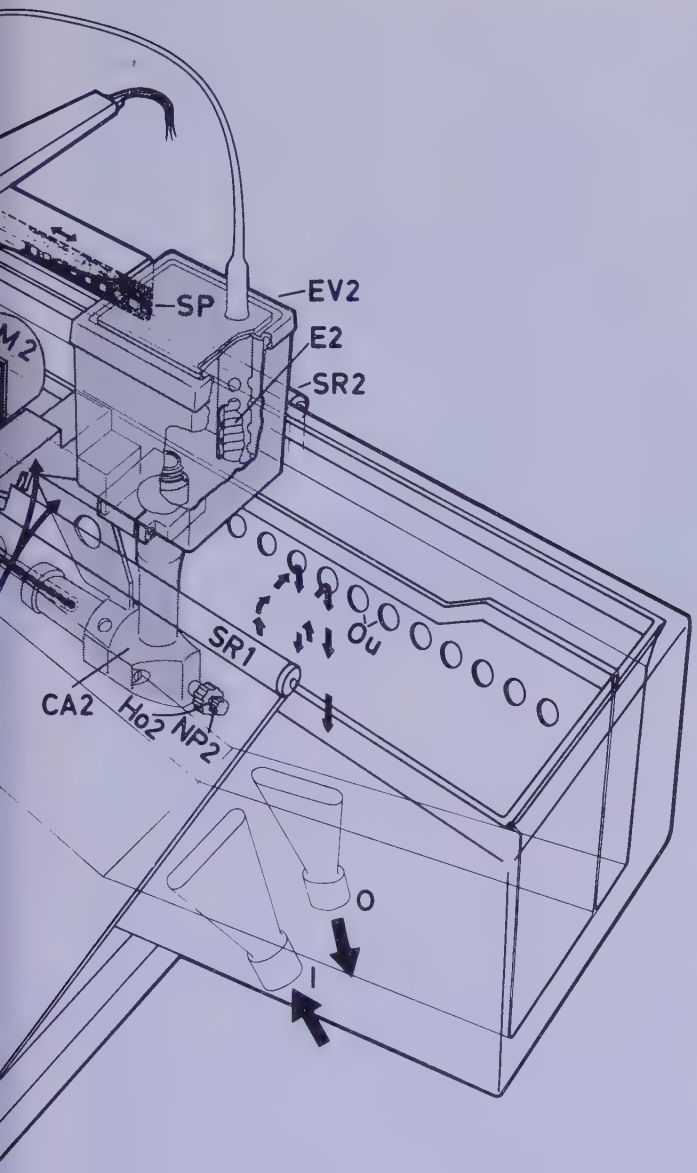

brass rod; E1, E2: electrodes; EV1, EV2: electrode vessels; ET: electrophoresis tube; CA1, buffer is introduced (or withdrawn) for hydrodynamic compensation of electroendosmotic SM1: synchronous motor for rotation of electrophoresis tube ET; SM2: synchronous motor SM2; UV: ultraviolet scanning beam; PM: photo multiplier; SP: shutter plate (part of the water; Ou: over-flow outlets; SF: support frame; W3, W4: quartz windows.

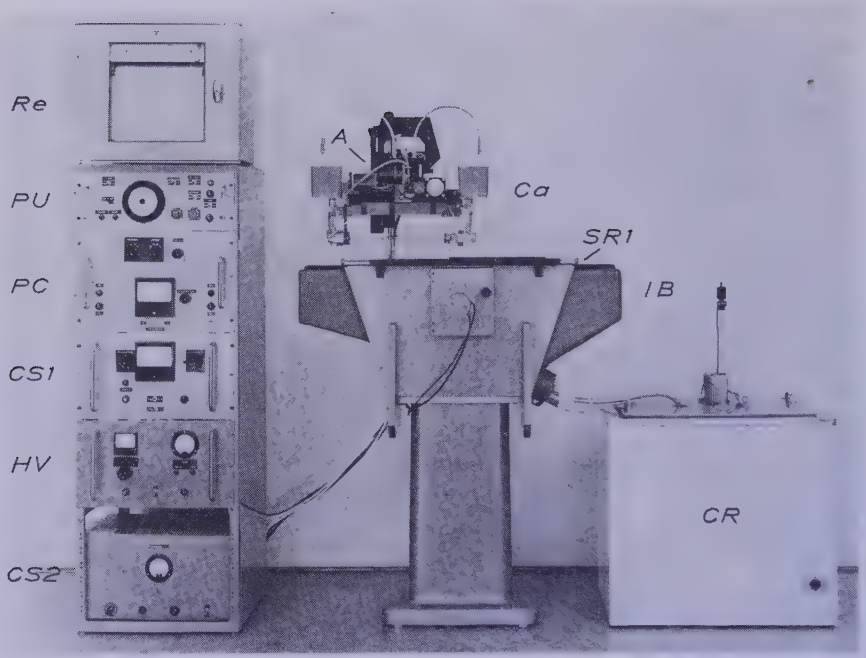

Fig. 7. Photograph of the complete free zone electrophoresis equipment (cf. Fig. 6). Ca: carriage with electrophoresis tube and electrode vessels; A: carriage-positioning arm; IB: immersion bath; SR1: steel rod on which the carriage Ca rides during the scanning maneuver (the other steel rod, SR2, is obscured by SR1); CR: cooling reservoir; CS2: current stabilizer for the hydrogen lamp; HV: high voltage source for the electrophoresis tube; CS1: current stabilizer for the electrophoresis tube; PC: pulse comparator for measuring UV-transmission of zones in the electrophoresis tube; PU: programing unit; Re: recorder.

The electrode vessels and the horizontal, revolving electrophoresis tube are mounted on a carriage. To achieve efficient dissipation of the joule heat, the electrophoresis tube is immersed in a water bath. At predetermined time intervals the carriage moves horizontally, transporting the electrophoresis tube past a stationary beam of UV-light. This permits photoelectric recording of light-absorbing zones. Referring to Fig. 6, I shall now outline briefly the construction of the equipment. A more complete description is given in the following sections. The quartz electrophoresis tube ET is rotated slowly (40 rev./min) during the introduction of the sample and throughout the run by means of belt Be driven by motor SM1. The buffer in the electrophoresis tube is connected to the buffer in electrode vessels EV1 and EV2 through arms CA1 and CA2. The short gel plug GP (Fig. 8) permits passage of the electric current but prevents hydrodynamic streaming through the electrophoresis tube. Consequently, a zone will not be washed

out of the tube even when the liquid levels in the electrode vessels are different. The sample is introduced into the revolving tube through hole Ho2 (Fig. 8) by means of a capillary syringe. To introduce the sample, the carriage Ca bearing the electrophoresis tube and the electrode vessels is raised out of the immersion bath IB containing circulating cooling water. The carriage Ca is mounted on wheels so that it can be moved back and forth smoothly on the steel rods SR1 and SR2 by the motor SM2. When during such a carriage movement a UV-absorbing zone in the tube passes through the light beam UV from a hydrogen lamp H (Fig. 9), the current from the photo multiplier PM is reduced, thereby producing a peak on the chart of a recorder. Such scans are made automatically at preset time intervals. When a conventional scanning system was tried with the free zone electrophoresis equipment, the baseline was very irregular [14]. Therefore, a scanning arrangement based upon a new principle was devised. This device and all the other different units of the equipment are described in some detail below. A photograph of the entire equipment is shown in Fig. 7.

B. The Separate Units

B:1. The Carriage Bearing the Electrophoresis Tube and the Electrode Vessels

a. General Description

The carriage Ca is built around a brass rod BR (Fig. 6; cf. Figs. 7 and 13*a*) The electrode vessels EV1 and EV2 are placed at its ends and the synchronous motors SM1 and SM2 are mounted on top of it. The motor SM1 is geared to rotate the electrophoresis tube ET at 40 rev./min. The reduction gears of motor SM2 are chosen such that pinion PG, which is friction-coupled to its axis, rotates at 5 rev./min. This drives the carriage at 20 cm/min along the steel rods SR1 and SR2. The motor SM2 is mounted such that its weight is supported by the rack Ra. The motor is surrounded by a soft iron shield which prevents the magnetic field of the motor from affecting the amplification of the photo multiplier PM. The additional weight that the iron shield represents increases the pressure of the pinion PG on the rack Ra. This smooths the movement of the carriage on the steel rods SR1 and SR2. To move the carriage manually the motor SM2 with the pinion PG are disengaged from the rack Ra by turning the knob Kn. This lifts the drive unit off the rack by means of an eccentric cam.

b. Leakage-Free Sealing of the Electrophoresis Tube

The milliammeter connected in series with the electrodes E1 and E2 (Fig. 6) will provide a correct measure of the current in the electrophoresis tube

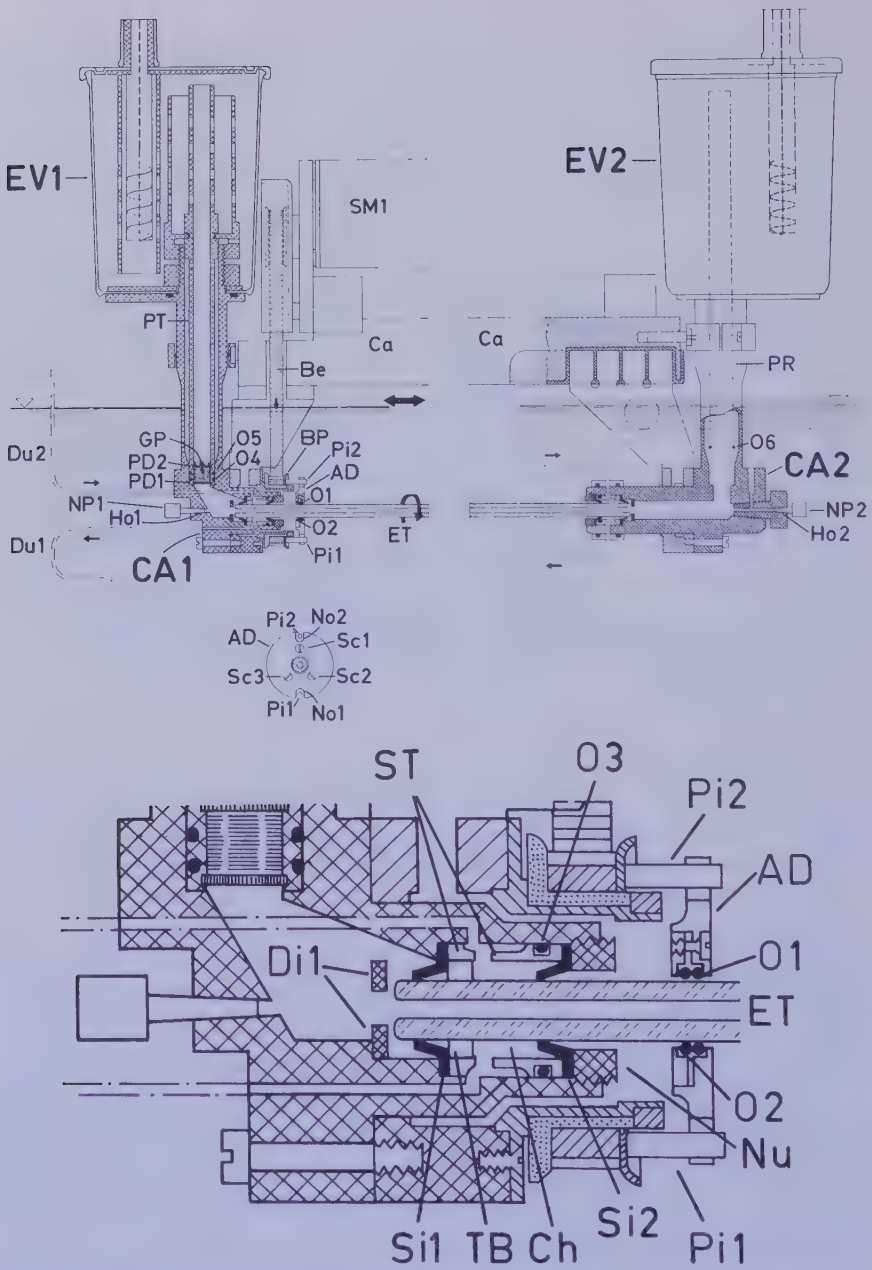

Fig. 8. Electrode vessels (EV1 and EV2) with connecting arms (CA1 and CA2) showing bearing, seals and drive coupling for the electrophoresis tube ET. Ca: carriage; SM1: synchronous motor; Be: cogged belt; BP: cogged belt pulley; PD1, PD2: porous polyethylene discs confining gel plug GP in plexiglass tube PT; NP1, NP2: nylon plugs for holes Ho1 and Ho2; 01, 02, 03, 04, 05, 06: O-rings; Du2: duct through which dry

only if there is no leakage of current into the cooling water. Considerable leakage of current can occur if the seals in which the electrophoresis tube rotates are not tight. Therefore, many different sealing arrangements were tested. The one illustrated in Fig. 8 works very well. To simplify the discussion I will refer only to the arrangement at the left end of the tube; the arrangement at the right end is similar. The plexiglass disc Di1 and its partner at the other end of the tube prevent the tube from moving longitudinally. The tube rotates in a teflon bearing TB, which is force-fitted inside the spacer tube ST, made of plexiglass. The two Simrit rings[g] Si1 and Si2 comprise the seal. Provided that the chamber Ch, bounded by these rings, is filled with dry air and that the quartz tube ET is perfectly circular along its contact surface with the Simrit rings, no current leakage occurs. If the chamber Ch contains moist air a water film can form by condensation when the electrophoresis tube is cooled to the temperature of the immersion bath (IB in Figs. 6 and 7). The formation of such a water film will cause a high leakage of current. Sometimes leakage begins suddenly during a run even if the chamber Ch has contained dry air at the start of the electrophoresis. This is due to saturation of the air in the chamber by water vapor arising from the water film that exists between the quartz tube and the Simrit ring. To avoid this source of leakage the chambers at both ends of the tube are flushed continuously with dry air during each run by means of a peristaltic pump attached to the carriage Ca. The air intake of the pump is a glass tube filled with silica gel.

c. The Coupling between the Belt Pulley and the Electrophoresis Tube

The belt pulley BP is connected to electrophoresis tube ET in the manner shown in Fig. 8 (cf. Figs. 6, 7 and 9). The aluminium disc AD is friction-coupled to the tube by two 0-rings 01 and 02 (the ring pressure can be regulated by the screws Sc1, Sc2, and Sc3). The disc AD is connected to the pulley by two pins, Pi1 and Pi2, which fit into the notches No1 and No2

[g] The Simrit rings are manufactured by C. Freudenberg, Simrit-Werke, Weinheim, Germany.

air is supplied to chamber Ch; Du1: air outlet duct; PR: plexiglass rod; Di1: perforated plexiglass disc for fixing longitudinal position of electrophoresis tube ET; AD: aluminium disc with notches No1 and No2 for the drive pins Pi1 and Pi2; Sc1, Sc2, Sc3: stainless steel screws; Si1, Si2: Simrit rings; ST: spacer tube of plexiglass; TB: teflon bearing; Nu: nut.

of the disc. The diameter of the pins is a few tenths of a mm less than the width of the notches. This "loose" coupling of the belt pulley BP to the electrophoresis tube ET is important for many reasons.

B:2. The Quartz Electrophoresis Tube

The scanning system is so constructed that at maximum amplification 15 % absorption (the ratio between the 280 mμ pulse and the 313 mμ pulse is then 0.85) corresponds to full scale deflection (25 cm) of the recorder pen. To utilize this high sensitivity, electrophoresis tube ET (Fig. 9), made of quartz to transmit UV-light, must be of high optical quality; otherwise the recorded baseline will be too irregular to allow good peak definition. Ideally, the tube should be perfectly straight and should have the same wall thickness and cross-sectional area throughout its length. Commercially available quartz tubes are not usable. Therefore, we had to develop ourselves a method for making tubes with the required tolerances. The high quality of these quartz tubes is demonstrated by the fact that they provide a baseline which is stable enough to permit detection of a peak corresponding to only 0.04 % absorption (99.6 % transmission). See, for example, the second fastest migrating zone in Fig. 31*a*. It is beyond the scope of this monograph to describe our method for making such quartz tubes, especially since the method is still under development. It will be described elsewhere at some future time. A $3 \times 7.8 \times 360$ mm quartz tube was used for all the experiments described in this monograph.

B:3. The Carriage-Positioning Arm

The carriage can be attached to an arm A (Fig. 7) that can be raised and lowered in the vertical plane by means of a crank. With this device the carriage can be lifted off the steel rods SR1 and SR2 (Fig. 6). The device also allows the carriage to be rotated into a vertical position. This is required for calibrations and for the application of samples by the layering technique (see section C:3, p. 54 ff.).

B:4. The Cooling Reservoir and the Immersion Bath

The UV-transmission of the coolant (distilled water) inevitably decreases with time due to microbial growth, dust, and a constant release of UV-absorbing material from the surfaces in contact with the cooling water. To minimize such decreases in the UV-transmission a preservative (e.g. formaldehyde) was added to the water and a large (80 l), covered cooling reservoir made from stainless steel was used. Under these conditions the same cooling water could be used for several weeks.

The cooling water can be maintained to within 0.5° of any temperature between 0° and room temperature. As is pointed out in section B, p. 69 ff. precise thermostating is not required.

Water from the cooling reservoir CR (Fig. 7) is pumped into the immersion bath IB via the inlet I (Fig. 6). From a horizontal row of over-flow outlets Ou at the top of this bath, the water is returned to the cooling reservoir through outlet O. The outlet is connected to a tight filter of cotton cloth which removes dust, etc., from the cooling water.

The optical parts of the scanning system (hydrogen lamp H; lenses L1 and L2; filter cuvettes C1 and C2; mirror Mi; motor SM with the cuvettes C3 and C4; aperture plate AP; quartz windows W1, W2, W3 and W4; and filter F) and photo multiplier PM are attached to the walls of the immersion bath (Figs. 9 and 6).

B:5. The Scanning Device

a. The Need for a Scanning Device

Valuable information regarding the special experimental conditions required for high resolution in the free zone electrophoresis technique was obtained in the earliest runs, which also indicated the limitations of the method. As predicted, dilute zones could be stabilized better than concentrated ones (see section A, p. 91 ff.). Furthermore, I soon discovered that rotation could not provide satisfactory zone stabilization in tubes larger than about 3 mm in inner diameter (see section A, p. 91 ff.). Since stabilization could thus be achieved only with very dilute zones and in cells of short optical path, zones could not be detected visually unless the substances were intensely colored. However, most materials of biological origin are colorless. Therefore, a technique for the detection of such substances was required. One approach to the problem of localizing non-visible zones involved serial withdrawal of 1-cm fractions from the revolving electrophoresis tube (see section B, p. 93 ff.). Each fraction was then analyzed by some appropriate means, such as the ninhydrin or the Folin reaction. Unfortunately, the withdrawal could not be done accurately enough to allow more than approximate determinations of mobilities. Furthermore, the chemical analyses were not sensitive enough to provide reliable patterns with complex mixtures such as serum. Although the development of better withdrawal techniques and more sensitive analytical methods might eliminate these problems, any procedure that involves withdrawal has the inherent serious disadvantage that the run cannot be resumed. Therefore, I directed my attention to the development of a sensitive scanning device that could be used to follow the migration of zones without interrupting or disturbing the run.

b. The Earliest Version of the Scanning Device

b:1. *The Principle*

The first version of the scanning system was built according to the principles of conventional photometry. It consisted of a hydrogen lamp as the source of ultraviolet light, a filter for the isolation of the wavelength desired, and a photo multiplier connected to a recorder [14]. These units (the recorder excepted) were mounted on a slide which was moved by a motor along the electrophoresis tube. When a UV-absorbing zone in the tube was encountered by the light beam from the hydrogen lamp, a peak was recorded on the chart.

b:2. *The Disadvantages*

Although many useful experiments were performed with this scanning arrangement it was extremely difficult to handle and did not give reproducible results for the following reasons.

(1) The two pairs of long quartz windows present in the cooling mantle had to be very clean throughout the run. They had to be removed and washed before each run.

(2) Any air bubbles that formed on the outer surface of the electrophoresis tube during a run could not be removed easily. Such bubbles produced irregularities in the baseline on the recorder chart.

(3) Vibrations in the hydrogen lamp and the photo multiplier that occurred during scanning also contributed to an uneven baseline.

(4) The open structure of the scanning system made it very sensitive to stray light. Therefore, the experiments had to be done in a room with very weak illumination.

(5) Variations in the intensity of the hydrogen lamp, defects in the quartz tube, and dirt on its surfaces also caused an irregular baseline.

c. The New Version of the Scanning Device

c:1. *The Principle and Its Advantages*

Problems (1)–(4) were eliminated by moving the electrophoresis unit instead of the detection system. Problem (5) was solved by the use of a new and unique ratio-recording arrangement (see section c:4, p. 45 ff.). In the present equipment only small quartz windows are required and these need not even be perfectly clean. Unlike the original, more conventional arrangement, the new scanning system has the advantage that the straightness of the baseline is not affected by transmission changes that occur in the quartz windows in the intervals between scans. The new scanning system is described more in detail below.

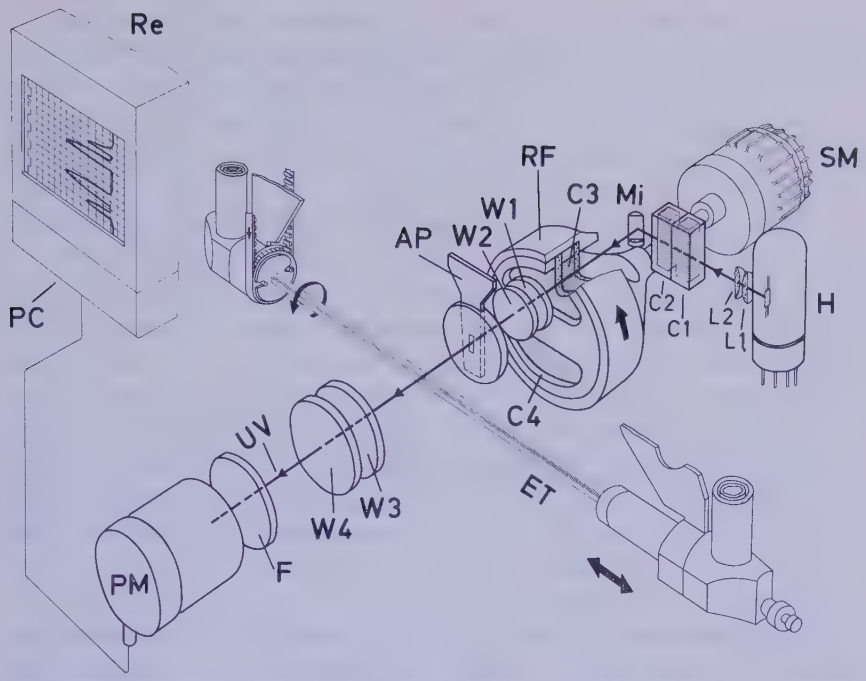

Fig. 9. Optics of the scanning system. H: hydrogen lamp (arc current 0.5A; filament voltage 4V); L1, L2: quartz lenses; C1, C2: quartz cuvettes for filter solutions; Mi: mirror; SM: synchronous motor; RF: rotating filter with quartz cuvettes C3 and C4; W1, W2, W3, W4: quartz windows; AP: aperture plate; ET: electrophoresis tube; UV: ultraviolet scanning beam; F: quartz blocking filter (UG5) for absorption of visible portion of spectrum; PM: photo multiplier; PC: pulse comparator; Re: recorder. The synchronous motor SM drives the dual filter RF which chops the scanning beam. The transmission characteristics of the filter F and the solutions in C1, C2, C3 and C4 are such that the wavelengths of the flashes are centered around 280 (or 260) and 313 mμ (see Fig. 10).

c:2. *The Optics*

1. *General Description.* The UV-light from the hydrogen lamp H (Fig. 9) is collimated by quartz lenses L1 and L2. The parallel beam then passes through a cuvette C1 containing nickel sulfate and a cuvette C2 containing ethylenediaminetetraacetic acid. These and other filters are described in the following sections. The filtered light beam is deflected 90° by an aluminized mirror Mi and is chopped by a rotating liquid filter RF consisting of two compartments, C3 and C4. One compartment contains potassium chromate and the other contains gentisic acid or 2.7-dimethyl-diaza-3.6-cycloheptadien-1.6-perchlorate. The light enters the immersion bath IB (Fig. 6) through the two quartz plates W1 and W2 (Fig. 9), passes through

the electrophoresis tube ET, leaves the immersion bath through the two quartz plates W3 and W4, and strikes the photo multiplier PM. The photo multiplier is protected from the influence of wavelengths in the visible part of spectrum by a UG5 filter. The spaces between the quartz windows W1 and W2 and between W3 and W4 are flushed with dry air to prevent the condensation of water vapor on the windows.

2. *The Light Filter Units.* Interference filters with a narrow band width and a high transmission in the ultraviolet region of the spectrum are not commercially available. The preparation of such filters has been reported [15], but no details of the procedure are given. Therefore, I have used liquid filters, which, unfortunately, usually are less stable to ultraviolet irradiation. To decrease instability arising from microbial growth, all the solutions should contain chloroform or some other non-UV-absorbing preservative.

Many substances of biological origin have absorption maxima at 260 mμ or 280 mμ. Therefore only filter combinations with peak transmission near these wavelengths and 313 mμ—the reference wavelength—will be described. The filter combinations consist of the following units (see Fig. 10).

(a) Nickel sulfate dissolved in water [16].

(b) UG5, a 3 mm thick quartz filter manufactured by Jenaer Glaswerk, Schott und Gen., Mainz, Germany. The filters (a) and (b) have a high UV-transmission and when used in series they virtually eliminate all wavelengths above 360 mμ.

(c) Gentisic acid dissolved in 0.01 *M* hydrochloric acid. Although the isolation of wavelengths around 280 mμ is often required for photometry of biochemical substances, (e.g., proteins) no convenient liquid filters for this purpose seem to have been described. Therefore, many likely substances were tested. Of these, gentisic acid proved to have the most satisfactory transmission characteristics.

(d) 2.7-Dimethyl-diaza-3.6-cycloheptadien-1.6-perchlorate dissolved in water [16, 17]. This solution has a transmission maximum at 260 mμ and is, when combined with filters (a) and (b) particularly suitable for the detection of purines and pyrimidines and substances which contain these bases.

(e) Potassium chromate dissolved in water [16]. The peak wavelength of the light used for the reference flash (see section c:4, p. 45 ff.) should be fairly close to the wavelengths that are absorbed by the substances to be detected. A chromate solution has a transmission maximum at 313 mμ, which is a very suitable reference wavelength for sample flashes around 280 mμ. Therefore, protein zones can be scanned conveniently by filling one compartment of the rotating filter (RF in Fig. 9) with solution (c) and the other with solution (e). Filter (e) has also been used in combination

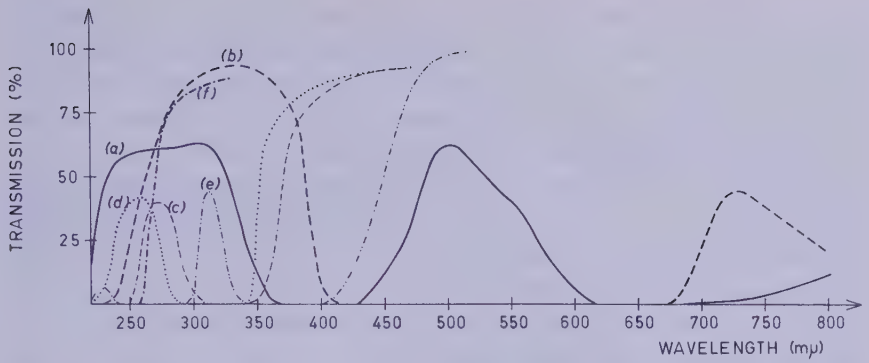

Fig. 10. Transmission characteristics of the optical filters. (a) Nickel sulfate solution; (b) a 3 mm thick quartz filter, UG5; (c) a solution of gentisic acid; (d) a solution of 2.7-dimethyl-diaza-3.6-cycloheptadien-1.6-perchlorate; (e) a solution of potassium chromate; (f) a solution of ethylenediaminetetraacetic acid. For the transmission of bands centered around 260, 280 and 313 mμ the combinations (a) + (b) + (d), (a) + (b) + (c) + (f) and (a) + (b) + (e) are used, respectively.

with filter (d); in this case, a shorter reference wavelength would be better, but I have not yet found any appropriate liquid filter that is sufficiently stable to ultraviolet radiation.

(f) Ethylenediaminetetraacetic acid (EDTA) dissolved in water [18]. The pH is adjusted to 6.8 with ammonia. The filter cuts off wavelengths below 275 mμ.

3. *Filter Combination for Samples with Absorption Maxima Near 280 mμ.* For detecting proteins and other substances that absorb strongly near 280 mμ, cuvette C1 (Fig. 9) is filled with solution (a), cuvette C2 is filled with (f), one side (e.g., C3) of the rotating filter RF is filled with (c) and the other side (C4) is filled with (e). The cathode of the photo multiplier PM is covered by a filter that absorbs most of the visible region of the spectrum. The filter (b) serves this purpose satisfactorily. When filter RF rotates, light flashes of wavelengths around 280 mμ (1, 3, 5 ... in Fig. 11) and 313 mμ (2, 4, 6 ... in Fig. 11) are obtained. When the electrophoresis tube contains only buffer (no sample), the 280-mμ flash should give a voltage pulse (S) only slightly lower than that given by the 313-mμ flash (R). To achieve this when a Philips 51 UVP photo multiplier (or one with the same spectral sensitivity) is used, the concentrations of the various filter solutions should be chosen such that the filters give transmission curves very similar to those shown in Fig. 10. If necessary, fine adjustments of the pulse heights can be made easily by changing the EDTA concentration in cuvette C2. An oscilloscope is very useful for following adjustments of the filter concentrations.

4. *Filter Combination for Samples with Absorption Maxima Near 260 mμ.* The filter units mentioned in the previous section are used, except that filter (c) is replaced by filter (d) and cuvette C2 is removed. Such a filter combination has a maximum transmission at 260 mμ and is therefore useful for detecting nucleic acids and their hydrolysis products, and viruses, and ribosomes. Since these materials also absorb rather strongly around 280 mμ they can often be detected even with the 280 mμ-filter combination. Therefore the latter combination can be used routinely for most biological substances.

5. *The Width of the Aperture.* The aperture plate AP (Fig. 9) gives the scanning beam a rectangular cross-section.

Irregularities in the quartz tube or poorly formed starting zones can cause distortions of the peaks in the electropherograms. The distortion is smaller when the scanning beam is wide, but increasing the width decreases the ability to resolve peaks that are very close together. Therefore, a compromise must be made. In most experiments we have used a 2 mm wide scanning beam. If the quartz tube is especially good optically the aperture can be reduced to 1 mm when the sample consists of low molecular weight substances, since small molecules diffuse rapidly to form well defined zones even if the sample is not applied uniformly.

6. *The Height of the Aperture.* If the scanning beam traverses only the central part of the electrophoresis tube an uneven zone can give recorder deflections that are strongly dependent on the angular coordinate ωt (ω = the angular velocity of the rotating electrophoresis tube; t = the time). In such cases, successive scans will not give identical patterns. To minimize this source of variation, the height of the scanning beam should not be smaller than the inner diameter of the electrophoresis tube. One must remember, however, that increases in the height of the beam decrease the sensitivity. In practice, the optimum height is determined empirically.

c:3. *The Photo Multiplier*

If the quartz tube is not perfectly straight the scanning beam (or part of it) will move up and down on the photo cathode with a periodicity determined by the rotational speed of the tube. Even if the number of photons striking the photo cathode does not change during such oscillations of the light spot, the motion of the spot will still cause alterations of the photo current because the sensitivity varies somewhat from point to point on a photo cathode. The result is a wavy baseline on the recorder chart. To get a smoother baseline an end window photo multiplier has been used (Philips 51 UVP). The particular photo multiplier used had been selected by the manufacturer for uniform sensitivity over the whole photo

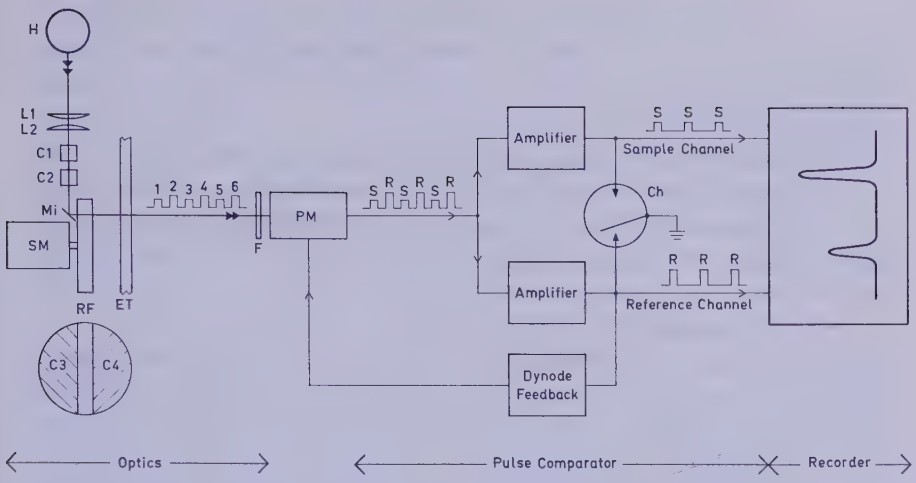

Fig. 11. Schematic diagram illustrating the operation of the ratio-recording arrangement (cf. Fig. 9). H: hydrogen lamp; L1, L2: quartz collimating lenses; C1, C2, C3, C4: cuvettes; Mi: mirror; SM: synchronous motor; RF: rotating filter; ET: electrophoresis tube; F: blocking filter (UG5) removing the visible part of spectrum; PM: photo multiplier; Ch: chopper; R: reference pulse, corresponding to the light flashes 2, 4, 6, ...; S: sample pulse, corresponding to the light flashes 1, 3, 5, ...

cathode surface. Since the "waviness" of the baseline depends on local variations in the sensitivity of the photo cathode one can also reduce the amplitude of the "waves" by spreading the scanning beam (after passing the quartz tube) over a larger area of the photo cathode. However, with the photo multiplier selected, we have not found it necessary to utilize this expedient.

c : 4. *The Ratio Recording System*

1. *The Principle.* As seen in Fig. 11 (cf. Fig. 9), the scanning beam passes through a rotating filter RF. The light striking the photo multiplier PM thus consists of a series of flashes. The quartz filter F and the solutions in the cuvettes C1, C2, C3, C4 are assumed to have transmission characteristics such that the wavelengths of two successive flashes are centered around 280 and 313 mμ, respectively. If we assume that flashes 1, 3, 5, ... consist of the 280-mμ light, the other flashes (2, 4, 6, ...) are 313-mμ light. The corresponding voltage pulses from the photo multiplier are identified by the letters S (sample) and R (reference). As the filter RF is rotated by a synchronous motor SM, the chopper Ch diverts the reference pulses to ground during one half of a cycle and the sample pulses to ground during the other half. Thus, one of the channels of the recorder is fed only reference

pulses and the other channel only sample pulses. The recorder is connected such that its deflection is linearly related to the ratio of the pulse heights (h_{280}/h_{313}). By a dynode feedback system the height of the reference pulse is kept constant.

Most substances of biological origin absorb at 280 mμ but not at 313 mμ. Thus the change in the ratio h_{280}/h_{313} produced by a zone of such a substance is due only to changes in h_{280}: the deflection of the recorder pen is proportional to the transmission at 280 mμ. For filter combinations that give the ratio h_{260}/h_{313} see section 4, p. 44 ff.

2. *The Advantages.* The main advantage of the ratio recording is that the recorder pen is not deflected when h_{280} (or h_{260}) and h_{313} are changed in the same proportions. Therefore, variations in the voltage across the hydrogen lamp, irregularities in the quartz tube, dirt on its surface, dust in the cooling water and the buffer, etc., usually have very little effect on the stability of the recorder baseline. Since reflection, refraction, scattering, and absorption depend on the wavelength of the light, the wavelength of the reference flash must be close to the wavelength of the sample flash (but not so close that the sample absorbs the reference wavelength) if one wishes to realize fully the benefits of ratio recording as regards baseline stability.

c:5. *The Pulse Comparator*

This unit (see Figs. 7 and 11) was constructed according to the principles used in the electronic system of the Spectronic 505, a spectrophotometer manufactured by Bausch and Lomb, Rochester, New York. To meet our particular demands, some modifications were introduced. Since the sample concentration varies from one experiment to another the pulse comparator is equipped with four sensitivity ranges that provide full recorder pen deflections at 85, 75, 50 and 0 % transmission, or, more correctly at the ratios 0.85, 0.75, 0.50 and 0 respectively, between the heights of the 280 mμ (or 260 mμ) pulse and the 313 mμ pulse.

c:6. *The Recorder*

A 5 mV Philips potentiometer recorder, type PR 2210 A/21 was adapted to measure the ratio between the heights of the sample and reference pulses (see Figs. 7 and 11). This recorder was chosen chiefly because it is equipped with a very efficient damping system based on tachometer feedback. The balancing time for full scale deflections is 1 sec. The recorder chart has a width of 25 cm. The chart speeds are 2, 8, 15 and 60 cm/min. Determinations of mobilities are usually performed at the medium chart speeds. The highest speed is used for quantitative measurements in order to get larger peak areas, which allows more accurate planimetry (see section A:3, p. 79 ff.).

B:6. High Voltage Source with Stabilizer for the Electrode Current

For the supply of DC voltage to the electrodes (E1, E2 in Fig. 6) and for stabilization of the current through the electrophoresis tube we have used a regulator (Fig. 7) similar to that used in the Tiselius-Svensson moving boundary electrophoresis apparatus (manufactured by LKB-Produkter AB, Stockholm, Sweden). However, the maximum output voltage has been increased to 4500 volts (maximum current 100 mA). The leakage current (i.e., the current flowing to ground) can be read on a μA-meter.

B:7. Current Stabilizer for the Hydrogen Lamp

This unit (Fig. 7) was constructed according to the design described by Anker [19], with modifications which give a higher current strength (500 mA). Any current stabilizer can be employed, however, since the ratio recording system can compensate for relatively large variations in the intensity of the hydrogen lamp. Therefore, fluctuations of a few per cent in the arc current produce very little recorder response.

B:8. Automation Devices

a. Programing Unit for Scanning

A schematic wiring diagram for the programing unit (PU in Fig. 7) is shown in Fig. 12. The time interval between successive scans can be set on the timer T. When the mode selector switch S is at the "Aut" (automatic mode) position the recorder chart drive motor CM and the motor SM2 (Fig. 6) are restarted each time the preset period has elapsed, whereupon the carriage Ca (Fig. 6) bearing the electrophoresis tube moves from one end of the immersion bath to the other. Electrophoresis is interrupted for the duration of each such scanning maneuver, since the high voltage HV to the electrodes is switched off at the beginning of each scanning traverse by the relay HVR. When the carriage reaches the end of its traverse the switch M1 (or M2) is depressed, stopping the motor SM2 and the recorder chart drive motor CM, and the high voltage HV to the electrodes is switched back on.

The carriage remains at the end position until the time set on the timer has elapsed, whereupon it makes a traverse back to the other end of the bath. The scanning maneuver is repeated at the preset time interval as long as the run is allowed to proceed. The operation is fully automated: after the sample has been introduced into the electrophoresis tube and the experiment has been started, the equipment requires no further attention until the run is completed.

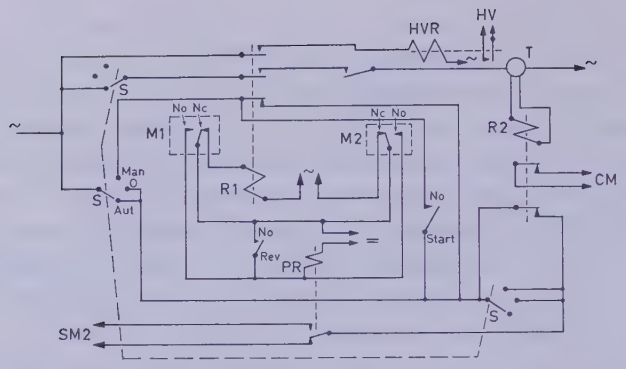

Fig 12. Wiring diagram of the programing unit. R1, R2: relays; PR: pulse relay; HVR: high voltage relay; HV: high voltage to the electrodes; M1, M2: microswitches (No, normally opened; Nc, normally closed) placed at the left and right ends, respectively, of the immersion bath (IB in Figs. 6 and 7); S: selector switch; T: timer (0–13 min); SM2: synchronous motor (see Fig. 6); CM: recorder chart motor. The positions of the switches and the relays in the diagram correspond to the phase in which the carriage Ca (Fig. 6) is moving.

When the mode switch S is set at the "0" position, the carriage moves back and forth continually. The carriage can be started manually by pressing the "Start" button when the mode switch is set at "Man" (manual).

The direction of movement of the carriage can be reversed by reversing the motor SM2. In practice, this is done by pressing the "Rev" (reverse) button.

b. Zone-Position Indicator Unit

Distances of migration are determined simply and precisely by the use of a self-calibrating distance scale that is automatically inscribed along one margin of the record during each scanning maneuver. The construction of the scale-marking unit ensures that each segment of the crenellated distance scale (Sc in Figs. 13*a* and 13*b*) always represents a distance of exactly 1 cm along the electrophoresis tube, whatever chart speed or scanning speed is used.[h]

The design of the scale-marking arrangement is illustrated in Fig. 13*a*. An aluminium plate SP containing a series of rectangular openings Op is attached to the movable carriage Ca bearing the electrophoresis tube ET. The length, a_2, of each opening and the distance, a_1, between consecutive openings is 1.00 cm. A photo transistor PT and a tungsten lamp TL are mounted on the rear wall of the support frame SF in such a way that the perforated plate is interposed between them when the carriage is in the

[h] The scale Sc is visible in many of the recordings presented in this monograph.

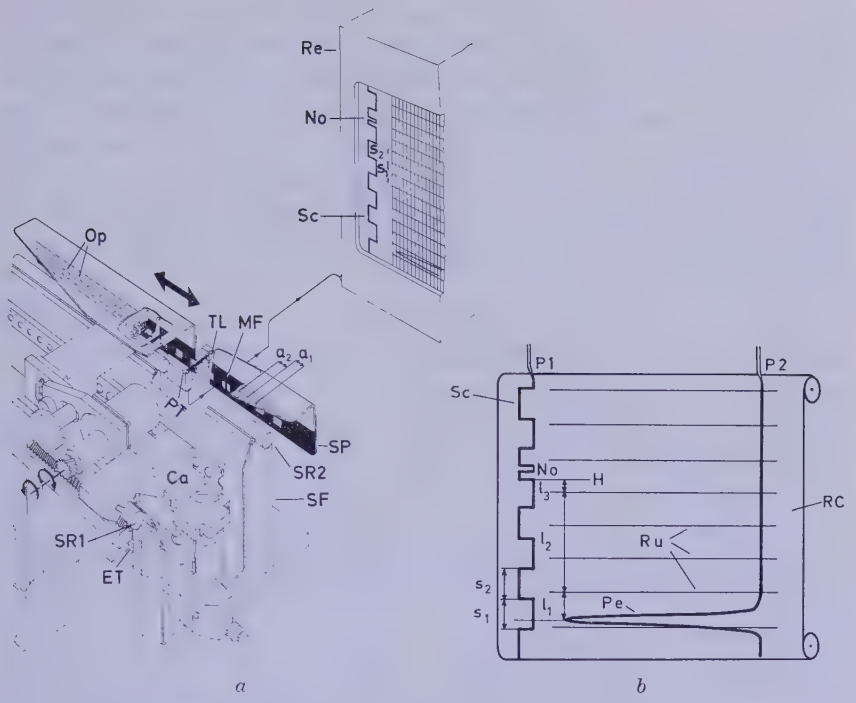

Fig 13a. Zone position indicator unit. SP: shutter plate attached to the carriage Ca, bearing electrophoresis tube and electrode vessels; Op: rectangular openings; MF: metal foil; TL: tungsten lamp; PT: photo transistor connected to the event marker of recorder Re; SF: support frame (cf. Fig. 6); SR1, SR2: steel rods (cf. Fig. 6); ET: electrophoresis tube (cf. Fig. 6). When the carriage Ca moves laterally the photo transistor is exposed alternately to light and dark, thereby producing the distance scale Sc, in which the distances s_1 and s_2 represent the distances a_1 (1.00 cm) and a_2 (1.00 cm) along the plate SP (or the revolving electrophoresis tube ET); the extra notch No is produced by the metal foil MF.

Fig. 13b. Determination of the position and distance of migration of a zone by means of the distance scale Sc (for details see section b, p. 48 ff.; see also Fig. 13*a*). RC: recorder chart with rulings Ru (spacing 1.00 cm); P1: event-marker pen, producing distance scale Sc; P2: UV-transmission recording pen; Pe: recorded peak, corresponding to a zone in the electrophoresis tube; s_1 and s_2: segments corresponding to distances of 1.00 cm along the electrophoresis tube; No: reference notch used to identify index line H.

operating position (e.g., resting on the steel rods SR1 and SR2). When the carriage makes a scanning traverse the perforated plate acts as a multiple shutter for the narrow collimated beam from the tungsten lamp, exposing the photo transistor alternately to equal periods of light and dark. The photo transistor is connected to the solenoid-operated event-marking

unit of the recorder. The trace Sc representing the alternating light and dark conditions of the photo transistor is thus a distance scale wherein the distances s_1 and s_2 represent the distances a_1 and a_2 (1.00 cm), respectively.

One of the openings in the shutter plate is divided into two unequal sections by a narrow strip MF of aluminium foil. (In Fig. 13*a* the left hand section is the shorter.) This strip produces an extra notch (No in Figs. 13*a* and 13*b*) in the otherwise regular distance scale. The stroke H (Fig. 13*b*) closest to this reference notch is always used as the index of the distance scale.

Obviously, the stroke H is made when the beam from the distance marker lamp encounters the edge on the left section of the masked opening in the shutter plate. Since the slit for the distance marker beam is positioned exactly above the slit for the scanning beam, the position in the electrophoresis tube represented by the index stroke H is that at which a vertical plane containing the above-mentioned edge cuts the electrophoresis tube at a right angle. If the electrophoresis tube contained a zone at this position, the corresponding peak in the recorder chart would appear directly opposite the stroke H: there is no offset between the distance scale and the scanning trace.

It is neither necessary nor desirable to make an index mark on the quartz electrophoresis tube itself. Instead, provision has been made for attaching a centimeter scale to the carriage directly above the electrophoresis tube. The scale is attached in such a way that its zero-line is at the position defined by the above-mentioned index plane. With the scale in place to guide the operation, any zone recorded on the chart can be withdrawn from the electrophoresis tube (cf. section B, p. 93 ff.). For example, the peak Pe in Fig. 13*b* is 4.7 segments away from the index stroke H of the distance scale. In the electrophoresis tube, the zone corresponding to the recorder peak Pe would be found 4.7 cm to the left of the zero-line of the attached centimeter scale.

The points discussed in the last two paragraphs regarding the means by which zones recorded on the chart are located in the electrophoresis tube are important only in cases where one wishes to withdraw particular zones for further analysis. By the use of the inscribed distance scale, mobilities can be calculated in a simple way from chart records obtained at different times during a run without reference to the electrophoresis tube itself.

The measurements and calculations involved in the determination of accurate mobility values are described in detail in section d, p. 87 ff.

II:3 *Experimental Procedure*

A. Coating the Electrophoresis Tube with Methyl Cellulose to Eliminate Electroendosmosis

A:1. The Coating Solution

Methyl cellulose (0.4 g) is dissolved in 100 ml distilled water.[i] Formic acid (7 ml) and then formaldehyde (35 ml) are added, with stirring. This solution can be used repeatedly for at least six months if stored in a refrigerator.

A:2. The Coating Procedure

The quartz tube is washed thoroughly in a detergent solution with the aid of pipe-cleaner and is then rinsed alternately with hot and cold tap water. Before drying, the tube is rinsed with distilled water. The methyl cellulose solution is drawn into the clean, dry tube by suction. After 5 min, the methyl cellulose solution is allowed to run out slowly, leaving a thin film of uniform thickness on the tube wall. After draining for 5 min the tube is placed in an oven at 120° for 40 min. A second treatment with methyl cellulose is recommended. Throughout the coating procedure it is important that air bubbles do not adhere to the tube wall and that the quartz tube is kept in a vertical position. Otherwise, the coating may be uneven.

Formaldehyde is known to cross-link methyl cellulose at elevated temperatures, thereby reducing its solubility in water.[j] Such cross-linked coatings can be used for many experiments over several days. The condition of the coating can be determined by electrophoresis of a dye such as naphtol green. If the dye forms a parabolic zone, electroendosmosis is operative (see section B, p. 56 ff.) and the coating should therefore be renewed. Such tests should be performed at low current strengths to ensure that zone deformation is not caused by excessive heating (see section A, p. 64 ff.).

B. Preparation of the Gel Plug (GP in Fig. 8)

To prevent hydrodynamic streaming of buffer through the electrophoresis tube from one electrode vessel to the other the tube PT (Fig. 8) contains a gel plug GP immobilized between two porous polyethylene discs PD1

[i] A methyl cellulose with a molecular weight of about 200,000 and a degree of substitution of 1.64–1.92 has been used. This product can be obtained from the Dow Chemical Company, Midland, Michigan, U.S.A., under the trade name Methocel MC, visc. 7000 cps.

[j] The author is much indebted to Dr. Rolf Mosbach for his advice to cross-link the methyl cellulose.

and PD2.[k] The tube PT is made from plexiglass and has, consequently, a hydrophobic surface. Since the gel plug has to be hydrophilic, it must be soft in order to adhere firmly to the wall of the tube. A polyacrylamide gel of a total concentration $T = 5\,\%$ (w/v) and a cross-linking concentration $C = 3\,\%$ (w/w) has proved to be suitable for this purpose. For a more precise definition of the parameters T and C, see ref. 20. Since the procedure for the preparation of polyacrylamide gels is described in detail in that reference only a short description is required here. The monomers (2.43 g acrylamide and 0.075 g N,N′-methylenebisacrylamide), the initiator (0.1 g ammonium persulfate) and the accelerator (0.1 ml β-dimethylaminopropionitrile) are dissolved in 50 ml of the buffer (thoroughly deaerated) to be used for electrophoresis. The resulting solution is sucked up through the two porous polyethylene discs PD1 and PD2 to a level about one cm above PD2. After 10–30 min a gel will form. The unpolymerized top layer is rinsed away with buffer. Excess ammonium persulfate and charged UV-absorbing substances are easily removed from the gel plug by electrophoresis before application of the sample [21]. The buffer in the gel plug can also be changed electrophoretically, allowing the same plug to be used repeatedly for several months in many different buffers. The discs PD1 and PD2, which are tightly pressed into slots in the tube PT, are renewed whenever a new gel plug is prepared.

Some of the initiator molecules might be polymerized into the polyacrylamide matrix by a chain transfer process [22, 23]. Therefore, in order to avoid electroendosmosis in the gel plug GP, one probably ought to use an uncharged initiator, such as hydrogen peroxide, instead of the charged persulfate ion. In our experience, however, either of these initiators provides gels in which neutral reference substances, such as DNP-ethanolamine [24], do not migrate upon the application of an electric field, indicating the absence of electroendosmosis.

Instead of a gel plug, one can use reversible electrodes as is done in the Tiselius moving boundary electrophoresis apparatus [1]. Since the gel plug arrangement described above is easier to handle, it was used in all the experiments described in this monograph.

C. Application of the Sample

C:1. General

A starting zone can be applied either by injection or by layering. Before these two techniques are described separately, some general comments on them will be given. When the injection technique is employed the starting

[k] Available from Bel-Art Products, Pequannock, New Jersey, U.S.A.

Fig. 14. Microsyringe for the application of the sample. Ba: barrel (inner diameter: 0.5 mm); Pl: stainless steel plunger; Tu: polyethylene tubing; Pi: 10–20 μl constriction pipette made of glass (the inside diameter of the pipette orifice should be about 0.2 mm).

zone consists of small liquid elements that behave according to the mathematical relations derived in section B, p. 14 ff. When the layering technique is used, the starting zone fills the whole cross-section of the electrophoresis tube and there is, consequently, no (or only slight) tendency for convection. However, if a zone formed by the layering technique somehow becomes skewed during a run, part of the zone will begin to behave like an injected liquid element of large diameter. As mentioned in section e, p. 18 ff., such liquid elements move relatively rapidly toward the tube wall. To reduce the incidence of this undesirable phenomenon the concentrations of layered starting zones must, in general, be less than those allowed by the injection technique: the maximum starting zone concentrations are about 0.4 % and 1 %, respectively, in the case of proteins (cf. section A, p. 91 ff.). In practice, this does not limit the usefulness of the layering technique, since for a given sample concentration a layered zone absorbs more light than an injected one. This is due to the fact that an injected starting zone consists of small liquid elements surrounded by buffer. Obviously, such a zone has a shorter effective optical path than a layered one, wherein the concentration is uniform from wall to wall. The injection technique thus requires a higher sample concentration than the layering technique in order to produce a given recorder deflection in the scanning of the starting zone.

Samples are applied with the microsyringe illustrated in Fig. 14. The barrel Ba and the plunger Pl are of stainless steel. A 10–20 μl glass constriction pipette Pi is connected to the syringe barrel by a piece of polyethylene tubing Tu. This tubing also prevents the steel syringe-barrel from touching, and perhaps scratching, the inner wall of the rotating quartz tube during the introduction of the sample. If samples are applied by injection the orifice of the constriction pipette used should be very small in order to minimize convective disturbances, as discussed in section e, p. 18 ff. The risk of convective disturbances is greatest during the application of the sample and decreases quickly after the current is applied, particularly if the sample separates rapidly into several components (see section g, p. 23 ff.).

In cases where the sample solution contains foreign ions some precautions must be taken if accurate mobilities are desired, as discussed in section c, p. 86 ff.

C:2. Application by Injection

After filling the apparatus with buffer, one should remove any air bubbles that might be present in the quartz electrophoresis tube ET or in the connecting arm CA1 (Fig. 6). The tube PT containing the gel plug GP is then inserted (Fig. 8). To achieve temperature equilibration the electrophoresis tube ET (Fig. 6) is lowered into the immersion bath IB by cranking the carriage Ca down onto the steel rods SR1 and SR2. The motor SM1, that rotates the electrophoresis tube, is started. After about five min in the immersion bath the buffer in the electrophoresis tube has reached the temperature of the cooling water and the carriage Ca is cranked up. Then the nylon plug NP2 is removed and the plexiglass rod PR is inserted (Fig. 8). The sample is sucked up into the constriction pipette of the microsyringe (Fig. 14). The syringe is then inserted into the rotating electrophoresis tube through the hole Ho2 and the sample is pressed out by a slow motion of the plunger. The syringe is withdrawn slowly, the plexiglass rod PR is removed and the nylon plug NP2 is inserted. Immediately, the carriage Ca is cranked down onto the steel rods SR1 and SR2. At this stage it is very important that the buffer has about the same temperature as the cooling water. Otherwise there is a risk that the starting zone will be deformed by volume changes in the buffer in the quartz tube or in the chamber below the gel plug GP.

This application technique, as well as that described below, should be practiced with colored substances, e.g. pH indicators.

C:3. Application by Layering

A snug-fitting 1 mm thick disc of porous hydrophilic linear polyethylene[k] is pressed into the methyl cellulose-treated quartz tube to the level at which one wishes to apply the sample. Owing to the high electrical resistance of such a disc and the consequently great heat generation air bubbles can form in the disc during a run, particularly when the voltage gradient is steep. However, this problem can be avoided by using a gel plug of cross-linked polyacrylamide instead of the polyethylene disc. The gel plug is prepared as described in section B, p. 51 ff. When a gel plug is used a pre-run must be done to remove UV-absorbing material [21]. When the buffer in the electrophoresis apparatus has come to temperature equilibrium with the cooling water as described above, the apparatus is cranked up out of the immersion bath and is turned from the horizontal to a vertical position. With the orifice of the constriction pipette just above the polyethylene

[k] See footnote [k], p. 52.

disc (or the polyacrylamide plug) the sample is pressed out slowly.[1] The motor SM1 (Fig. 6) is then started. The carriage is rotated back to the horizontal position and is cranked down onto the steel rods SR1 and SR2.

It is relatively easy to create even starting zones by the layering technique, while the injection technique requires considerable practice. However, as a layering support must be used in the former method, the latter is generally preferred.

D. Condensed Instructions for the Performance of a Run

An over-all outline of the procedures involved in performing a typical run with the free zone electrophoresis apparatus is given below. For details regarding the different units of the apparatus and the various manipulations mentioned in this brief description the reader is referred to the preceding sections.

First, the buffer to be used is filtered to remove dust, etc., and is then de-aerated. The electrode vessels and the electrophoresis tube are carefully filled with the buffer and the peristaltic pump attached to the carriage Ca (Fig. 6) is started to flush the chambers Ch (Fig. 8) with dry air. The carriage is cranked down onto the steel rods SR1 and SR2 (Fig. 6) to immerse the electrophoresis tube in the bath IB for temperature equilibration. At this stage, one should check for current leakage (see section B:6, p. 47 ff.) using the same voltage as will be used in the run. A good seal allows no detectable current leakage. In no case should the leakage current exceed 1 per cent of the total current read on the milliammeter connected in series with the electrodes.

After applying the sample, two scans (one from left to right and the other *vice versa*) are made to determine the position of the starting zone. The high voltage to the electrodes is switched on during the second scan. The scan interval is then set on the timer T (Figs. 7 and 12): thereafter, the scans are performed automatically.

At the end of the electrophoresis run, zones can be recovered for further analyses, etc., as described in section B, p. 93 ff.

II:4. *Electroendosmosis*

A. General

The term electroendosmosis refers to the process by which immovable charges present on surfaces exposed to a conducting liquid (for instance

[1] The addition of foreign substances, such as sucrose, to the sample in order to increase the density difference between sample and buffer is often done in other types of zone electrophoresis to facilitate layering [21]. This expedient cannot be used here because of the convective disturbances that would result during the electrophoresis.

that in an electrophoresis channel) cause the liquid to move when an electric field is applied. In their discussion of the microscope technique for electrophoretic studies of particles, Brinton and Lauffer [25] state that "electroosmotic streaming of liquid past the cell walls cannot be eliminated or counteracted by any known method". This was the situation several years ago when I began to investigate the possibility of developing a free zone electrophoresis method in which zone stabilization would be provided by rotation. Although it did not take long to establish that convective disturbances could be virtually eliminated by rotation under conditions that were compatible with the performance of electrophoresis, I soon realized that this discovery could have no practical value unless disturbances arising from electroendosmotic effects could also be eliminated (see Fig. 17*a*).

A vigorous attack on the crucial problem of electroendosmosis led finally to the development of two effective methods, described in later sections, for the elimination of electroendosmotic disturbances. In the first method, electroendosmosis is not prevented, but the attendant reflow is cancelled by the application of a matching counterflow of liquid. The second method, which merely involves treating the walls of the electrophoresis tube with methyl cellulose, provides a simpler and more fundamental solution to the problem: the surface charges that cause electroendosmosis are screened or/ and their counter ions immobilized so that electroendosmosis does not occur at all. This method, treated in section E. p. 61 ff., has been used in all the experiments described in this monograph.

The same method for the preparation of electroendosmosis-free surfaces should be applicable in many other types of free electrophoresis, such as the microscope technique [25], flowing-film electrophoresis [9, 10], magnetically stabilized electrophoresis [26], and even the classical Tiselius moving boundary method [1]. In fact, I have already had some successful results with a micro-modification of the latter technique (see section B : 1, p. 82 ff.). It is probably the presence of electroendosmosis that has consistently frustrated previous attempts to develop a practical method for the performance of moving boundary electrophoresis on a micro scale.

B. Deformation of a Zone by Electroendosmosis

The electroendosmotic velocity $v_{eo,x}$ at the distance x from the wall of the quartz tube can be calculated from the following expression, derived by Helmholtz [27]

$$v_{eo,x} = \frac{ED}{4\pi\eta}(\zeta - \psi_x) \tag{51}$$

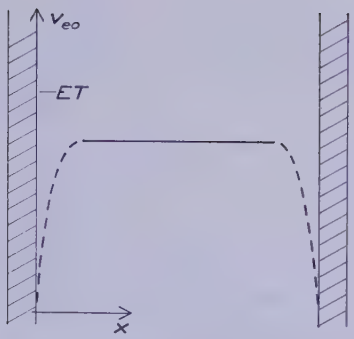

Fig. 15. The electroendosmotic velocity v_{eo} as a function of the distance (x) from the inner wall of the electrophoresis tube ET (eqn. (52)). The dashed part of the curve corresponds to a liquid film only 10–100 Å thick and can be neglected in practice (see Fig. 16*a*).

where

E is the strength of the electric field, produced by the voltage applied across the ends of the quartz tube,

D is the dielectric constant,

ψ_x is the potential at the distance x from the wall of the electrophoresis tube; (ψ_x arises exclusively from the surface charge of the quartz and has no connection with the applied voltage),

ζ is the potential ψ_x of the liquid layer that does not move relative to the wall of the quartz tube, and

η is the viscosity coefficient.

According to the Debye-Hückel theory, $\psi_x = \psi_0 \cdot e^{-\varkappa x}$, where $1/\varkappa =$ "the thickness" of the diffuse double layer [28]. Consequently,

$$v_{eo,x} = \frac{ED}{4\pi\eta}(\zeta - \psi_0 \cdot e^{-\varkappa x}) \tag{52}$$

This equation is represented diagramatically in Fig. 15 (the left half of the symmetrical curve). Since the "thickness" of the double layer is given by

$$\frac{1}{\varkappa} \sim \frac{3 \times 10^{-8}}{\sqrt{\text{ionic strength}}} \text{ [cm]}$$

(see ref. 29) and is thus an extremely small distance, the dashed part of the curve, which corresponds to the term $\psi_0 \cdot e^{-\varkappa x}$, can be neglected in practice. The bulk of the liquid in the tube thus moves at a constant speed $v_{eo,b}$ which is given by the relation [27]

$$v_{eo,b} = \frac{ED\zeta}{4\pi\eta} \tag{53}$$

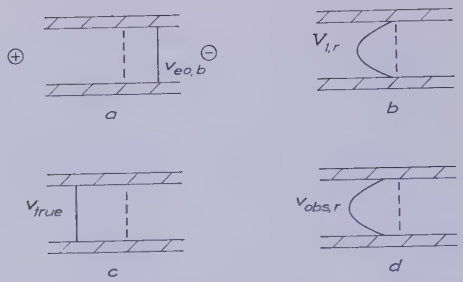

Fig. 16. The position and the shape of a zone as influenced by *a*) electroendosmosis only (eqn. (53)); the starting zone is indicated by a dashed line, *b*) hydrodynamic flow only (eqn. (54)), *c*) electrophoresis only [paragraph (a), p. 70], *d*) electroendosmosis, hydrodynamic reflow, and electrophoresis [the combined effect of a,)b), and c)]. The patterns are drawn for the case where the inner wall of the electrophoresis tube and the substance comprising the zone are negatively charged and the anode is at the left end of the tube. The notations $v_{eo,b}$, $V_{1,r}$, v_{true}, $v_{\text{obs},r}$ are defined in section C, p. 58 ff.

Consequently electroendosmosis itself only displaces a zone without affecting its shape (Fig. 16*a*). However, in most carrier-free electrophoresis methods, including free zone electrophoresis, a hydrodynamic return flow occurs. This return flow is described by the following equation [25], which applies to laminar streaming

$$V_r = \frac{P}{4\eta l}(R^2 - r^2) \tag{54}$$

where

V_r is the hydrodynamic velocity at the distance r from the axis of the tube,
P is the pressure drop between the ends of the tube,
R is the radius of the tube,
η is the viscosity coefficient, and
l is the length of the tube.

When this parabolic velocity distribution (Fig. 16*b*) is superimposed on the movements illustrated in Figs. 16*a* and 16*c*, the position and shape of the zone will be affected as shown in Fig. 16*d*. Efforts to avoid this ruinous consequence of electroendosmosis (see Fig. 17*a*) were directed along the lines discussed in the next sections.

C. Hydrodynamic Compensation of the Electroendosmotic Reflow

A continuous hydrodynamic flow can be applied in a direction opposite to that of the electroendosmotic reflow by means of a pump or a syringe connected to the hole Ho1 in Fig. 6. If the observed electrophoretic migra-

tion velocity of a zone at a distance r from the axis of the tube is $v_{\text{obs},r}$ and if, in the absence of electroendosmosis, the zone is assumed to migrate at a velocity v_{true} which is constant throughout the cross-section of the tube, the following relation holds:

$$v_{\text{obs},r} = v_{\text{true}} - v_{eo,b} + V_{1,r} - V_{2,r} \tag{55}$$

where $v_{eo,b}$, $V_{1,r}$, and $V_{2,r}$ are the velocities of the bulk electroendosmotic flow, the reflow, and the applied counterflow, respectively, at the distance r from the axis of the tube. The signs of the velocities in eqn. (55) apply for the directions of motion indicated in Figs. 16. Combining eqns. (54) and (55) we get:

$$v_{\text{obs},r} = v_{\text{true}} - v_{eo,b} + \frac{P_1}{4\eta l}(R^2 - r^2) - \frac{P_2}{4\eta l}(R^2 - r^2) \tag{56}$$

The zone in the electrophoresis tube will not be distorted if

$$\frac{\delta v_{\text{obs},r}}{\delta r} = 0$$

in which case

$$P_1 = P_2 \tag{57}$$

The condition represented by expression (57) can be maintained in a simple and direct fashion if a colored zone is present to guide the manipulations. Therefore, a colored substance is included in the sample, or, if that is objectionable, a colored zone is introduced into the revolving tube at some appropriate distance from the sample zone. The counterflow is then applied and maintained throughout the run at such a rate that the colored zone—and thereby, all the other zones present—retains its initial shape.

When condition (57) obtains, eqn. (56) is reduced to

$$v_{\text{true}} = v_{\text{obs}} + v_{eo,b} \tag{58}$$

The value of $v_{eo,b}$ can be calculated from the relation

$$v_{eo,b} = \frac{V'}{tq}$$

where q is the cross-sectional area of the electrophoresis tube and V' is the volume delivered by the syringe during the time t of the electrophoresis run.

If the colored zone used to indicate the rate at which the compensatory counterflow should be applied is an electrically neutral substance, e.g. DNP-ethanolamine [24], $v_{eo,b}$ is simply l/t, where l is the distance the neutral zone has been displaced; v_{true} can then be calculated from eqn. (58)

as before. If all distances are measured from the position of the neutral zone rather than from the original starting position, v_{true} can be calculated without evaluating $v_{eo,b}$. The mobility values reported in ref. 14 were determined in this way. The method described in this paragraph yields relative, rather than absolute mobility values, as all measurements or corrections are made with respect to a "neutral" substance whose electrophoretic mobility is presumed to be zero. However, the relative mobility values determined as described here with DNP-ethanolamine as the neutral reference substance agree well with the "absolute" values in all cases where comparisons have been made.

The main disadvantage of the hydrodynamic compensation method is that it requires constant attention throughout the electrophoresis run: the counterflow must be adjusted continually so that the colored zone remains undistorted. Some approaches that were explored in an attempt to find simpler methods for the elimination of electroendosmosis are described in the next two sections.

However, I should like to point out here that since the hydrodynamic compensation method allows accurate determinations of the electroendosmotic velocity, $v_{eo,b}$, free zone electrophoresis can be used to determine the ζ-potential of the inner surface of the revolving electrophoresis tube (see eqn. (53)).

D. Reduction of Electroendosmosis by Reducing the ζ-potential

Eqn. (53) shows that electroendosmosis would disappear if the ζ-potential were zero. Therefore the inner wall of the quartz tube was coated with plastics presumed to be electrically neutral. The following hydrophobic polymers were tried: methylsilicone (M 120 from Farbenfabriken Bayer Aktiengesellschaft, Leverkusen, Germany), phenylmethylsilicone (P 200, and P 850 from the same company), polyvinylacetal (Mowital B 30H from Farbwerke Hoechst AG., Frankfurt (M), Germany), polystyrene (L G from Badische Anilin- und Soda-Fabrik AG. (BASF), Ludwigshafen am Rhein, Germany), polyisobutylene (Oppanol B 200 from BASF), and polyamide (Ultramid 1C from BASF).

Of the materials mentioned, the first two were the most efficient in reducing electroendosmosis, but even these did not reduce it to acceptable levels. In order to determine whether these negative results might have reflected a failure of these hydrophobic polymers to adhere to quartz, homogeneous tubes of plexiglass, polystyrene, and polytetrafluoroethylene (Kel-F) were tested. However, all of these tubes also exhibited considerable electroendosmosis.

E. Reduction of Electroendosmosis by Increasing the Resistance to Flow in the Diffuse Double Layer

Helmholz' equation (eqn. 51) is based upon the assumption that the viscosity in the diffuse double layer at the tube wall is constant and equal to the value in the bulk of the solution. I shall now derive an expression for the case where the viscosity varies with the distance from the tube wall. Consider a cylindrical shell concentric with the long axis of the electrophoresis tube, which is assumed to be filled with buffer. This shell is presumed to lie in the diffuse double layer at a distance x from the tube wall and has a length a and a thickness Δx ($a <$ the length of the electrophoresis tube). As the shell is electrically charged, it will move when a voltage is applied across the electrophoresis tube. In the stationary state, the force exerted on the cylindrical shell by the electric field is equal to the frictional force that must be overcome to move the shell at constant speed. Accordingly

$$F(x+\Delta x) - F(x) = E \cdot \varrho_x \cdot a \cdot 2\pi(R-x)\Delta x \tag{59}$$

where

$$F(x) = \eta \cdot a \cdot 2\pi(R-x) \cdot \frac{dv_{eo,x}}{dx} \quad \text{and}$$

ϱ_x = volume charge density.

E, R, η, and $v_{eo,x}$ are defined in section B, p. 56 ff.

When Δx approaches zero eqn. (59) is transformed to

$$\frac{dF(x)}{dx} = E \cdot \varrho_x \cdot a \cdot 2\pi(R-x)$$

Integration gives

$$\eta(R-x) \cdot \frac{dv_{eo,x}}{dx} = E \int (R-x) \cdot \varrho_x \cdot dx + C_1$$

Introducing Poisson's formula $\left(\frac{4\pi\varrho_x}{D} = -\frac{d^2\psi_x}{dx^2}\right)$ we get,

$$\eta(R-x)\frac{dv_{eo,x}}{dx} = -\frac{ED}{4\pi}\int (R-x) \cdot \frac{d^2\psi_x}{dx^2} + C_1 \tag{60}$$

The "thickness" of the double layer is only 10–100 Å (see section B, p. 56 ff.) which is much less than the tube radius R. Within the double layer and also at all distances from the tube wall for which $x \ll R$, eqn. (60) can be simplified to

$$\eta \cdot \frac{dv_{eo,x}}{dx} = -\frac{ED}{4\pi} \cdot \frac{d\psi_x}{dx} + C_2 \tag{61}$$

The constant C_2 is zero, as the derivatives $\frac{dv_{eo,x}}{dx}$ and $\frac{d\psi_x}{dx}$ are zero outside the diffuse double layer.

Integration of eqn. (61) gives

$$v_{eo,b} - v_{eo,\text{slip}} = -\frac{ED}{4\pi} \int_{\psi_{\text{slip}}}^{\psi_{\text{bulk}}} \frac{1}{\eta} \cdot d\psi_x \tag{62}$$

As $v_{eo,\text{slip}}$, the velocity at the slipping plane, and ψ_{bulk}, the potential outside the double layer, are both zero, and $\psi_{\text{slip}} = \zeta$, eqn. (62) can be written

$$v_{eo,b} = \frac{ED}{4\pi} \int_0^{\zeta} \frac{1}{\eta} \cdot d\psi_x \tag{63}$$

At constant η this equation is equivalent to eqn. (53). The latter expression, which was derived for the case where η is constant throughout the solution, shows that an increase in the viscosity of the buffer in the electrophoresis tube decreases electroendosmosis. However, eqn. (63) indicates that, to decrease electroendosmosis, it is necessary to increase the viscosity only in the diffuse double layer. Therefore, the inner wall of the electrophoresis tube was coated with a thin layer of a very viscous hydrophilic polymer solution (methyl cellulose with a viscosity of about 100 centipoise). The coating was made less soluble in water by cross-linking the methyl cellulose with formaldehyde. The coating procedure is described in section A, p. 51 ff. The cross-linked methyl cellulose coating virtually eliminated electroendosmosis (see Fig. 17*b*).

I should mention here that no electroendosmosis was detected in an untreated electrophoresis tube when methyl cellulose was included in the buffer: a neutral marker, DNP-ethanolamine [24], did not move, and neither this nor any other of the zones applied showed any tendency to become curved. However, when the experiment was repeated with polyethylene glycol in the buffer, instead of methyl cellulose, electroendosmosis was considerable. Therefore, it is not clear whether the ability of methyl cellulose to eliminate electroendosmosis is due to an increase in viscosity or to a reduction in ζ-potential (or a combination of both). At any rate, the absence of charged groups in the methyl cellulose is essential to its effectiveness, since carboxymethyl cellulose does not eliminate electroendosmosis.

In the above treatment the increase in flow resistance near the tube wall has been attributed to an increase in viscosity. However, any other means of making the diffuse double layer less mobile than the bulk solution will also reduce electroendosmosis. Therefore, electroendosmosis will be suppressed by methyl cellulose even if it forms a stiff stationary gel layer rather than a very viscous solution as was assumed above.

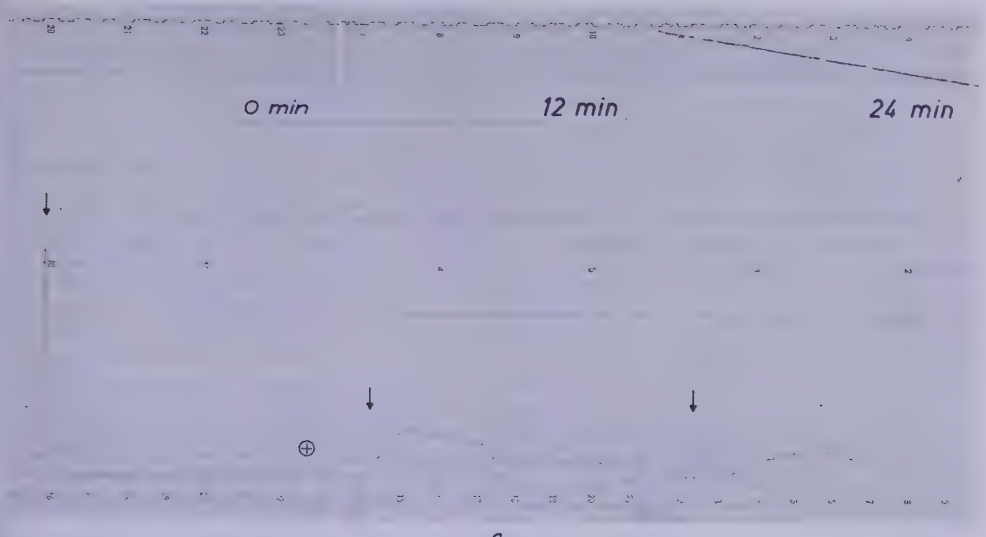

a

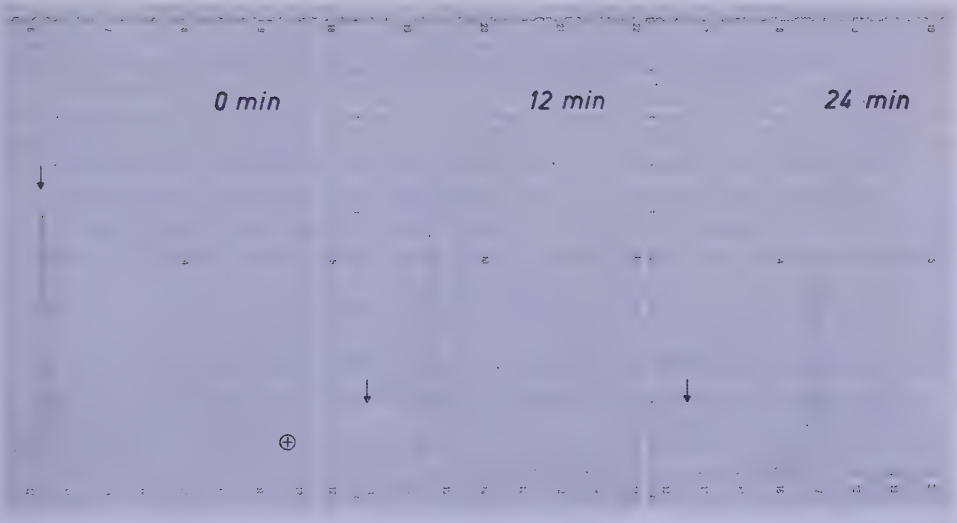

b

Fig. 17. a) Free zone electrophoresis of naphtol green in an *untreated* quartz electrophoresis tube. Buffer: 0.03 M sodium phosphate, pH 7.3. Sample: 1.6 μg naphtol green in 10 μl buffer. Inner diameter of revolving electrophoresis tube: 3 mm. Current: 5 mA. Voltage: 740 V. Temperature of cooling water: 16°. The arrow indicates the position of the starting zone. The scans were made at the times indicated. *b*) Run performed exactly as in *a*) except that the inner surface of the electrophoresis tube had been coated with methyl cellulose to eliminate electroendosmosis. A comparison between electropherograms *a*) and *b*) shows clearly the importance of eliminating electroendosmosis.

II:5. *The Electrophoretic Migration Velocity Profile*

A. The Migration Velocity as a Function of the Distance from the Axis of the Electrophoresis Tube

The evolution of heat attending the passage of current through the electrophoresis tube will inevitably produce a temperature gradient in which the temperature is highest at the axis of the tube and declines parabolically toward the periphery. Regions of a zone that differ in temperature will migrate at different velocites. To derive a quantitative expression for the resulting migration velocity profile we begin with the relation [27]

$$u = C \cdot \frac{D\zeta}{\eta} \tag{64}$$

where u is the electrophoretic mobility, C is a constant, D is the dielectric constant, ζ is the electrokinetic potential, and η is the coefficient of viscosity. Since the migration velocity, v, is equal to $u \cdot E$, the mobility times the field strength, the migration velocity in any part of a zone is given by the expression [28]

$$v = C \cdot \frac{D\zeta E}{\eta} \tag{65}$$

E has the same value everywhere in the electrophoresis tube even when a temperature gradient is present; D and ζ vary only slightly with temperature [30] and the variation is such that their product is essentially independent of temperature [30 b]. Accordingly, eqn. (65) can be approximated as

$$v = \text{constant} \cdot \frac{1}{\eta} \tag{66}$$

The shape of the migration velocity profile in a temperature gradient is thus determined almost entirely by the temperature dependence of the viscosity. The viscosity varies with the absolute temperature T according to the relation

$$\eta = A \cdot e^{\frac{B}{T}} \tag{67}$$

where A and B are constants. Therefore,

$$\frac{v_r}{v_w} = e^{\frac{B}{T_w} - \frac{B}{T_r}} \tag{68}$$

where v_w and v_r are the migration velocities at the wall and at the distance r from the axis of the electrophoresis tube, respectively, and T_w and T_r are the corresponding absolute temperatures.

Since in practical electrophoresis experiments the temperature difference $T_r - T_w$ must be small compared to T_w (usually < 1 per cent), the series expression obtained by expanding the exponential term of the above equation can be simplified to give

$$\frac{v_r - v_w}{v_w} = \frac{B(T_r - T_w)}{T_r T_w}$$

which is in turn approximated satisfactorily by

$$\frac{v_r - v_w}{v_w} = \frac{B(T_r - T_w)}{T_0^2} \tag{69}$$

where T_0 is the absolute temperature of the cooling water. The magnitude of B for water is about 2400°K. For values of T_0 in the normal operating range from 273–293°K, eqn. (69) can be approximated by

$$\frac{v_r - v_w}{v_w} = 0.03\,(T_r - T_w) \tag{70}$$

i.e., in this temperature range each degree of difference in temperature corresponds to a difference of about 3 per cent in migration velocity.

The factor $T_r - T_w$ in eqn. (69) can be approximated by the expression [31, 32, 33]

$$T_r - T_w = \frac{I^2}{4\varkappa\pi^2 R^4 \lambda}(R^2 - r^2) \tag{71}$$

where I is the current through the electrophoresis tube, $\varkappa$ is the electrical conductivity of the buffer at the temperature of the cooling water, and λ is the thermal conductivity of the buffer (varies only slightly with temperature [30]). The validity of a similar expression for the case of powder-stabilized media has been verified by Porath [32]. Insertion of eqn. (71) into eqn. (69) gives

$$\frac{v_r - v_w}{v_w} = \frac{BI^2(R^2 - r^2)}{4\varkappa\pi^2 R^4 \lambda T_0^2} \tag{72}$$

The parabolic velocity distribution represented by eqn. (72) is illustrated graphically in Fig. 18*a* for four different values of the current strength. The magnitude of the difference in steady-state velocity between the axis and the inside wall of the electrophoresis tube can be calculated simply by setting r equal to zero. Thus,

$$\frac{v_a - v_w}{v_w} = \frac{BI^2}{4\varkappa\pi^2 R^2 \lambda T_0^2} \tag{73}$$

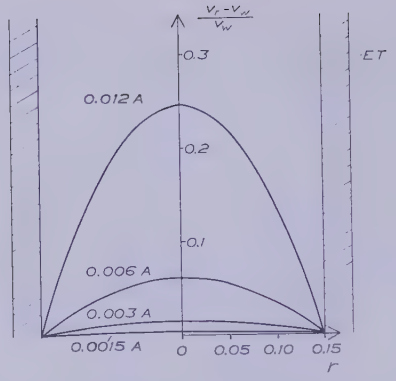

Fig. 18a. The migration velocity distribution in the electrophoresis tube ET. The curves are calculated from eqn. (72) for the four current strengths indicated. The other parameters in the equation have been given the following values: $B = 2400°K$, $R = 0.15$ cm, $\varkappa = 3.67 \times 10^{-3}$ ohm^{-1} cm^{-1}, $\lambda = 5.73 \times 10^{-3}$ joule sec^{-1} cm^{-1} degree^{-1}, $T_0 = 274°K$.

where v_a and v_w are the migration velocities at the axis and at the wall of the tube, respectively. Since $B = 2400°K$ and $\lambda = 5.73 \times 10^{-3}$ joule sec^{-1} cm^{-1} degree^{-1},

$$\frac{v_a - v_w}{v_w} = \frac{1.06 \cdot 10^4 \cdot I^2}{R^2 \varkappa T_0^2} \tag{74}$$

where I is expressed in amperes, R in cm, $\varkappa$ in ohm^{-1} cm^{-1}, and T_0 in °Kelvin.

Any difference in migration velocity between the center and the periphery of a zone will cause an initially planar zone to become curved upon migrating a few centimeters. This is true for all electrophoresis methods. The maximum current strength that can be used in any particular run depends on the degree of zone curvature that can be tolerated. In general, however, currents for which the calculated velocity difference $(v_a - v_w)/v_w$ exceeds 0.06 should not be used in any free zone electrophoresis experiment [as eqn. (74) obtains for a steady-state gradient, higher currents can be used if the run is completed before the steady state is established (see section C, p. 29 ff.)]. According to eqn. (70), this maximum permissable difference of 6 per cent in migration velocity corresponds to a temperature difference of only 2° between the axis and the inner wall of the electrophoresis tube. Under these conditions, the periphery of a zone would migrate only 20 cm while its center migrated 21.2 cm. The recorded peak corresponding to the curved zone would be noticably asymmetric and about 1 cm broader (about twice as broad) as the peak that would be obtained in the absence of curvature. (The usual peak width is about 1 cm, as evidenced by the many patterns

that appear in this monograph.) Since curved zones give broad and skewed recorder peaks, thereby decreasing the apparent resolution and prohibiting accurate mobility measurements, conditions that produce curved zones should be avoided.

The differences in migration velocity that occur in a temperature gradient, and which produce the type of zone deformation discussed above, are due primarily to the variation of viscosity with temperature, as is evident from eqn. (66). Of course, any temperature gradient will also produce a gradient of density. However, for any conditions whose use would not be obviated by the viscosity effects discussed above, the maximum difference in density represented by the temperature gradient developed is likely to be much smaller than the difference in density between the sample zone and the buffer. For example, within the temperature interval from 0 to 20°, a temperature difference of 2° corresponds at most to a density difference of only 0.00039 g cm^{-3}, whereas the difference in density between a buffer and a 1 per cent solution of protein equilibrated with that buffer (e.g., by dialysis) is about 0.0026 g cm^{-3}.[f] In free zone electrophoresis (cf., the alternating current experiment described in section C, p. 29 ff.) and in many other electrophoresis methods these small density differences of thermal origin produce no convective disturbances. In most cases, the marked zone broadening and consequent loss of resolution that occurs when excessive field strengths are used is due almost entirely to the formation of parabolic zones. If charged, colored substances are subjected to electrophoresis in the revolving tube or in transparent gels of agar, agarose or polyacrylamide, the zone curvature that occurs at excessive field strengths can be followed visually (see Fig. 18*b*). In general it is this zone curvature, and not convective disturbances, that prohibits the use of high field strengths. I stress this fact because I have the impression that it is not generally realized.

Theoretically, thermal zone deformations can be avoided at high field strengths by increasing the temperature of the cooling water continuously during the run in such a way that the parabolic gradient is flattened out. In practice, however, it is simpler to flatten curved zones by applying a counterflow of buffer, as described in section C, p. 58 ff. The use of the counterflow method to restore a curved zone to a flat shape in a vertical column of a 0.16 % agar suspension is illustrated in Fig. 18*c* (this technique is not applicable to electrophoresis columns of cellulose and similar granular bed materials). In order to facilitate the use of this adjustment method when the substance of interest is not visible, a colored zone of similar mobility should be applied to the revolving tube some distance away from

[f] See footnote [f], p. 23.

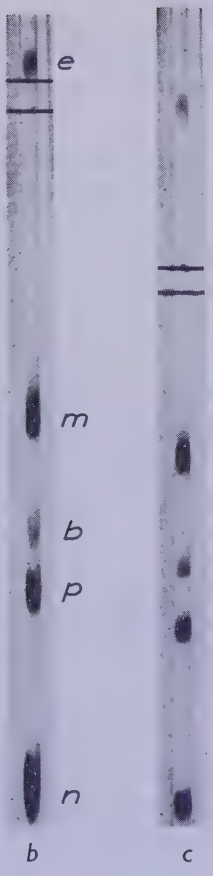

Fig. 18b. Curved zones caused by excessive voltage gradients (a practical demonstration of the effect described by the theoretical curves in Fig. 18*a*). The experiment shown in the photograph was performed in a 0.16 % agar suspension [43] but similar zone deformations also occur in other electrophoresis methods, including free zone electrophoresis. The five substances separated are (from the bottom): naphtol green, phenol red, bromothymol blue, methyl orange, and DNP-ethanolamine. Buffer: 0.03 M sodium borate, pH 8.9. Inner diameter of the stationary, vertical electrophoresis tube: 3.6 mm. Potential gradient: 60 volts/cm. Current: 7 mA. The position of the starting zone is indicated by two horizontal lines.

Fig. 18c. The curved zones in Fig. 18*b* have been flattened by forcing buffer through the tube in a direction opposite to that of electrophoretic migration (see also section C, p. 52 ff.). This hydrodynamic compensation was performed with reference to the phenol red zone (p), so the other zones are still somewhat parabolic.

the sample zone. Using this colored zone as a guide, the compensatory flow can be applied during or after the run.

A colored zone is not necessary, however, for the adjustment operation can be followed easily by the use of the scanning device. The recorder deflection will be maximum when the zone is flat. This is discussed further in section f, p. 90 ff.

When high field strengths are to be used, the buffer must be de-aerated thoroughly in order to prevent the formation of air bubbles as the temperature rises. Air bubbles can distort zones severely.

Of course, zone curvature need not have a thermal origin. Electroendosmosis also gives rise to parabolic zones, as discussed in section B, p. 56 ff. Effective methods for counteracting or eliminating the electroendosmotic effects have been described in section C, p. 58 ff. and in section E, p. 61 ff.

In certain buffers a temperature gradient will produce a significant pH

gradient.[m] This will also effect the migration velocity of weak electrolytes, but the effect is relatively minor compared to the viscosity effect discussed above. In general, the pH gradient will slightly augment the curvature of basic zones and reduce the curvature of acidic ones, as compared with that predicted by eqn. (72).

B. The Effect of Coolant Temperature on the Migration Velocity at Constant Current

Since the field strength, E, is equal to $i/\varkappa$, eqn. (65) can be written in the form

$$v_r = \frac{i_r}{\varkappa_r} \cdot C \cdot \frac{D\zeta}{\eta_r} \tag{75}$$

where v_r, i_r, $\varkappa_r$, and η_r denote the migration velocity, the current density, the electrical conductivity, and the viscosity, respectively, at the distance r from the axis of the electrophoresis tube.

Since

$$\varkappa = C_0 \cdot e^{-\frac{B}{T}} \tag{76}$$

where C_0 is a constant, and $\eta = A \cdot e^{B/T}$ (eqn. (67)), the product $\varkappa_r \cdot \eta_r = C_0 A$ is a constant, independent of the temperature and consequently of the tube radius. The product $D \cdot \zeta$ is also virtually independent of the temperature, as was mentioned in the discussion of eqn. (65). Therefore eqn. (75) can be written

$$v_r = C_1 \cdot i_r \tag{77}$$

where C_1 is a constant.

Assume now that we make two experiments that are identical except for the temperature of the cooling water. In one experiment the temperature at the inner wall of the electrophoresis tube is T_w and in the other it is $T_w + \Delta T_w$. Applying eqn. (77) to these two cases we obtain

$$\frac{v_{r,\,T_w+\Delta T_w}}{v_{r,\,T_w}} = \frac{i_{r,\,T_w+\Delta T_w}}{i_{r,\,T_w}} \tag{78}$$

where v_{r,T_w} and $v_{r,T_w+\Delta T_w}$ are the migration velocities at the distance r from the tube axis when the temperatures at the inside wall of the tube are T_w and $T_w + \Delta T_w$, respectively; $i_{r,T_w+\Delta T_w}$ and i_{r,T_w} are the corresponding current densities.

---

[m] For a 0.05 M Tris-HCl buffer, pH 7–8, $(d\,\mathrm{pH}/dt)_{t=25} \sim -0.028$ unit, degree^{-1} (ref. 34).

(a) First we shall consider the simple case where the total current I through the electrophoresis tube is so small that the temperature gradient can be neglected. The zones are then planar according to eqn. (69). In the absence of a temperature gradient the current density will be the same everywhere in the tube and equal to $I/\pi R^2$. If the total current is kept constant the current density will not change when the temperature of the cooling water is changed, so eqn. (78) can be simplified to $v_{r,\,T_w+\Delta T_w} = v_{r,\,T_w}$. Accordingly, the migration velocity is independent of the temperature of the cooling water when the total current is maintained constant.

(b) We shall now proceed to the more complicated general case where the current is high enough to produce a significant temperature gradient, which in turn gives rise to a parabolic migration velocity profile as discussed in the preceding section.

The assumption that the total current is maintained constant is formulated as follows:

$$\int_0^R i_{r,\,T_w} \cdot 2\pi r\,dr = \int_0^R i_{r,\,T_w+\Delta T_w} \cdot 2\pi r\,dr \tag{79}$$

As the field strength $E(=i_r/\varkappa_r)$ is at every moment constant throughout a cross-section of the tube, i.e. independent of r, eqn. (79) can be transformed to

$$E_{T_w} \cdot \int_0^R \varkappa_{r,\,T_w} \cdot 2\pi r\,dr = E_{T_w+\Delta T_w} \cdot \int_0^R \varkappa_{r,\,T_w+\Delta T_w} \cdot 2\pi r\,dr$$

or

$$\frac{i_{r,\,T_w}}{i_{r,\,T_w+\Delta T_w}} = \frac{\varkappa_{r,\,T_w}}{\varkappa_{r,\,T_w+\Delta T_w}} \cdot \frac{\int_0^R \varkappa_{r,\,T_w+\Delta T_w} \cdot 2\pi r\,dr}{\int_0^R \varkappa_{r,\,T_w} \cdot 2\pi r\,dr} \tag{80}$$

where $\varkappa_{r,\,T_w}$ and $\varkappa_{r,\,T_w+\Delta T_w}$ are the conductivities at the positions where the current densities are $i_{r,\,T_w}$ and $i_{r,\,T_w+\Delta T_w}$, respectively.

The concentration gradient that arises as a consequence of thermodiffusion contributes only slightly to altering the conductivity distribution in the tube and can be neglected. Therefore, the conductivity at any point in the tube is determined almost solely by the temperature at that point according to the formula $\varkappa = C_0 \cdot e^{B/T}$ (eqn. (76)). If we use the expanded form of this equation given in footnote[n], we see that

[n] Applying Lagrange's mean value theorem to eqn. (76) one obtains $\varkappa_{T_2} \approx \varkappa_{T_1} \cdot [1 + (B/T_1^2)\ (T_2 - T_1)]$, where $\varkappa_{T_1}$ and $\varkappa_{T_2}$ are the conductivities at the temperatures T_1 and T_2, respectively. As B/T_1^2 ($B = 2400°\mathrm{K}$) varies only slightly with temperature for moderate temperature alterations, this expression is approximated satisfactorily by $\varkappa_{T_2} = \varkappa_{T_1}[1 + C_1 \cdot (T_2 - T_1)]$, where $C_1 = 0.03$ degree^{-1}.

$$\varkappa_{r,T_w} = \varkappa_{R,T_w} \cdot \{1 + C_1[T_{r,T_w} - T_w]\} \tag{81}$$

$$\varkappa_{r,T_w+\Delta T_w} = \varkappa_{R,T_w+\Delta T_w} \cdot \{1 + C_1[T_{r,T_w+\Delta T_w} - (T_w + \Delta T_w)]\} \tag{82}$$

Eqns. (81) and (82) apply for the cases where the temperatures at the inner wall of the tube are T_w and $T_w + \Delta T_w$, respectively; $\varkappa_{R,T_w}$ and $\varkappa_{R,T_w+\Delta T_w}$ are the conductivities at the inner wall of the tube when the temperatures there are T_w and $T_w + \Delta T_w$, respectively. Upon combining eqns. (78) and (80), inserting relations (81) and (82), and then utilizing eqn. (71) we get,

$$\frac{v_{r,T_w+\Delta T_w}}{v_{r,T_w}} = \frac{1 + \dfrac{C}{\varkappa_{T_w+\Delta T_w}}(R^2 - r^2)}{1 + \dfrac{C}{\varkappa_{T_w}}(R^2 - r^2)} \cdot \frac{1 + \dfrac{C}{\varkappa_{T_w}} \cdot \dfrac{R^2}{2}}{1 + \dfrac{C}{\varkappa_{T_w+\Delta T_w}} \cdot \dfrac{R^2}{2}} \tag{83}$$

where $C = C_1 \cdot \dfrac{I^2}{4\pi^2 R^4 \lambda}$

We will now investigate this expression for three different cases.

(1) $v_{r,T_w+\Delta T_w} = v_{r,T_w}$. Insertion of this condition into eqn. (83) gives $r = R/\sqrt{2}$, i.e. there exists in the tube an isobestic cylinder along which the migration velocity is independent of the temperature of the cooling water (Fig. 19).

(2) $v_{r,T_w+\Delta T_w} > v_{r,T_w}$. According to eqn. (83) this inequality obtains for $R \geqslant r > R/\sqrt{2}$. The greatest difference between $v_{r,T_w+\Delta T_w}$ and v_{r,T_w} in this interval occurs for $r = R$, i.e. at the tube wall. To get an idea of the magnitude of this maximum difference we insert into eqn. (83) a set of values from a typical experiment for the case where the cooling water temperature is changed so much that $\Delta T_w = 10°$. Using $C_1 = 0.03$ degree^{-1}, $I = 0.005$ A, $R = 0.15$ cm, $\lambda = 5.73 \times 10^{-3}$ joule sec^{-1} cm^{-1} degree^{-1}, $\varkappa_{T_w} = 3.7 \times 10^{-3}$ ohm^{-1} cm^{-1}, and $\varkappa_{T_w+\Delta T_w} = 1.3 \times 3.7 \times 10^{-3}$ ohm^{-1} cm^{-1} we get

$$\frac{v_{R,T_w+\Delta T_w}}{v_{R,T_w}} = 1.005$$

which means that an increase of 10° in the temperature at the wall will increase the migration velocity at the wall by only 0.5 per cent (Fig. 19). If the current is 0.010 A instead of 0.005 A the increase will be 1.7 per cent.

(3) $v_{r,T_w+\Delta T_w} < v_{r,T_w}$. This obtains for $0 \leqslant r < R/\sqrt{2}$. The maximum difference between v_{r,T_w} and $v_{r,T_w+\Delta T_w}$ in this interval occurs for $r = 0$, i.e. at the tube axis. To estimate this maximum difference we use the same values for the various parameters as were used in (2). We then get

$$\frac{v_{0,T_w+\Delta T_w}}{v_{0,T_w}} = 0.996 \text{ for } I = 0.005 \text{ A}$$

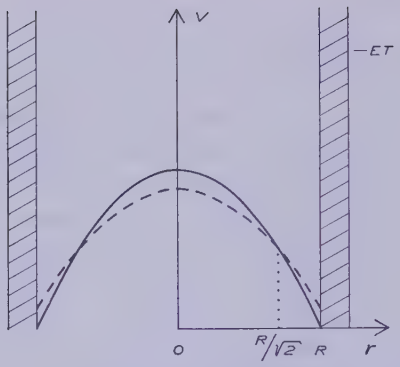

Fig. 19. The migration velocity v as a function of the distance r from the axis of the electrophoresis tube ET for two different temperatures of the cooling water when the current through the tube is the same (cf. eqn. (83)). The dashed curve corresponds to the higher temperature. The difference between the two curves is exaggerated in the figure and can often be neglected in practice.

and = 0.985 for $I = 0.010$ A. The migration velocity at the tube axis thus decreases somewhat when the temperature of the cooling water is increased by about 10° (Fig. 19).

From the paragraphs 1–3 one can conclude that moderate changes in the temperature of the cooling water have little effect on the migration velocity profile in the tube, and even less effect on the migration velocities as measured from the peaks in an electropherogram, since the decrease in migration velocity at the tube axis is partly compensated by an increase at the tube wall and the maximum in peak height corresponds to a position in the electrophoresis tube somewhere between the center and the periphery of a zone. This statement that the migration velocity at constant current is approximately independent of the temperature has been verified by determinations of the migration velocities of *R*-phycoerythrin and naphtol green in 0.03 *M* sodium phosphate (pH 7.6) at constant current (= 0.007 mA) first at a cooling water temperature of 10° and then at 21°. No significant differences in migration velocities could be detected for this temperature difference of 11°.

In the above theoretical treatment we have assumed that the variation of mobility with temperature is due only to the change in viscosity of the medium (eqn. (64)). However, if also the ζ-potential of the solute should change, for instance, by interaction with buffer ions or with other substances in the electrophoresis medium, differences in migration velocities can occur when experiments are performed at the same constant total current but at different temperatures. A determination of the temperature coefficient

of the migration velocity at constant current could perhaps form the basis of a method for the study of such an interaction. In such determinations one should remember that some buffers change their pH relatively strongly with temperature, which also may affect the migration velocities (see footnote [m], p. 69); one should also take into account the temperature dependence of the dissociation constants of the substances to be analyzed.

As the free zone electrophoresis equipment is fitted with a current stabilizer, one can also conclude from what has been said above that the temperature of the cooling water can fluctuate during a run without causing detectable variations in migration velocity. Therefore, the cooling reservoir can be equipped with a very inexpensive device for thermostating.

The fact that the observed migration velocity is approximately independent of temperature at a constant current strength, is, of course, not true for the calculated mobility. Tiselius [35] has pointed out that if a run is performed at one temperature and the conductivity that is used for calculation of the mobility according to eqn. (87) is determined at another temperature the mobility has been calculated for the latter temperature. Tiselius [35] has also shown that the relation $\eta_{t_1} u_{t_1} = \eta_{t_2} u_{t_2}$ holds for the transformation of mobilities from one temperature (t_1) to another (t_2).

A comparison between the solid and the broken curve in Fig. 19 shows that in all types of electrophoresis methods the temperature of the cooling system should be chosen as high as other factors (e.g. the stability of the sample) permit because the curvature of a zone then is less pronounced.[o] High voltage electrophoresis is in general performed at low temperatures, which, however, must be unfavorable as regards the degree of zone curvature. The selection of low cooling water temperatures is probably due to the fact that the temperature dependence of the migration velocity profile has not been analyzed previously.

II:6. *Analytical Runs*

A. Quantitative Analysis

A:1. Changes in the Intensity and Direction of the Scanning Beam Caused by the Electrophoresis Tube

The ensuing paragraphs describe how the scanning beam is affected by reflection and refraction as it traverses the electrophoresis tube. In this treatment, the scanning beam is assumed to consist of exactly parallel

[o] This does not apply for moving boundary electrophoresis, where experiments should be conducted at the temperature where the boundaries are most stable, i.e., at about +4° (ref. 31).

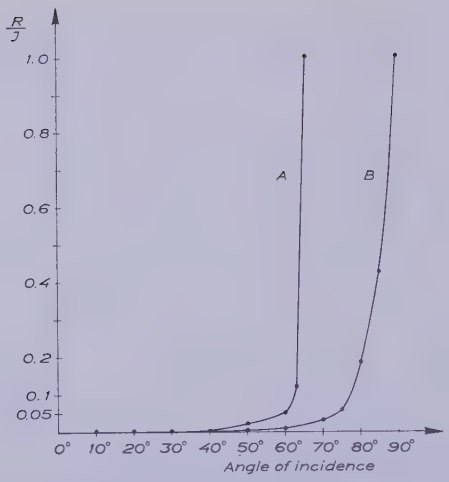

Fig. 20. Diagrammatic representation of the ratio between the intensities of reflected and incident light (R/I) as a funtion of the angle of incidence. The curves are calculated from Fresnel's formula (eqn. (84)) for a wavelength of about 280 mμ ($n_{\text{quartz}} = 1.50$; $n_{H_2O} = 1.37$). Curve A applies to light rays passing from quartz to water and curve B applies to rays travelling in the opposite direction.

rays and to have a constant intensity throughout its cross-section before it strikes the tube.

When a light beam strikes a boundary between two transparent materials, part of the light is reflected and part is refracted. The fraction that is reflected increases with the angle of incidence. The ratio R/I between the intensities of the reflected and incident light is given by Fresnel's formula [36]

$$\frac{R}{I} = \frac{1}{2}\left[\frac{\sin^2(i_1 - i_2)}{\sin^2(i_1 + i_2)} + \frac{\tan^2(i_1 - i_2)}{\tan^2(i_1 + i_2)}\right] \tag{84}$$

where i_1 is the angle of incidence and i_2 is the angle of refraction.

The curves shown in Fig. 20 were calculated by this equation for light with a wavelength of 280 mμ passing from quartz to water (curve A) and from water to quartz (curve B). For angles of incidence below 60° less than 5 per cent of the light is reflected upon striking the quartz-to-water interface. For light passing in the opposite direction, the reflection losses are less than 5 per cent for angles of incidence up to 75°. Rays I and II in Fig. 21 have angles of incidence of 60 and 75°, respectively, corresponding to 5 per cent reflection for the two cases just mentioned. These rays are part of a homogeneous light beam which strikes the quartz tube. According to this diagram, a zone in the tube will be illuminated evenly everywhere except at its upper and lower edges.

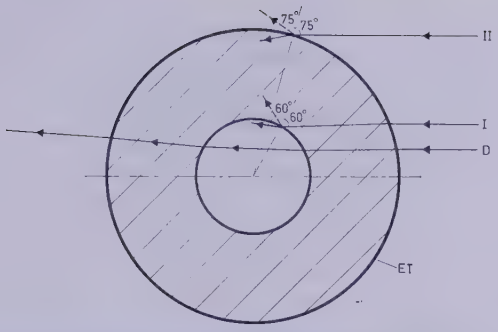

Fig. 21. Reflection and refraction of the scanning beam upon traversing the buffer-filled quartz electrophoresis tube ET (inner diameter: 3 mm; outer diameter: 7.8 mm). The light rays striking the quartz tube are assumed to be parallel and to consist of wavelengths around 280 mμ. The ray D is drawn to show that the light converges only slightly as it traverses a zone in the tube. The reflection losses greater than 5 % occur only for rays when angles of incidence exceed those of rays I and II (cf. Fig. 20).

The reflection losses are very small because quartz and water have similar refractive indices (1.50 and 1.37, respectively, for light of 280 mμ). For the same reason, the light beam converges only slightly as it traverses the buffer in the tube (see ray D in Fig. 21).

A:2. The Relationship between Transmission and Sample Concentration (Calibration Curve)

a. The Theoretical Curve

In a rigorous treatment one would have to take into account the convergence of the light upon traversing the quartz tube (Fig. 21) and the light losses incurred by reflection at the various water/quartz boundaries. The reflection losses vary with the angle of incidence according to Fresnel's formula (eqn. (84)). The exact expression for the intensity of the transmitted beam would thus be extremely complicated.

However, since the reflection losses are small and the convergence is slight, as discussed in the preceding section, the treatment can be simplified considerably with little loss of accuracy by ignoring the reflection losses and assuming that the light rays remain parallel upon traversing the tube. To derive an expression for the transmission as a function of the sample concentration we shall also assume that the sample pulse consists entirely of wavelengths that can be absorbed by the solute (or more strictly, that the light is monochromatic) and that the intensity of the beam is everywhere the same when it strikes the sample zone. The intensity of the incident beam is designated I_0, and is expressed in terms of the number of photons impinging on a unit area per second.

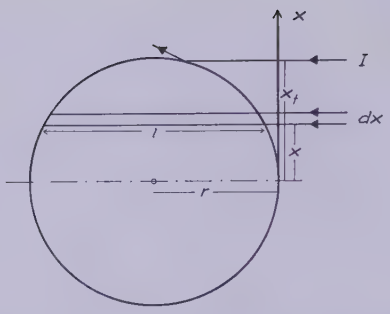

Fig. 22. Diagram used to determine the relationship between transmission and sample concentration. Total reflection occurs with rays having angles of incidence greater than that of ray I; $l = 2\sqrt{r^2 - x^2}$.

Consider an infinitesimal portion of the scanning beam; namely, a light bundle with the height dx and a narrow width a (Fig. 22). The number of photons passing a cross-section of this bundle per second, and therefore, the number that impinge per second on a corresponding infinitesimal area of the sample zone is $I_0 a \cdot dx$. The sample zone is assumed to be cylindrical in shape, with a radius r corresponding to the inner radius of the electrophoresis tube. The solute concentration is uniform throughout the width a. The number of photons that leave the area $a \cdot dx$ at the opposite side of the zone per second (e.g., the number transmitted per second by this thin slice of the zone) is dN. If Beer's law obtains, $dN = I_0 a \cdot dx \cdot e^{-kcl}$, where k is the absorption coefficient, c is the concentration, and l is the length of the optical path ($l = 2\sqrt{r^2 - x^2}$). The total number (N) of photons transmitted by the entire zone per second is:

$$N = I_0 a \int_{-x_t}^{+x_t} \exp\left(-2kc\sqrt{r^2 - x^2}\right) \cdot dx$$

where x_t is the ordinate at which total reflection occurs. The limits for the integration should properly be slightly less than x_t, but the use of x_t instead of the proper limit has very little effect on the value of N (x_t can be calculated easily from r and the refractive indices of quartz and water for the mean wavelength of the sample flash of the scanning beam).

If the transmission, T_{true}, is defined as the number of photons that leave the zone per second divided by the number that enter it per second, then

$$T_{\text{true}} = \frac{1}{2x_t} \int_{-x_t}^{+x_t} \exp\left(-2kc\sqrt{r^2 - x^2}\right) \cdot dx \qquad (85)$$

This integral cannot be solved in closed form. Therefore, T_{true} was evaluated numerically by means of a computer. The result is shown graphically in Fig. 23. Since k depends on the wavelength of the incident light and x_t

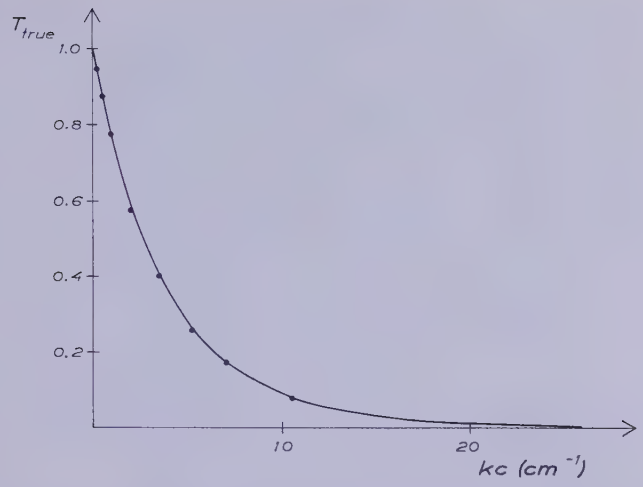

Fig. 23. Plot of the transmission (T_{true}) against kc (k = the absorption coefficient, c = the sample concentration). The curve was calculated from eqn. (85) by a computer for the case where $r = 0.154$ cm and $x_t = 0.142$ cm. The points represent experimental values (see Fig. 24).

on the wavelength and the tube radius, any such calibration curve applies for only one tube size and one scanning wavelength.

To check the validity of eqn. (85), T_{true} and kc were determined experimentally for each of a series of eight solutions and the values were plotted in the diagram shown in Fig. 23. All of the experimental points (filled circles) fall very near the theoretical curve (solid line). The experimental procedure used for the determination of T_{true} and kc was as follows.

A solution of adenosine 5′-phosphate (AMP) was prepared in 0.025 M ammonium formate, pH 3.61. Equal aliquots of this solution were diluted with different volumes of the same buffer. The electrophoresis tube was then filled with these AMP-solutions and their true transmissions were determined as described in the next section. A 1-cm cuvette filled with one of the eight AMP-solutions was then placed in the light beam traversing the water-filled immersion bath IB (Fig. 6). The true transmission of this solution was then determined. Using Beer's law, written in the form $kc = -\log_e 10 \times \log_{10} T_{\text{true}}$, kc for the solution was obtained. The kc-values of the other AMP-solutions were calculated from the known dilution ratios. The true transmissions were plotted against the kc-values (Fig. 23).

b. The Empirical Curve

The numerical calculation of eqn. (85) is very time-consuming unless one has access to a computer. Therefore I shall describe how a calibration curve can easily be prepared experimentally.

The transmissions read directly from the recorder chart are not the true transmissions, as these are defined by eqn. (85), because some of the assumptions under which this equation was derived are not fulfilled in practice. Thus (1) the height of the scanning beam is somewhat larger than the inner diameter of the electrophoresis tube and (2) the filters used have such undesirable transmission characteristics that the sample pulses (1, 3, 5, ... in Fig. 11) contain wavelengths that are not absorbed by the sample. Therefore, the height of the sample pulse is not zero even when the sample concentration is "infinite". This means that the recorder pen will never show 0 per cent transmission, which is equivalent to full deflection; i.e., the printed scale on the recorder chart will not give the true transmission.[p] This complication can be circumvented, however, provided the recorder deflection is determined for a solution of "infinite" concentration. This deflection is then used as a reference for the transmission zero. The practical details are as follows.

By means of the arm A (Fig. 7), the carriage Ca with the electrophoresis tube ET is turned to a vertical position, the tube being closed at its bottom with a rubber stopper. A series of solutions of different but known concentrations has previously been prepared from the substance one wants to determine quantitatively in a subsequent electrophoretic analysis. These solutions are layered on top of each other in the electrophoresis tube. To avoid convection the solutions must be introduced in the order of decreasing densities. Above these layers another layer is applied, which consists of the buffer in which the various solutions were prepared, i.e. the buffer to be used for the electrophoresis. If one wants the true transmissions—and not the apparent ones—the bottom solution must have an "infinite" concentration. In the experiments described here it is justified to consider the concentration of a solution as "infinite" if further increase in concentration does not increase the deflection of the recorder pen or if the transmission of the solution is zero when analyzed at its absorption maximum in a grating or prism spectrophotometer with negligible stray light (e.g. Zeiss or Beckman instruments). After the electrophoresis tube has been filled with the different solutions, the rotation of the tube by the motor SM1 (Fig. 6) is begun. The carriage is brought to the horizontal position and a scan is immediately done. The appearance of such a recording is shown in Fig. 24. In this case the bottom solution had an "infinite" con-

[p] To avoid the introduction of constants and thus make the treatment more intelligible, we assume in this section that the sensitivity knob of the pulse comparator (see section c : 5, p. 46 ff.) is put into such a position that full deflection of the recorder pen is obtained when all light corresponding to the sample pulse is absorbed (the lowest sensitivity range).

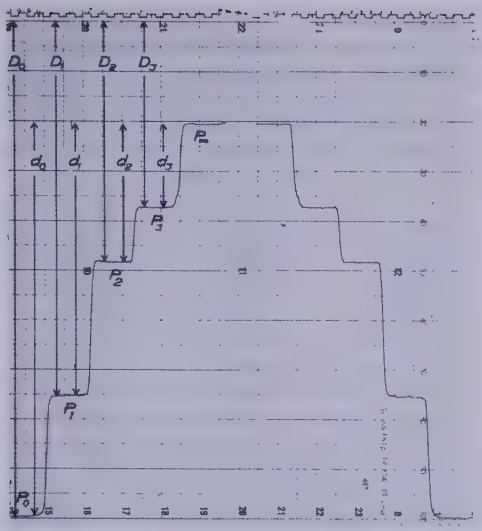

Fig. 24. Chart record obtained in an experiment performed to establish relationship between pen deflection and sample concentration. The plateaus P_0, P_1, P_2, P_3, and P_∞ correspond to sample concentrations of 0, c_1, c_2, c_3, and "infinity", respectively. The true and apparent transmissions are d_i/d_0 and D_i/D_0, respectively, where $i = 1, 2, 3$. The experimental points in Fig. 23 were obtained from a similar recording.

centration and the other solutions the concentrations c_1, c_2 and c_3 ($c_1 < c_2 < c_3$). The true transmission (T_{true}) of a solution of the concentration c_i ($i = 1, 2, 3$) is accordingly d_i/d_0 (d_i corresponds to the concentration c_i); d_i and d_0 are defined in Fig. 24. The apparent transmission (T_{app}) is D_i/D_0 ($i = 1, 2, 3$). T_{app} or preferably T_{true} is then plotted against c_i (or against kc_i as in Fig. 23). The resulting calibration curve can be used for the determination of the amount of substance in an electrophoresis zone as shown in the next section. In the experiment described there and in the verification of eqn. (85) (see Fig. 23) the true transmissions were used.

A:3. The Accuracy of Quantitative Determinations

The accuracy of quantitative analysis was evaluated in the following way. Four zones of different but known concentrations of adenosine 5′-phosphate (AMP) were injected into the quartz tube. The volume of each zone was about 15 μl. To determine this volume more exactly the syringe (Fig. 14) was weighed before and after each application. Ten minutes after the application of the fourth zone two successive scans were made. A high recorder chart speed was used in order to get wider peaks and consequently greater accuracy in the subsequent planimetry. The true transmission was

Table 2. The accuracy of quantitative determinations. Four zones of adenosine 5′-phosphate (AMP) were applied. The one of the highest concentration was chosen as a reference zone and showed that a corrected peak area of 1 cm^2 corresponded to 0.0534 μg. From this relation and the corrected areas of the three other peaks, the weight of material in the zones could be established.

Vol. of sample (μl)	Conc. of sample ($\mu g/\mu l$)	Weight of sample (μg)	Corrected peak area (cm^2)	Calculated weight of sample (μg)
16.2	0.0314	0.51	9.09	0.49
16.5	0.0523	0.86	16.9	0.90
14.0	0.0785	1.10	20.6	1.10

calculated as described in the previous section at intervals of 2 mm along the chart axis. The corresponding concentrations, obtained from an empirical calibration curve were plotted directly on the recorder chart. A curve was drawn through the points obtained and its area determined by a planimeter. This corrected peak area is, of course, proportional to the amount of material in the zone. The largest of the four peaks was used as a reference peak; i.e., from its corrected area and the amount of AMP applied in this zone, the amount of material in the other three zones could be calculated. The values obtained are given in Table 2. The area tabulated for each sample applied is a mean for two scans (one was made when the carriage moved from the left to the right and the other when it moved in the opposite direction). From this table and from results obtained in other experiments, it is evident that the errors are less than five per cent.

The accuracy obtained is much dependent on the regularity of the starting zone. For quantitative determinations it is therefore often preferable to apply the sample by layering instead of injection (these two techniques are described in section C, p. 52 ff.). The injection technique was used in the experiment described here because it permits the application of more than one zone. However, when the injection technique is employed the starting zone consists of small liquid elements of the sample surrounded by buffer (see section C, p. 52 ff.). Therefore, we chose a low molecular weight substance, AMP, as test material. This compound will diffuse rapidly to form a uniform zone.

The error of 2–3 per cent involved in the determination of the always small amount of material applied contributes to the inaccuracy of the above quantitative analyses. However, in most electrophoresis experiments

only a single zone is applied and one is usually interested only in the relative amounts of any separated components. Such relative data are more reliable than the absolute values.

The free zone electrophoresis will be automated for quantitative analyses. To do this the recorder must be modified such that the deflections of the pen are proportional to the sample concentration. This means that eqn. (85) will form the basis for the necessary reconstructions or, as shown in the next section, more conveniently the relation (86).

A:4. Approximation of Eqn. (85)

For $1.0 \geqslant T_{true} \geqslant 0.13$ (or $0 \leqslant -\log_{10} T_{true} \leqslant 0.9$) eqn. (85) reduces to

$$-\log_{10} T_{true} = C \cdot kc \tag{86}$$

The constant C varies with the inside diameter of the electrophoresis tube. The relation (86) can be proved most easily by taking the logarithms of the T_{true} values obtained by a computer calculation of eqn. (85) for different kc-values, and then plotting $-\log_{10} T_{true}$ against kc. Such a plot is shown in Fig. 25. This figure demonstrates that eqn. (86) is valid. The computer calculations on which Fig. 25 is based were performed for an electrophoresis tube with a radius r of 0.154 cm. However, the validity of eqn. (86) could also be demonstrated for r-values of 0.080 and 0.250 cm. This is an important finding because it shows that this linear relation holds for any tube radius that can be used in free zone electrophoresis. Accordingly, as long as the

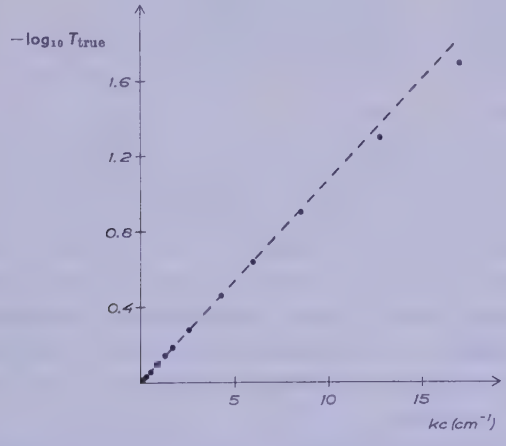

Fig. 25. Plot of $-\log_{10} T_{true}$ against kc (k = the absorption coefficient, c = the sample concentration). The values of T_{true} corresponding to different values of kc were calculated from eqn. (85) by means of an electronic computer. The deviation from linearity is extremely small for values of $-\log_{10} T_{true} \leqslant$ about 0.9 (or $T_{true} \geqslant 0.13$).

transmission exceeds 0.13 it is not necessary to prepare or use a calibration curve. One can simply plot $-\log_{10} T_{true}$ for different points on the recorded peak *versus* the position of these points. The area of the peak obtained will then be proportional to the amount of material in the corresponding zone.[q] Another consequence of the fact that relation (86) applies for any radius in the usable range, is that the planned attachment for automatic quantitative analysis need not be reconstructed for every new electrophoresis tube. The requirement that T_{true} must be larger than 0.13 creates no difficulties in practice, since none of the experiments performed to date have required concentrations corresponding to a T_{true} below 0.2.

By a serial expansion of the exponential term in eqn. (85) and subsequent integration, it can be shown that C can be approximated by 0.720 r. From a comparison between eqn. (86) and Beer's law one can therefore conclude that, within the validity range of eqn. (86), the quartz tube is equivalent in light transmission to a conventional cuvette with a rectangular cross-section and an optical path of $\log_e 10 \times 0.720$ r $= 1.66$ r.

B. Mobility Determinations

B:1. The Moving Boundary Method

Moving boundary electrophoresis has been used with success for mobility determinations for the last three decades. The serum proteins are still classified on the basis of their relative mobilities and by the positions in which they appear in the moving boundary pattern. The standard Tiselius *U*-cell used in moving boundary electrophoresis has a cross-section of 3×25 mm and requires about 11 ml of a sample solution with a concentration of 0.3–1.5 per cent, which amounts to 33–165 mg of material. Since this is far more material than is available in many cases where electrophoretic analysis by the moving boundary method is desired, many attempts have been made to devise a suitable cell of smaller dimensions. Unfortunately, the small cells do not afford the resolution that is attainable with the larger one, because: (1) any decrease in the height of the channel decreases the allowed migration distance; (2) a reduction in the depth decreases the length of the optical path, thereby decreasing the sensitivity of the optical observation system; (3) a decrease in the width increases the importance of electroendosmosis and provides practical problems as regards the alignment of the light beam.

[q] This plotting technique was checked experimentally on the same electropherograms to which the data given in Table 2 apply. The calculated weights of the material in the zones were very similar to those listed in the table, which gives the values obtained by the use of a calibration curve.

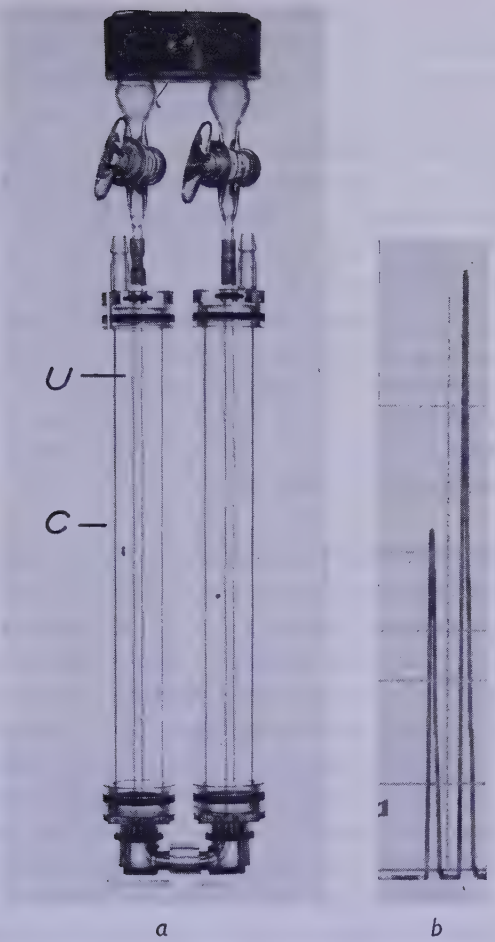

Fig. 26. a) *U*-tube used for moving boundary electrophoresis on a micro scale. The inner diameter of the quartz tube *U* is about 3 mm; *C* indicates the cooling mantle. *b*) The boundaries can be detected by a derivatizing photoelectric scanning system which measures the light absorption at 280 mμ.

Another approach that has been explored in attempts to reduce the amount of sample required has been to use low sample concentration and interference optics, which are more sensitive than the conventional schlieren system [3, 37]. When the sample concentration is very low, however, the difference in density between the buffer and the sample is so small that the boundaries will be very susceptible to distortion by liquid currents arising from thermal convection and electroendosmosis. Therefore, the alternative of using very low sample concentration is not workable unless the latter two effects can be virtually eliminated. To reduce electroendos-

mosis Troitskii and Kobozev [38] replaced the conventional glass U-cells with cells of plexiglass. They found that the use of plexiglass allowed the cell dimensions to be reduced to the extent that satisfactory analyses could be performed with only 0.5 ml of rabbit or bull serum, provided the protein concentration was 2.5 %. The amount of material required was thus still considerable (12.5 mg). Most of the problems involved in adapting moving boundary electrophoresis to a micro scale are solved by the use of a cell of the type shown in Fig. 26*a*, if the limbs of the U-tube are coated with methyl cellulose (see section E, p. 61 ff.). Electroendosmosis is eliminated by the methyl cellulose coating and thermal convection can be suppressed effectively because the small dimensions of the cell (the diameter of the U-tube is only 3 mm) allow efficient cooling. In such a coated cell, protein solutions of concentrations as low as 0.1 per cent can be analyzed. The derivative of the concentration in the boundary can be recorded by a photoelectric scanning system (Fig. 26*b*).

B:2. Zone Electrophoresis in a Supporting Medium

Due to the many problems encountered in attempts to use micro cells in the moving boundary technique, several efforts have been made to develop other electrophoresis methods suitable for analysis of small amounts of material. Most of these are zone methods that involve the use of a supporting media to suppress convection. Many of the support-stabilized zone-electrophoresis methods can provide extremely good resolution. However, the presence of the support prohibits the determination of absolute mobilities, because migration velocities can be affected by "tortuosity" phenomena, by adsorption to the supporting medium, and by streaming due to electroendosmosis or evaporation. Reference substances must therefore be used and various empirical corrections must be applied to transform observed migration velocities to those in free solution [39, 40, 41].

Of the various stabilizing media used, agarose suspensions generally show the least adsorption [42, 43]. Furthermore, the hindrance to electrophoretic migration is very low, because the concentration of agarose required for a satisfactory stabilization is only 0.15 % (w/v). For these two reasons, mobilities calculated from an electrophoresis in an agarose suspension usually require correction only for electroendosmosis (see the table in ref. 43).

B:3. Free Zone Electrophoresis

a. The Range of Application

Any hydrophilic substance can be studied by moving boundary electrophoresis provided that (1) it does not sediment during a run, and (2) the

concentration required to obtain a stable and detectable boundary is not so high that pronounced "boundary anomalies" appear. Whole cells, such as erythrocytes, are ruled out by the first condition and low molecular weight substances by the second.

The application range of zone electrophoresis in a supporting medium is in general limited to molecules: particles as large as mitochondria and bacteria have difficulty in passing through the channels in the bed.

With free zone electrophoresis mobility determinations and other analyses can be performed on a micro scale with ionic materials ranging in size from inorganic ions to whole cells. However, certain types of cells sometimes clump suddenly after a few minutes of electrophoresis. The cause of this abrupt clumping is not known.

b. Construction Details Affecting the Accuracy of Mobility Determinations

In order to obtain accurate mobility data with a free zone electrophoresis apparatus constructed along the lines of that described herein, the following ideal requirements must be very nearly met: (1) the electrophoresis tube must have the same bore throughout its length; (2) the carriage (Ca in Fig. 6) must move at constant speed along the steel rods SR1 and SR2; (3) the response time of the recorder must be short so that the pen does not lag behind the input signal from the photo multiplier; (4) the recorder chart must be fed at constant speed; (5) there must be no current leakage at the Simrit rings (Si1 and Si2 in Fig. 8). With the present equipment, mobilities in the range of $10^{-4}-10^{-5}$ cm^2 sec^{-1} V^{-1} can be measured with a precision of about 1 per cent, as evidenced by the data presented in Table 3, p. 89. The FSH runs described in section B, p. 102 ff. also demonstrate the high reproducibility attainable with the apparatus.

Free zone electrophoresis can reveal very tiny differences in mobility if the substances whose mobilities are to be compared are applied to the electrophoresis tube as separate zones a few centimeters apart. Unless the substances have almost exactly the same mobility, the distance between the peaks will increase or decrease perceptibly as the zones migrate along the tube. A difference of 1 mm can be significant in such an experiment. By the use of this technique, Roos [44] was able to show that urinary and pituitary FSH differ very slightly in mobility. Of course, the same technique can be used for identification purposes if the appropriate reference substances are available (see Fig. 35*b*).

c. The Influence of the Composition of Sample Solution on the Accuracy of a Mobility Determination

In general, one cannot obtain meaningful mobility values by moving boundary electrophoresis unless the sample solution is nearly identical to that used above the boundaries as regards the composition and concentration of all ions other than the solutes of interest. Therefore, the sample is usually dialyzed against the desired buffer until osmotic equilibrium is achieved.

Ideally, samples to be examined by free zone electrophoresis should also be equilibrated with the buffer in which the run is to be done. In practice, however, this is seldom necessary. If the sample happens to be available in very concentrated form or in the dry state, it can simply be diluted up in the proper buffer for application to the tube.

Provided that a few important conditions, all discussed below, are fulfilled, the free zone electrophoresis technique has the advantage that relatively large differences in ionic composition and/or concentration between the applied sample solution and the surrounding medium will neither impair separations nor preclude accurate mobility measurements. However, the fundamental requirement for zone stability, namely, that the difference in density between the zone and the surrounding medium be less than 0.3 per cent, should not be violated (see section A, p. 91 ff.). If the sample solution is less than 0.3 per cent more dense than the buffer, the conductivity difference is not likely to be great enough to cause undue zone broadening even if the density difference is due almost entirely to small ions.

Since the conductivity of the applied zone is not very critical, one can compensate for high sample concentrations by applying the sample in a buffer that is more dilute (i.e. less dense) than the electrophoresis medium. Beyond certain limits, however, this practice can become self-defeating, for if the conductivity of the applied zone is too low, the zone will sharpen to the extent that the density difference will exceed the allowed limit anyway [7, 45].

In most electrophoresis experiments there will appear a stationary zone in the position of the starting zone long after the particular ions that were present there originally have migrated away. This zone corresponds to the ε- and δ-boundaries encountered in moving boundary electrophoresis and consequently contains the same constituents as the buffer but differs from it only as regards the concentration of the constituents (cf. section B, p. 111 ff.). Therefore, some modifications of the conventional way to perform an electrophoresis must be introduced in order to detect such a stationary zone by a UV-scanning of the electrophoresis tube.

The peak II in Fig. 38 corresponds to such a stationary zone (the zone

does in fact migrate very slowly). The difference in ionic concentration between the stationary zone and the surrounding medium increases with the difference in conductivity between the buffer and the applied sample solution. Accordingly, unless the sample has been equilibrated with the buffer used for the run, mobility measurements should not be made until the solute of interest has migrated clear of the starting position.

It should be emphasized that a mobility measurement can become very inaccurate if the sample contains a foreign ion (e.g. a small ion that is not present in the electrophoresis buffer) that migrates with about the same velocity as the solute to be analyzed, since the presence of even minor amounts of foreign ions in the migrating zone may contribute considerably to its conductivity. Fortunately, this is a rare case, particularly when this solute is a macromolecule (e.g. a protein) and the foreign ion is a small molecule (e.g. a simple inorganic or organic ion), because the difference in mobility between these two types of substances often is great.

d. Performance of Mobility Determinations

d:1. *The Mobility Equation*

The mobility u is calculated by the use of the equation

$$u = \frac{C \cdot v_{app} \cdot q \cdot \varkappa}{I} \tag{87}$$

where the apparatus constant C converts the apparent migration distance measured on the recorder chart to the true migration distance in the electrophoresis tube; v_{app} is the apparent migration velocity (cm/sec) measured from the recorder chart; and q, $\varkappa$ and I are the cross-sectional area (cm^2) of the tube, the electrical conductivity ($ohm^{-1}\ cm^{-1}$), and the current strength (amp), respectively.

d:2. *Determination of C in Eqn. (87)*

Since each segment of the crenellated distance scale inscribed on the left margin of the recorder chart (see Fig. 13*b* and section b, p. 48 ff.) corresponds to a distance of 1.00 cm along the axis of the electrophoresis tube, C is simply the length, in cm, of the distance scale segments on the chart record. C is determined most accurately as a/n, where a is the length, in cm, of n (e.g. 10) segments.

d:3. *Determination of v_{app} in Eqn. (87)*

A thin pencil line is drawn through the peak Pe parallel to the rulings Ru of the chart paper (see Fig. 13*b*). The distance l_1 between the peak and an adjacent ruling is then read with a magnifier containing a scale graduated in tenths of a millimeter. The distance l_3 between a ruling and the reference

line H is determined in the same way. The total distance L between the reference line H and the peak is thus $l_1+l_2+l_3$; since the distance between adjacent rulings of the chart is 1.00 cm, l_2 can be read directly from the chart record.

The migration velocity v_{app} can then be determined as the slope of the line obtained by plotting the L-values measured for a series of consecutive scans against the time (t), in seconds, at which the scans were made (the scanning interval is set on the timer T in Fig. 12). In general, however, I prefer to calculate v_{app} in a more objective fashion as the slope of the regression line for the regression of L on t (ref. 46):

$$v_{app} = \frac{\Sigma t \cdot \Sigma L - n\Sigma tL}{(\Sigma t)^2 - n\Sigma t^2}$$

where n is the number of (t, L)-values. This formula was used in the comparative mobility determinations described below.

d:4. *Determination of q in Eqn. (87)*

The area of the inner cross-section of the electrophoresis tube is determined as the inner volume divided by the length of the tube. The inner volume is determined by weighing the tube empty and filled with water or mercury.

d:5. *Determination of $\varkappa$ and I in Eqn. (87)*

Since the solute to be analyzed is in low concentration in most free zone electrophoresis experiments, one can use for $\varkappa$ in eqn. (87) the conductivity of the buffer instead of that of the migrating zone without introducing any grave errors. One must remember, however, that a mobility value calculated by eqn. (87) applies for the temperature at which $\varkappa$ was determined, and not for the temperature at which the run is done, unless, of course, the two temperatures are the same. The buffer pH can be measured at any temperature, but the temperature should be stated because the pH values of some buffers have relatively high temperature coefficients. The pH measured at room temperature and at the temperature of the cooling water can in some cases differ by 0.5 units (see footnote [m], p. 69). Such a pH difference may correspond to an inaccuracy in mobility of several per cent.

The leakage current should not exceed 1 per cent of the total current.

e. A Comparison of Mobility Values Determined by Moving Boundary Electrophoresis and Free Zone Electrophoresis

e:1. *The Moving Boundary Experiment*

In free zone electrophoresis, the lower limit of sample concentration that can be used is determined entirely by the sensitivity of the detection system.

There is no lower limit of concentration as regards zone stability as the susceptibility of a zone to convective disturbances decreases continuously with the solute concentration (see section A, p. 91 ff.). This is exactly opposite to the situation in moving boundary electrophoresis, where the stability of boundaries increases with the sample concentration. However, as pointed out in section f, p. 90 ff., the boundary anomalies increase with the sample concentration and consequently also the inaccuracy in mobility determinations. Therefore, to obtain accurate mobilities one should use low sample concentrations, but not so low that the boundaries will be unstable. In the experiments from which the data given in Table 3 were derived, a protein concentration of 0.3 per cent was used. This is such a low concentration that the boundaries would have been thermally distorted if the runs had not been conducted at low current densities. The intense color of phycoerythrin, the test protein, permitted visual examination of the boundaries, and therefore we could easily establish that no distortion was apparent when a current strength as low as 10 mA was used.

To suppress further the boundary anomalies, the electrophoresis was conducted in a cacodylate buffer, because, at the pH used, the mobility of the cacodylate ion is about the same as that of phycoerythrin (see section f, p. 90 ff.).

The mobility values were calculated from the descending boundary, using the conductivity value for the original dialyzed phycoerythrin solution. The conductivity value that should be used to calculate the mobility of phycoerythrin from an ascending boundary is difficult to determine.

Table 3. A comparison of mobility values obtained by moving boundary electrophoresis and by free zone electrophoresis.

Sample: a 0.3 % solution of *R*-phycoerythrin dialyzed against the buffer. Current: 10 and 2.5 mA, respectively. Cross-section of the U-cell: 3×25 mm. Inner diameter of the rotating electrophoresis tube: 3 mm. Buffer: sodium cacodylate-acetic acid, 0.1 M in cacodylate. The pH of the buffer at room temperature was 6.70. All experiments were performed at a cooling water temperature of 1°. The conductivity values used for the calculation of the mobilities were also determined at 1°.

Moving boundary electrophoresis ($cm^2\ sec^{-1}\ V^{-1} \times 10^{-5}$)	Free zone electrophoresis ($cm^2\ sec^{-1}\ V^{-1} \times 10^{-5}$)
5.92	5.85
5.97	5.89
5.97	5.85
Mean: 5.95	Mean: 5.86

e:2. *The Free Zone Electrophoresis Experiment*

The determination of the mobility of phycoerythrin by free zone electrophoresis was performed as described in section d, p. 87 ff. The same protein solution was used as in the moving boundary experiment. The sample was applied by injection. The conductivity value used to calculate the mobility values in the free zone electrophoresis experiment was that of the buffer.

Both sets of values given in Table 3 have a precision of better than 1 per cent, and the difference between the mean values is only 1.5 per cent. The question as to which of the two methods gives the most accurate mobility has not been explored.

f. Interpretation of Electropherograms

Great precautions should be taken when electropherograms, including those obtained from free zone electrophoresis, are used to decide whether a sample solution is homogeneous or not. A narrow, symmetrical peak is a strong indication of electrophoretic homogeneity. However, a common misinterpretation is that asymmetry of a peak is equivalent to heterogeneity. Therefore it should be stressed that a completely symmetrical electrophoresis peak can not be expected in all experiments, even if the sample is quite homogeneous. This is due to the fact that the electrical conductivity and the pH in a zone are rarely the same as in the surrounding buffer [47, 48]. Therefore, the front of a zone often migrates with a different velocity than the rear, and this difference will manifest itself as an asymmetric peak (in moving boundary electrophoresis this effect corresponds to differences in migration velocities of the ascending and descending boundaries). To suppress these so called "anomaly effects", the sample concentration should be low and the mobility of the substance to be examined should be as near as possible to the mobility of the buffer ion that has the same sign as this substance [3, 37, 49]. Thus, it is of importance to have recourse to a sensitive scanning system which enables analysis at low zone concentrations, not only in order to spare sample material but also to obtain more readily interpretable results and higher accuracy in mobility determinations.

Electroendosmosis, excessively high field strengths, and leakage that causes buffer flow in the electrophoresis tube can also distort a zone so much that it will be recorded as an asymmetric peak even if it consists of homogeneous material. Eqns. (54) and (69) and Figs. 16 and 18*b* show that a zone distorted in one of these ways will be parabolic and can therefore be restored to a flat shape by a counter flow in the same way as described in section C, p. 58 ff. After such a restoration, the recorder deflection will, of course, be higher than before. To evaluate whether the asymmetry

of a peak is due to a parabolic shape of the zone one can therefore proceed as follows.

Buffer is pressed into the electrophoresis tube by screwing down stepwise the plexiglass tube PT (Fig. 8). After each step the zone is scanned. If in one or more of these scans the recorded peak is higher than it was before buffer was forced into the electrophoresis tube, it is very probable that the asymmetry developed during the electrophoresis was due to a parabolic zone deformation with the vortex pointing toward the left. The total buffer volume pressed into the electrophoresis tube should be so small that the center of the zone is displaced no more than one or two centimeters. If the peak height should continuously decrease during the above attempts at hydrodynamic compensation, one ought to find out whether the peak asymmetry is due to a parabolic zone profile with vortex toward the right. For this purpose the tube PT is brought back to its original position. Buffer is then forced out of the electrophoresis tube by screwing up PT stepwise and the height of the peak is examined as before.

If a migrating zone is recorded as an ill defined or exceptionally broad peak, this may be due to heterogeneity of the applied sample or convective disturbances. To distinguish between these two possible causes of distortion one can reverse the direction of electrophoretic migration by reversing the current[r] (see ref. 50). Should the zone increase in height and decrease in width while migrating back toward its starting position the sample is probably heterogeneous; in any case, convective deformations are not affected by reversal of the current direction. Many proteins tested have shown such a reversible zone spreading, which might be due to differences in primary structure, or in secondary, tertiary, and quaternary structure, including effects of allosteric transitions [51, 52]. One should also remember that a homogeneous substance can give an asymmetric peak or even multiple peaks as a result of interactions with the buffer components [53].

II:7. *Preparative Runs*

A. The Capacity

The susceptibility of a zone to distortion decreases with the difference in density, $\varrho_p - \varrho_m$, between the zone and the surrounding buffer, as is evident from the fact that both γ_1 (eqn. (15)) and $\sqrt{k^2+l^2}$ (eqn. (26)) become smaller as $\varrho_p - \varrho_m$ becomes smaller. Since

[r] If the zone is parabolic due to electroendosmosis or to the use of an excessive field strength it must first be restored to a flat shape by a hydrodynamic compensation as described above. Otherwise, the recorder peak will increase in height upon reversal of the current even if the zone represents a homogeneous substance.

$$\varrho_p - \varrho_m = c(1 - \bar{v} \cdot \varrho_m) \tag{88}$$

where c and $\bar{v}$ are the concentration and partial specific volume of the solute [54], respectively, it follows that for a given value of $\bar{v}$ the most dilute zone will be the most stable. The minimum sample concentration that can be used in practice depends entirely on the sensitivity of the detection system. In the case of electrophoretically homogeneous viruses, a sample concentration of 0.02 per cent is usually adequate when the scanning is done at 280 mμ (Fig. 36*a*), and a considerably lower concentration can be detected by scanning at 260 mμ. This means that about 3 μg of a pure virus preparation is sufficient for an electrophoretic run. In the case of proteins, the sample concentration must be at least 0.1 per cent when the scanning is done at 280 mμ.

As mentioned above there is no lower limit to the solute concentration that can be used as far as zone stabilization is concerned. There is, however, an upper limit. In simple aqueous buffers, a zone can be very susceptible to deformation if it differs in density from the surrounding medium by more than about 0.003 g cm^{-3} [s] (0.3 per cent). The sample concentration corresponding to this density difference varies with the partial specific volume of the sample substance (eqn. (88)). However, as most biopolymers have values of this parameter ranging from 0.60 to 0.75 cm^3 g^{-1}, the maximum permissible sample concentration for substances of this type is usually about 1 per cent,[t] according to eqn. (88).[u] Samples which differ in density from the buffer by more than 0.003 g cm^{-3} can sometimes be run successfully if they contain a mixture of substances that separate rapidly into a number of less concentrated zones. For example, in the serum sample used for the run shown in Fig. 31 the protein concentration was 2.2 per cent. This is the highest protein concentration that has been used so far, and I doubt that it can be exceeded. Since the sample volume should not exceed 20 μl, the maximum amount of protein that can be applied is thus about 0.44 mg.

Free zone electrophoresis is inherently a micro method. The scale cannot be increased appreciably by increasing the radius of the electrophoresis

[s] This figure refers to the case where the sample is applied by injection. When the layering technique is used the highest permissible density difference is about 0.001 g cm^{-3} (see section C:1, p. 52 ff.).

[t] For substances with a low molecular weight, the partial specific volume varies considerably with the nature of the substance. Therefore, for small molecules the maximum permissible sample concentration can differ greatly from 1 per cent.

[u] We have assumed here that the sample is equilibrated with the buffer so that the difference in density between the starting zone and the surrounding buffer is due only to the solute of interest (i.e. no foreign substances are present).

tube because, as eqn. (54) shows, an increase in the radius increases the tendency for convection in the longitudinal direction. The inner diameter of the tube used for all the experiments described in this monograph is 3 mm, which seems to provide the optimum balance between stability and capacity.

The capacity figures given above apply for conventional aqueous buffers. The capacity can be increased considerably beyond these limits by the use of additives (e.g., sucrose, polyethylene glycol, methyl cellulose, etc.) that increase the viscosity of the buffer medium. This is evident from eqn. (54), which shows that longitudinal convection is suppressed by an increase in viscosity, and from Fig. 3*b* and eqn. (27) which reveal that γ_1 and $\sqrt{k^2+l^2}$ respectively, can be very small, even for relatively large values of $\varrho_p - \varrho_m$, provided that the viscosity is high enough. Therefore, the use of very viscous buffers will allow both the bore of the tube and the sample concentration to be increased substantially beyond the limits that obtain in ordinary buffers. There are, however, some disadvantages associated with the use of viscous buffers. First, the migration velocity of any substance is inversely proportional to the viscosity at a given potential gradient (see eqn. (65)), so the time required for a certain separation will increase roughly in proportion to the viscosity of the buffer used. Second, the required "viscogenic" additives can be troublesome to remove. In general, therefore, the flowing-curtain method [9, 10] is much more convenient than free zone electrophoresis for large scale preparative separations in the absence of a carrier.

B. Recovery of Zones from the Electrophoresis Tube

Zones can be recovered from the rotating tube by the following procedure.

1) The voltage to the electrodes is turned off and a scan is made immediately.

2) The carriage Ca (Fig. 6) is then cranked up to raise the electrophoresis tube ET out of the immersion bath IB.

3) The electrode vessel EV2 and the connecting arm CA2 are emptied. There is no risk that this will cause liquid to stream through the electrophoresis tube, since the buffer in the other electrode vessel is separated from that in the electrophoresis tube by a tight gel plug GP (Fig. 8).

4) A special centimeter scale is mounted below and parallel to the rotating tube. (The scale is clipped onto the two connecting arms, CA1 and CA2, by means of a rigid mounting bracket at each end.) With the scale in place, the zones corresponding to the various peaks in the chart record can be located accurately in the electrophoresis tube as described in section b, p. 48 ff.

5) Using the scale as a guide, 1-cm fractions are withdrawn serially from the right end of the tube by means of a micro-syringe (Fig. 14) inserted through the hole Ho2 (Fig. 6). Owing to the small diameter of the electrophoresis tube, the meniscus is quite stable and will merely recede as successive fractions are withdrawn. Therefore, the buffer will not run out of the tube during the withdrawal operation. In order to minimize zone distortion the orifice of the syringe should be held at the receding meniscus throughout the withdrawal of each fraction.

6) The fractions are transferred to tiny test tubes, etc., for further analysis.

Fig. 32 illustrates one of the many experiments in which this recovery technique has been used to advantage.

III. APPLICATIONS

III:1. *Low Molecular Weight Substances*

Among the low molecular weight substances that have been submitted to free zone electrophoresis are inorganic and organic ions, amino acids, peptides, corticosteroid hormones, and hydrolysis products of nucleic acids. The results obtained show that free zone electrophoresis is a convenient method for studying all these types of substances. Here, I shall only describe a few experiments performed with inorganic ions and various hydrolysis products of nucleic acids. (Experiments with some other low molecular weight substances are described in refs. 12 and 90.)

I should mention here that the UV-scanning device illustrated in Fig. 9 can be used to follow the migration of low molecular weight substances even if they have no ultraviolet absorption (Fig. 38). The basis for this is discussed in section B, p. 111 ff.

A. Inorganic Ions

If strong electrolytes, such as inorganic ions, are to be electrophoretically analyzed, they should be applied in low concentrations in order to avoid excessive boundary anomalies, which seriously reduce resolution by causing the peaks to become broad and skewed. Therefore, the detection technique must be sensitive enough to permit localization of dilute zones of such ions. At low ion concentrations narrow and well defined peaks are obtained, as illustrated in Fig. 27. Notice the short time (1 min) required for the analysis. Electrophoretic separations of inorganic ions have previously been performed almost exclusively on paper or agar gel as supporting media [55, 56].

B. Hydrolysis Products of Nucleic Acids

Knowledge of the chemical composition of nucleic acids is of fundamental importance in many branches of biochemistry. Accordingly, it is essential to have means for separation, characterization and quantitative determination of such degradation products of nucleic acids as purine and pyrimidine bases, nucleosides, and nucleotides. Great efforts have therefore been made to develop chromatographic and electrophoretic methods suitable for this purpose [57]. Most of the experiments have been performed in a supporting medium, often filter paper. The spots (zones) can be located in the sup-

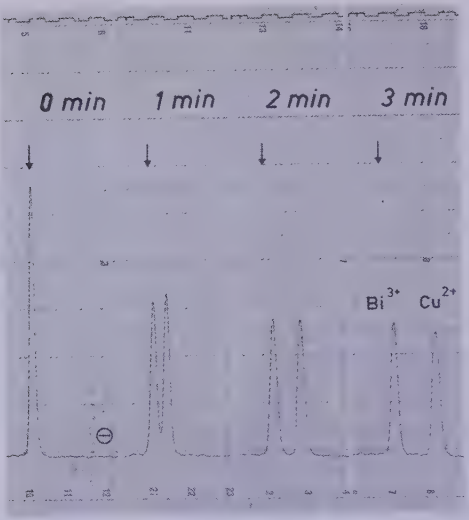

Fig. 27. Separation of inorganic ions (Cu^{2+} and Bi^{3+}) by free zone electrophoresis. Medium: 0.1 *M* lactic acid. Sample: 10 μg of $Cu(NO_3)_2 \cdot 3H_2O$ and 7 μg of $Bi(NO_3)_3 \cdot 5H_2O$ in 8 μl of 0.1 *M* lactic acid. Inner diameter of electrophoresis tube: 3 mm. Current: 8 mA. Voltage: 2540 V. Temperature of cooling water: 16°. The arrow indicates the position of the starting zone. The scans were made at the times indicated.

porting medium by photography or by visual inspection in ultraviolet light. For quantitative measurements, the supporting medium is divided into pieces, which then are eluted. The amounts of the different compounds are determined spectrophotometrically.

For the applications mentioned above free zone electrophoresis is more rapid, reproducible, and accurate than the electrophoretic and chromatographic techniques reported previously. Figs. 28–30 show fractionations of different types of hydrolysis products of nucleic acids. The peaks were identified in the manner used for native and denatured DNA (Fig. 35). The accuracy of the quantitative determinations is illustrated in Table 2, p. 80. Another advantage of free zone electrophoresis is the fact that the relative mobilities observed are close to those predicted from the net charges of the hydrolysis products. Using pk_a-values or plots of charge as a function of pH [58, 57], one can easily select the pH that ought to provide optimal resolution for any particular case. However, when the electrophoresis is performed in the presence of a supporting medium, the separations expected often do not occur and the appearance of the electropherogram might be quite different from that predicted [59]. This is due to interaction with the supporting medium and is particularly pronounced with bases and nucleosides.

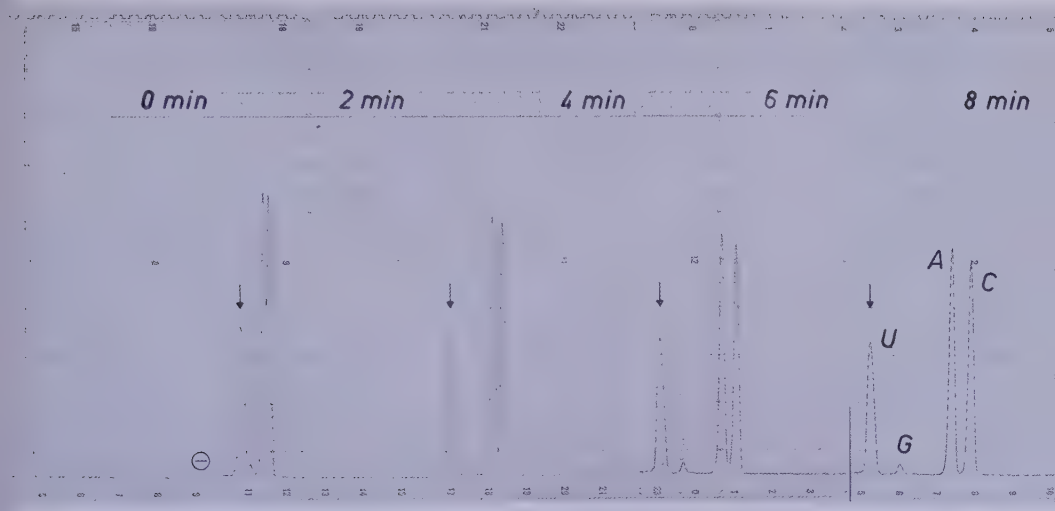

Fig. 28. Separation of the bases cytosine (C), adenine (A), guanine (G), and uracil (U). Buffer: 0.025 *M* ammonium formate, pH 3.61. Sample: 3 μg in 15 μl buffer. Inner diameter of electrophoresis tube: 3 mm. Current: 8 mA. Voltage: 3040 V. Temperature of cooling water: 20°. The arrow indicates the position of the starting zone. The scans were made at the times indicated.

B:1. Purine and Pyrimidine Bases

The analytical method used most widely for the separation of the nucleic acid bases is paper chromatography. More recently, thin layer techniques have been developed with cellulose powder as the carrier medium [60]. In the thin layer technique the running time is only 1.5 hours, a substantial decrease from the 28 hours required with paper. However, considerable time is required for subsequent quantitative analyses.

An electrophoretic separation of the bases as complete as that obtained by the chromatographic method has been considered difficult to achieve [56]. To my knowledge the best result published heretofore was obtained with agar as an anticonvection agent [61]. This technique does not adequately resolve cytosine and adenine, whereas the four common bases can easily be separated completely by free zone electrophoresis (Fig. 28). Only 6 min is required for such a run.

B:2. Nucleosides

Paper chromatography is usually employed for the fractionation of these substances. Only few successful electrophoretic experiments have been reported. Apparently, a complete separation of these substances by electro-

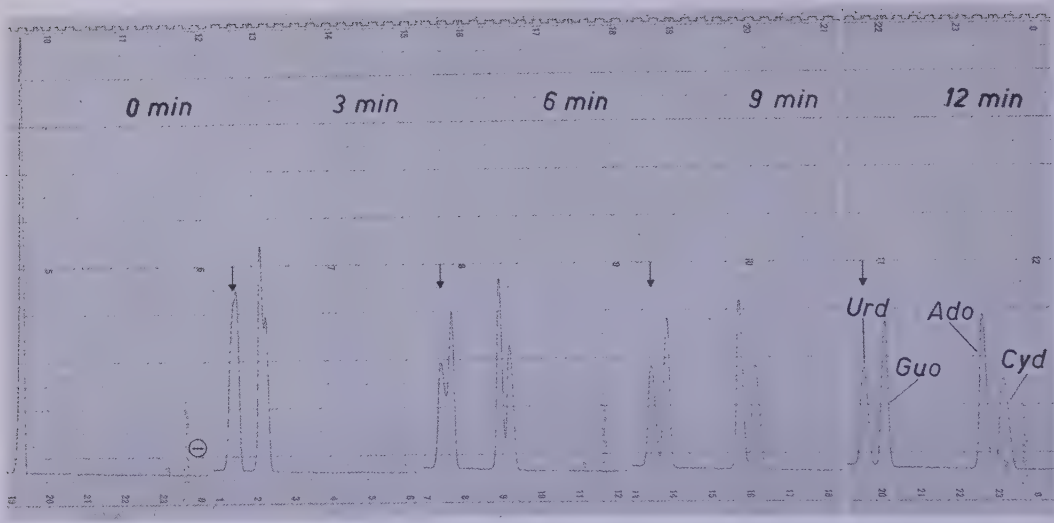

Fig. 29. Separation of the nucleosides cytidine (Cyd), adenosine (Ado), guanosine (Guo), and uridine (Urd). Buffer: 0.05 *M* ammonium formate, pH 2.85. Sample: 4 μg in 15 μl buffer. Inner diameter of electrophoresis tube: 3 mm. Current: 9 mA. Voltage: 3520 V. Temperature of cooling water: 20°. The arrow indicates the position of the starting zone. The scans were made at the times indicated.

phoresis has been accomplished only by Werkheiser and Winzler [62]. They did the run at pH 2.3 in a modified Kunkel-Tiselius paper electrophoresis apparatus [39]. Attempts to utilize the complex-forming properties of borate ions have also been reported [63, 64], but the results were not entirely satisfactory. Free zone electrophoresis can be used with advantage as an alternative to these methods since this technique achieves complete separation of the four nucleosides, as shown in Fig. 29.

B:3. Nucleotides

Paper electrophoresis has been more successful with nucleotides than with the positively charged nucleosides and bases. This reflects the lack of supporting media free of negative charges. Free zone electrophoresis is therefore particularly valuable for fractionating these basic hydrolysis products as shown above, but can also be used with advantage for nucleotide separations as Fig. 30 indicates.

I should mention here that adenosine 5′-monophosphate (AMP), adenosine 5′-diphosphate (ADP), and adenosine 5′-triphosphate (ATP) can be separated very easily by free zone electrophoresis at pH 3. This fractionation appears to be difficult to perform reproducibly with paper as a supporting medium [56].

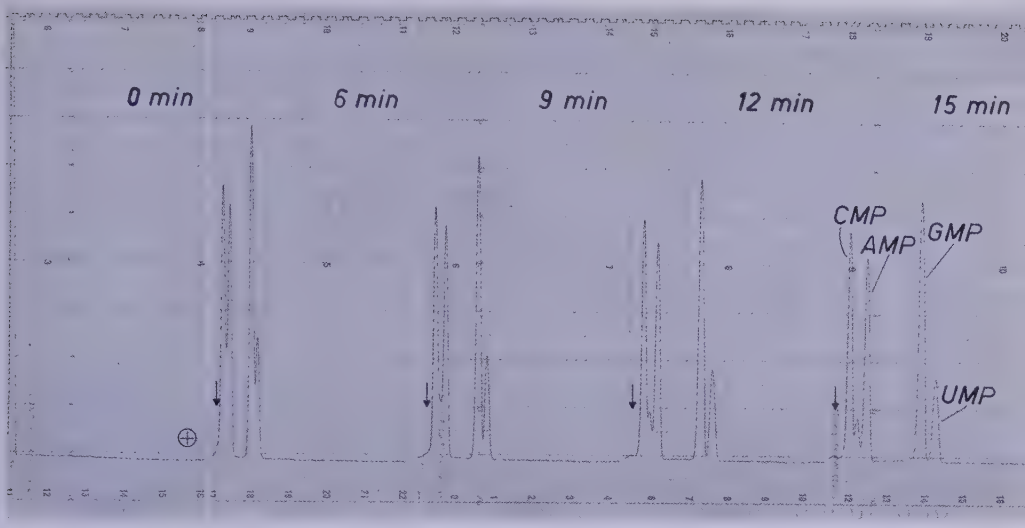

Fig. 30. Separation of the nucleotides uridine 5′-phosphate (UMP), guanosine 5′-phosphate (GMP), adenosine 5′-phosphate (AMP), and cytidine 5′-phosphate (CMP). Buffer: 0.017 *M* ammonium formate, pH 3.61. Sample: 4 μg in 15 μl buffer. Inner diameter of electrophoresis tube: 3 mm. Current: 5 mA. Voltage: 2660 V. Temperature of cooling water: 20°. The arrow indicates the position of the starting zone. The scans were made at the times indicated.

III:2. *Proteins*

A. Normal Human Serum

For many reasons serum is an excellent protein mixture for testing the usefulness and the resolution of an electrophoresis method. First, serum is easy to obtain and electrophoretic patterns are already available for many different experimental conditions, e.g. different pH's and buffer compositions [4, 65]. Second, some serum components are present in high and others in extremely low concentrations. The ability of a carrier free electrophoresis method to reveal the minor components is a good measure of the degree to which convection has been suppressed. Third, the publication of serum electropherograms containing new information, or ones obtained by a new technique offering greater convenience and versatility, should be of interest in many laboratories, since serum is certainly the most widely studied of all protein systems.

Undialyzed serum was mixed with 2.2 parts of water. The run illustrated in Fig. 31*a* was performed with 10 μl of the diluted serum. After 12 min 4 peaks are present and after 24 min 8 peaks, which are better resolved

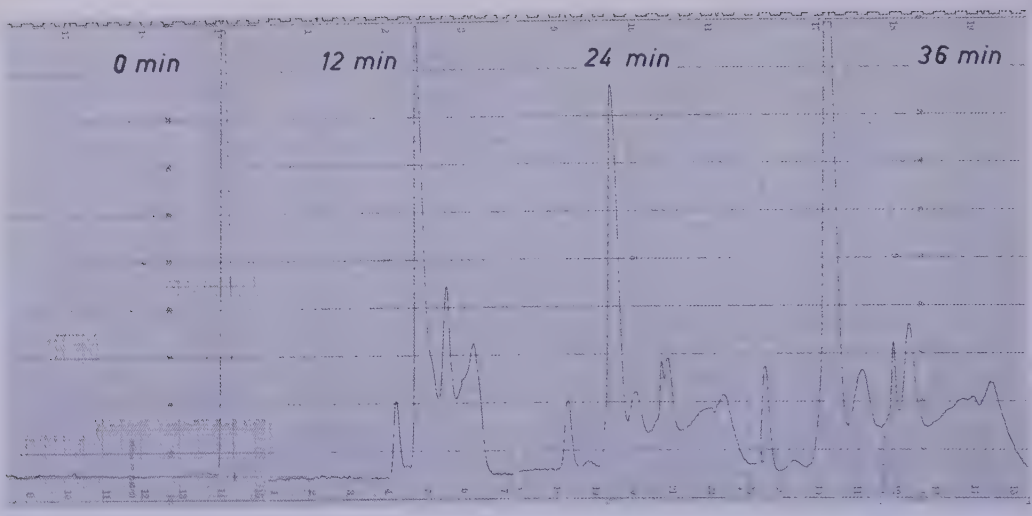

Fig. 31a. Free zone electrophoresis of normal human serum. Buffer: 0.1 *M* Tris-HCl, pH 8.7. Inner diameter of electrophoresis tube: 3 mm. Current: 5 mA. Voltage: 1320 V. Temperature of cooling water: 26°. Sample: 10 μl of a 2.2 % solution. The scans were made at the times indicated.

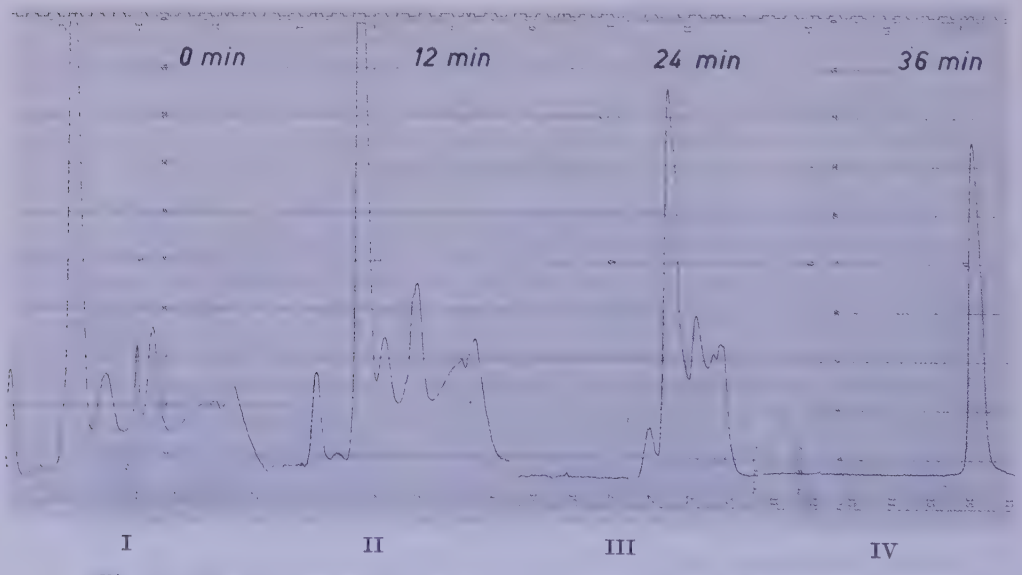

Fig. 31b. Electropherogram showing the migration of the separated components in Fig. 31*a* back into a single zone upon reversing the direction of the current. The convective disturbances are thus very small despite the high sample concentration. The recordings III and IV were made at a lower amplification to show the shape of peaks which go off scale at the higher amplification.

after 36 min. The main peak contains albumin. The zones following this probably contain α_2-globulins, β-lipoprotein, transferrin, and γ-globulins. The electropherogram also shows two minor zones ahead of the albumin. The slower of these may be prealbumin; the faster one is not present when dialyzed serum is used as starting material and is therefore presumed to contain low molecular weight compounds.

The protein concentration of the applied sample was greater than 2 % in this run. In order to determine whether the rotation of the electrophoresis tube had effectively suppressed convection at this comparatively high sample concentration, the direction of the current was reversed immediately after the last scan in Fig. 31*a*. The result is shown in Fig. 31*b*. Only one peak is present after 36 min reverse electrophoresis. Convective deformation of the zones is thus negligible. The scans were made at different amplifications. In the scan IV made at the end of the reverse electrophoresis a relatively low amplification was used so that the shape of the whole peak could be examined.

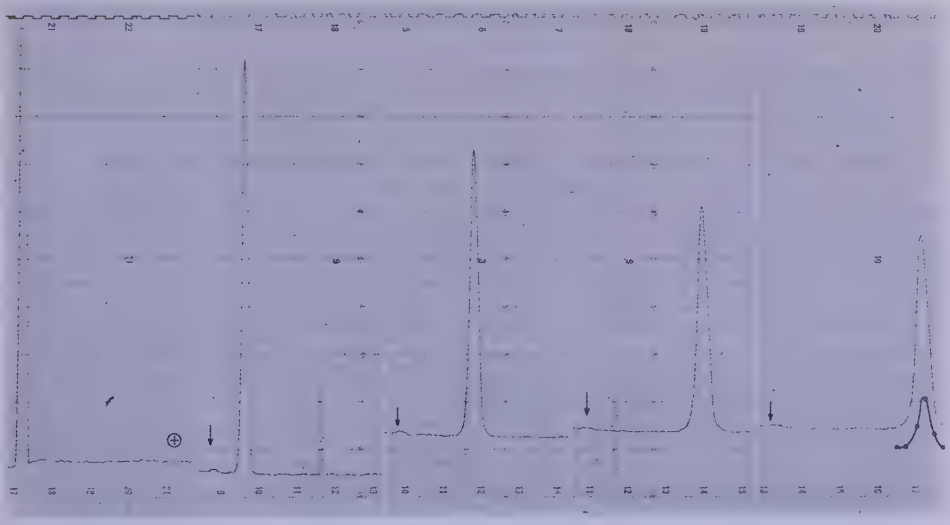

Fig. 32. Free zone electrophoresis of cellulase from *Penicillium notatum*. Buffer: 0.1 *M* Tris-acetic acid, pH 5.5. Sample: 10 μl of a 0.15 % solution. Inner diameter of electrophoresis tube: 3 mm. Current: 6 mA. Voltage: 1020 V. Temperature of cooling water: 1.2°. The arrow indicates the position of the starting zone. The final pattern was obtained after 180 min electrophoresis. Immediately thereafter the run was terminated and fractions were withdrawn from the revolving tube for determinations of cellulase activity. The result of the activity measurements is shown in the last pattern. The activity curve follows the UV-curve, indicating electrophoretic homogeneity. For further details see ref. 68.

B. Some Other Proteins

The need for micro scale analytical methods is great in biochemical fractionation work, since materials of biological origin are often very precious and difficult to obtain. Free zone electrophoresis is sometimes a valuable technique in such work. Thus, Roos [66, 67] has used it to study the homogeneity of a pituitary protein hormone (FSH) and determined its mobility, using only 60 μg of his hormone preparation. The mobility in 0.1 M Tris-HCl, pH 8.7 (temp. = 1°) was -6.1×10^{-5} cm^2 sec^{-1} V^{-1}. A previous determination with an earlier version of the free zone electrophoresis apparatus gave a value of -6.0×10^{-5} cm^2 sec^{-1} V^{-1} at pH 8.6. The good agreement between the two mobility values indicates the reproducibility of the method. Fractions withdrawn from the electrophoresis tube at the end of a run were assayed in order to demonstrate that the hormone activity was associated with the recorded peak. Another example of the use of the withdrawal capability in conjunction with a homogeneity test is illustrated in Fig. 32 (see ref. 68).

Among other proteins studied by free zone electrophoresis are: a neurotoxin [69], a dextranase [70], an inhibitor against Picornaviruses [71], an

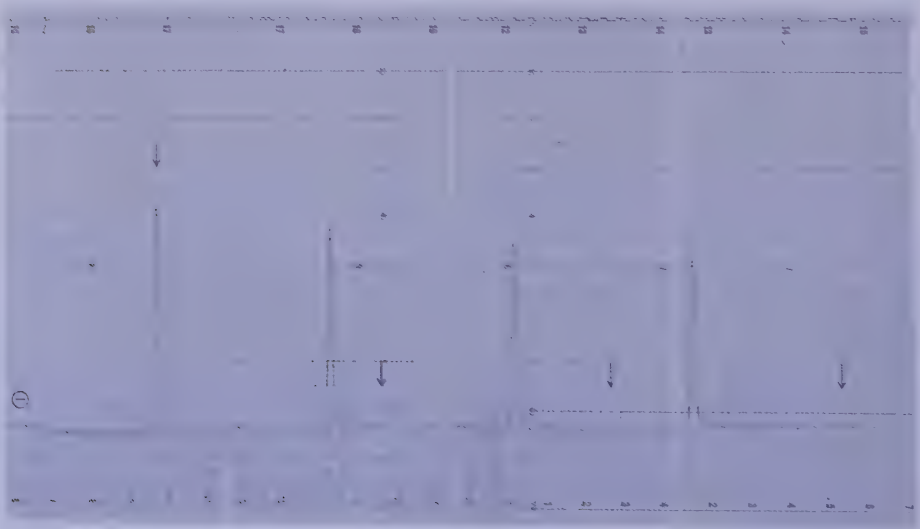

Fig. 33. Free zone electrophoresis of a proteolytic enzyme from a strain of *Arthrobacter*. Buffer: 0.1 M Tris-acetic acid, pH 8.6. Sample: 10 μl of a 0.4 % solution. Inner diameter of electrophoresis tube: 3 mm. Current: 3 mA. Voltage: 1520 V. Temperature of cooling water: 1.1°. The arrow indicates the position of the starting zone. The scans were made at 0, 84, 156 and 244 min. The fact that the zone is still very sharp after 4 hours of electrophoresis testifies both to the homogeneity of the sample and the zone stabilizing power of rotation. For further details see ref. 75.

α-hydroxysteroid dehydrogenase [72], γ-globulins [73], a 5′-nucleotidase [74], and a proteinase [75]. A run performed with the last mentioned protein is illustrated in Fig. 33. This electropherogram shows that a free zone electrophoresis of highly purified proteins can be continued for several hours (in this case four hours) without significant zone spreading.

III:3. *Nucleic Acids*

A. The Mobility of Free-Draining Molecules

Neglecting relaxation effects, the mobility, u, of "free-draining" polyelectrolytes is determined by the simple relation $u = e/f$, where e and f are the charge and friction factor per segment, respectively [76]. Since the mobility of such polyelectrolytes is accordingly independent of the degree of polymerization no prefractionation with respect to molecular size is required to get sharp peaks and accurate mobilities. The inability of electrophoresis to separate such substances according to size may, however, sometimes offer an advantage, for example, in the separation of two types of polyelectrolytes both of which are polydisperse.

B. Separation of Native and Thermally Denatured T2 DNA

DNA is hydrodynamically free-draining in electrophoresis [77, 78]. Thus, when size-heterogeneous DNA is submitted to electrophoresis one does not obtain diffuse peaks. This property allows, for instance, ion interaction [77, 78] and helix-coil transition [79] to be studied by free electrophoresis. The moving boundary technique has been used successfully for such studies. The applicability of free zone electrophoresis to similar problems is illustrated in Fig. 34, which shows a separation of native and thermally denatured T2 DNA. The DNA was prepared as described by Mandell and Hershey [80] and was a gift from Dr. L. Rudin of this Institute. DNA was denatured by incubating at 100° for 10 min on a water bath and was then rapidly cooled to 0° in ice water. The denatured DNA was added to native DNA and the mixture was introduced into the electrophoresis tube. The two peaks present in Fig. 34 were identified as native and denatured DNA by the following complementary experiments. (1) A similar run was done with a sample having a higher ratio of native to denatured DNA. In this run, the faster of the two peaks was elevated, as shown in Fig. 35*a*. (2) In another run the migration rates of the two peaks in Fig. 34 were compared to those of native and denatured DNA. For this purpose three separate zones were applied, the first consisting of native DNA (n), the second

Fig. 34. Separation of native and thermally denatured T2 DNA. Buffer: 0.05 *M* sodium acetate, pH 5.2. Sample volume: 10 μl. Sample conc.: about 0.05 %. Inner diameter of electrophoresis tube: 3 mm. Current: 6 mA. Voltage: 970 V. Temperature of cooling water: 17°. The arrow indicates the position of the starting zone. The scans were made at 0 and 12 min. The fast zone corresponds to native and the slow one to denatured DNA, as demonstrated in the experiments shown in Figs. 35*a* and *b*.

Fig. 35a. Separation of native and thermally denatured T2 DNA. The experimental conditions were similar to those mentioned in the legend to Fig. 34, except that the concentration of native DNA relative to that of denatured DNA was higher. A comparison of the heights of the two peaks in this electropherogram with those in Fig. 34 indicates that the fast zone corresponds to native and the slow one to denatured DNA.

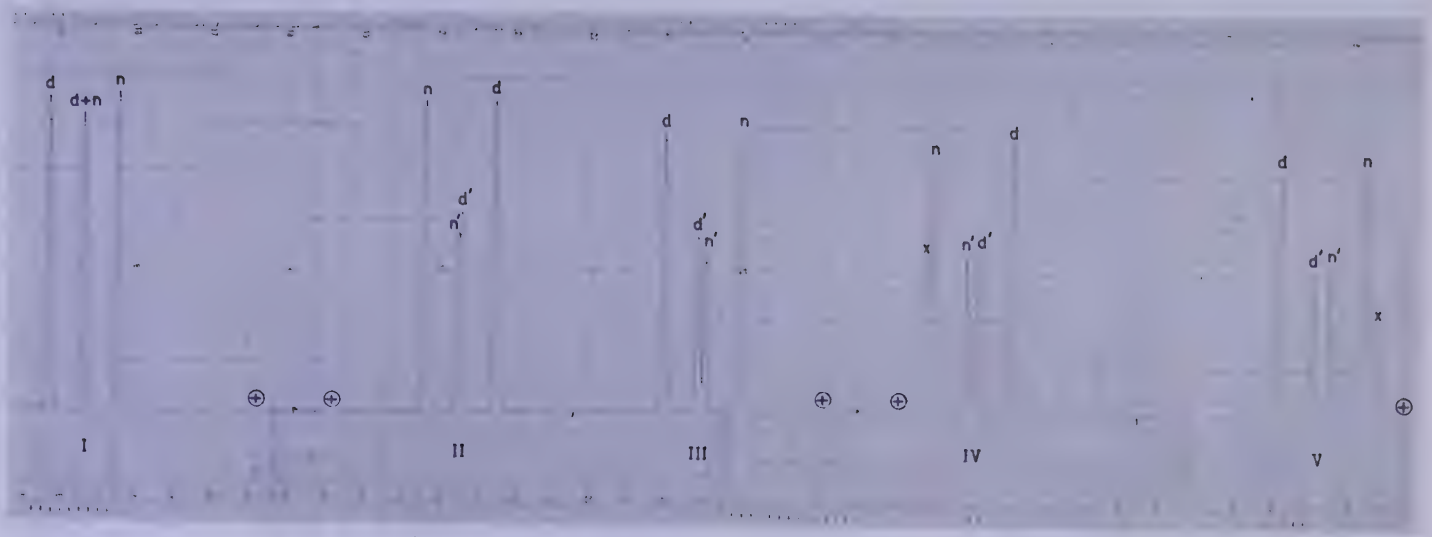

Fig. 35b. Three samples run simultaneously: *d* – denatured T2 DNA, *n* – native T2 DNA, and *d* + *n* – a mixture of the two. The samples were applied as three separate zones. The experimental conditions were the same as those mentioned in the legend to Fig. 34. The scans were made at intervals of 6 min. In scans I, III and V the direction of carriage movement was from right to left. Scans II and IV involved movement of the carriage from left to right. Consequently, consecutive patterns are reversed. The distance between the zones *d* and *d'* remained constant during the run, as did the distance between the zones *n* and *n'*, thus indicating that *n'* consists of native and *d'* of denatured T2 DNA. Observe the sudden appearance of peak *X*.

of the mixture ($n+d$) and the third of denatured DNA (d). The distance between the zones d and d' and between n and n' did not change during the run as seen in Fig. 35*b*. Experiments (1) and (2) show that the faster zone in Fig. 34 corresponds to native DNA and the slower to denatured DNA. Due to its simplicity and high accuracy the technique outlined here for the characterization of electrophoresis components has been used also in many other cases.

Sometimes in free zone electrophoresis of DNA a zone split suddenly into two or more zones. This is illustrated in scan IV (18 min) of Fig. 35*b*, wherein zone n has abruptly begun to separate into two peaks. The reason for this has not been explored. While studying T2 DNA by electrophoresis in a sucrose gradient Olivera, Baine and Davidson [81] also observed a "false" peak, which they ascribed, probably incorrectly, to electroendosmosis.

III:4. *Viruses*

The very high absorption of viruses in ultraviolet light allows very dilute zones of these substances to be located. If scanning is performed at 280 mμ a concentration of about 0.02 % is sufficient [82, 83]. Much lower concentrations can be detected when light of 260 mμ (the wavelength at which viruses have maximum absorption) is used.

Satellite tobacco necrosis virus (SV) and turnip yellow mosaic virus (TYMV) have been studied by free zone electrophoresis in collaboration with Fridborg *et al.* [82] and with Tiselius and Jerstedt [83], respectively. Höglund has utilized the same technique in an investigation of the linkage between T2 phage and its antibody [84]. Only the work on SV will be outlined here. Fig. 36*a*, reproduced from ref. 82, shows a pattern obtained with partially purified SV. At the end of the run, the stationary peak was withdrawn. Examination of the material by electron microscopy (Fig. 36*b*) indicated that electrophoresis had effected considerable purification. Therefore, similar experimental conditions were chosen for preparative electrophoresis in a column of an agarose suspension [43]. Free zone electrophoresis has been used in several other investigations in order to determine rapidly suitable conditions for preparative electrophoretic fractionation in non-sieving media.

III:5. *Subcellular Particles*

The mechanisms of cellular function cannot be elucidated simply by studying various molecules obtained from cells. It is also necessary to study the larger elements present in cells and the interaction among them [85].

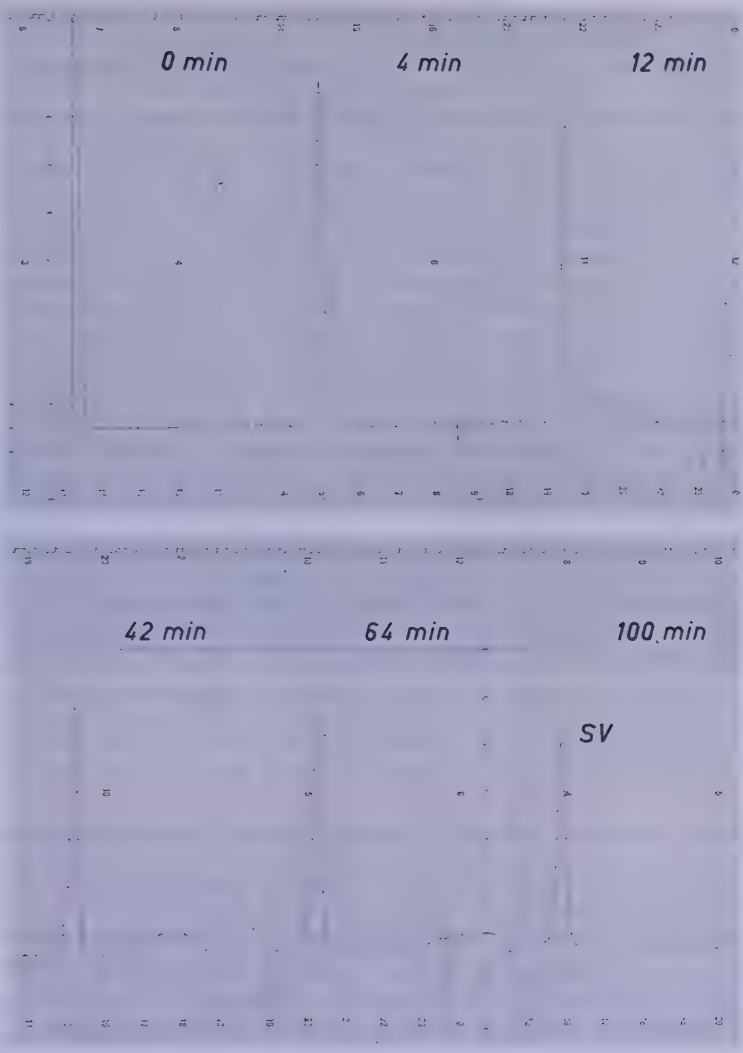

Fig. 36a. Free zone electrophoresis of a preparation of satellite tobacco necrosis virus (SV). Buffer: 0.07 *M* cacodylate-acetic acid, pH 6.35. Sample: 10 μl of a 0.02 % solution. Inner diameter of electrophoresis tube: 3 mm. Current: 8 mA. Voltage: ca. 1400 V. Temperature of cooling water: 1.5°. The scans were made at the times indicated. The material corresponding to the peak SV was withdrawn and analyzed by electron microscopy (Fig. 36*b*).

Efficient methods for the fractionation of subcellular particles are therefore required. Free zone electrophoresis is very suitable for analysis of such material, and for preparative experiments on a micro scale as well.

The cellular mechanisms involved in the synthesis, storage, and release

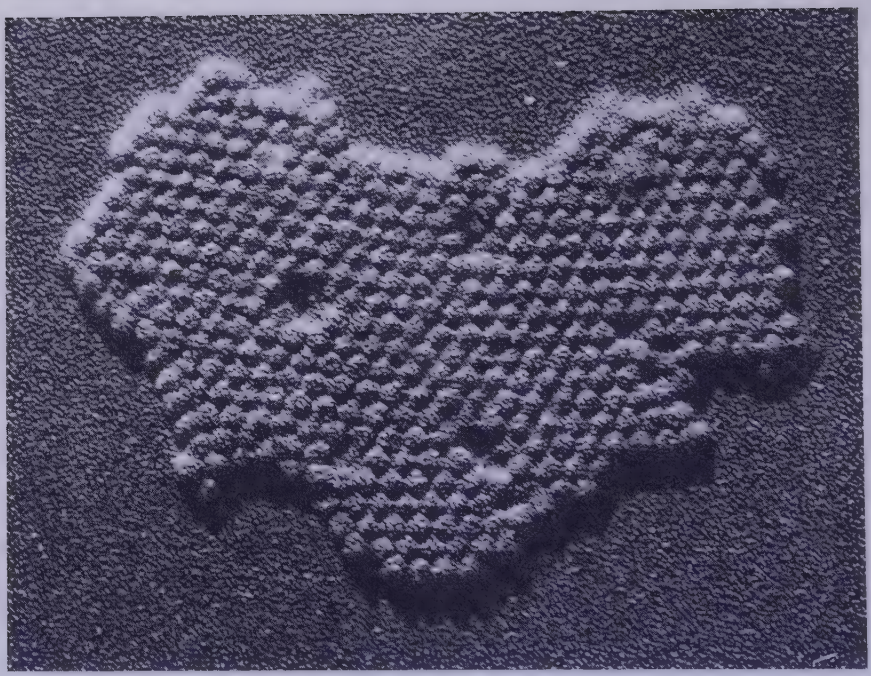

Fig. 36b. Electron micrograph of material corresponding to the peak SV (satellite tobacco necrosis virus) in Fig. 36*a*. For further details see ref. 82. The micrograph was taken by Dr. Höglund.

of insulin are poorly understood, mainly because most of the biochemical separation methods are not applicable with the very small amounts of B-cell material available. In a free zone electrophoresis experiment, however, a homogenate of B-cells from only two mice was sufficient to produce satisfactory recorder deflections, provided that a special dissecting technique was used, and the animals belonged to a strain with a recessive trait for obesity and hyperglycemia [86, 87] (Fig. 37). By analyzing aliquots of fractions withdrawn from the rotating electrophoresis tube at the end of a run, the fractions having the highest insulin content were located (see section B, p. 93 ff.). Electron microscopy showed that the insulin-rich fractions contained high concentrations of spherical granules. Thus it seemed likely that these granules contained the insulin. This hypothesis is supported by the fact that after sonication of the withdrawn fractions the insulin concentration was highest in the granule-rich fractions. Apparently, these granules are the storage sites for insulin. There has been no direct evidence for this heretofore. Ref. 88 contains further details of this work. These studies, performed in collaboration with Höglund and Hellman,

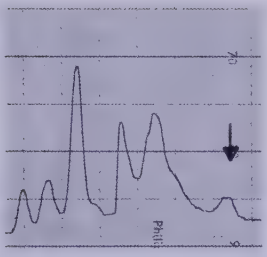

Fig. 37. Free zone electrophoresis of a homogenate of pancreatic *B*-cells from starved obese-hyperglycemic mice. Buffer: 0.067 *M* sodium phosphate, pH 7.3. Sample volume: 15 μl. Inner diameter of electrophoresis tube: 3 mm. Current: 10 mA. Voltage: 1040 V. Temperature of cooling water: 3°. The arrow indicates the position of the starting zone. The recording was made after 47 min electrophoresis. For further details see ref. 88.

seem to be the first successful studies of a specific structural element of the B-cells.

Ribosomes and several other kinds of particles are stable only in very dilute buffers. To suppress anomaly effects and obtain reliable mobility values the electrophoresis of such particles must be performed at extremely low particle concentrations. Under these conditions the moving boundary method is not satisfactory, as pointed out by Nomura and Watson [89]. Since free zone electrophoresis often permits detection of low particle concentrations (0.02 % is sufficient in the case of ribosomes) this method might allow more accurate mobility determinations in buffers of low ionic strength.

III:6. *Cells*

For a long time, the microscope method has been the only method available for analytical electrophoresis of cells [25, 27]. The method requires only a few cells. Free zone electrophoresis can be used for the same purposes, but many more cells are needed. However, free zone electrophoresis allows different fractions to be recovered for further analyses. The types of problems which have been attacked by determination of the migration velocities of cells by free zone electrophoresis are illustrated in the work performed in collaboration with Agarwal [90]:

Substances which react with sulfhydryl groups (e.g. *p*-hydroxymercuribenzoate) are known to cause lysis of erythrocytes *in vitro* [91]. Lysis can be prevented by certain corticosteroids [92]. To study these phenomena, the migration velocities of erythrocytes were determined before and after treatment with corticosteroids and sulfhydryl reagents. Velocities were also determined with these reagents present in the electrophoresis buffer.

No differences in migration velocity were observed. Apparently, therefore, the interaction between erythrocytes and the above reagents occurs *within* the cell. For further studies, methods other than electrophoresis must be used.

For electrophoretic fractionations on a larger scale, the continuous free flow method [9, 10] and the density gradient technique [93, 94] are more convenient. However, one must remember that the variations in osmotic pressure that exist in a density gradient column can damage cell walls.

IV. MODIFICATION OF THE METHOD FOR SPECIAL APPLICATIONS

IV:1. *Detection of Substances which have no UV-Absorption*

A. Detection by Analysis of Withdrawn Fractions

Fractions 1 cm long are removed from the rotating electrophoresis tube and are transferred to test tubes for analysis (see section B, p. 93 ff. and Fig. 32). This technique has some disadvantages, however, as discussed in section a, p. 39 ff.

B. Detection by Recording the Boundary Anomalies

The phenomena termed "boundary anomalies" can cause serious errors in an electrophoretic analysis. Therefore, the occurence of these anomalies is usually undesirable. However, one can also take advantage of these effects and utilize them for the detection of non-UV-absorbing materials. This technique has not been described in the literature previously and will therefore be discussed here.

In general, no ions, including the hydrogen ions, can have the same concentration on both sides of a boundary [3, 37, 49]. Since a zone is enclosed between two boundaries, every ionic species present in the zone has a different concentration within the zone than it has outside. Consequently, a zone corresponding to an ion which has no ultraviolet absorption can be localized with the scanning system described herein if the buffer contains ultraviolet absorbing ions. The sensitivity of this detection technique depends on the magnitude of the boundary anomaly. To obtain a high sensitivity, one should therefore select UV-absorbing ions whose mobilities differ greatly from those of the substances that are to be detected (for further details, see section f, p. 90 ff.). This is often easy to do when the solutes are small ions, particularly inorganic ions.

The principle of this detection technique is illustrated by an experiment performed in sodium barbiturate buffer, which has a moderate ultraviolet absorption around 280 mμ. About 0.02 g of sodium cacodylate was dissolved in 1 ml of the buffer and 15 μl of the resulting solution was introduced into the electrophoresis tube. The cacodylate had no effect on the absorbancy of the buffer (Fig. 38*a*). However, within 7 min after the application of current, two zones are recorded (Fig. 38*b*). One of the zones moves while

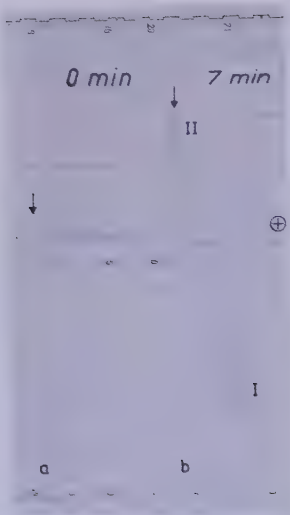

Fig. 38. Localization of a UV-transparent substance (cacodylate ion) in a UV-absorbing buffer by recording boundary anomalies. Buffer: sodium veronal: ionic strength 0.025, pH 8.6. Sample: 15 μl of a 1 % cacodylate solution. Inner diameter of electrophoresis tube: 3 mm. Current: 5 mA. Voltage: 1700 V. Temperature of cooling water: 16°. The arrow indicates the approximate position of the starting zone. The cacodylate zone (peak I) can be detected despite the fact that the ions themselves do not absorb the scanning beam. Peak II has arisen by the automatic adjustments in ion concentrations that must occur in the position of the starting zone in accordance with Kohlrausch's regulating function [95, 37].

the other remains stationary. The migrating zone (I) corresponds to cacodylate ions and the stationary one (II) represents the δ- and ε-boundaries encountered in moving boundary electrophoresis.

This means of detecting changes that occur in the buffer during a run should be useful also in theoretical investigations of electrophoresis.

The method has been used to study several organic ions in addition to cacodylate and several inorganic ions, such as chloride, as well.

IV:2. *Electrophoresis in a Medium Consisting of Buffer and an Additive*

A. The Use of Additives to Increase the Capacity

Convective disturbances can be suppressed by increasing the viscosity of the medium, as was discussed in section A, p. 91 ff. Thus, for preparative purposes more concentrated zones can be stabilized by including in the

buffer a substance which greatly increases the viscosity. Low molecular weight compounds, such as sucrose; and polymers, such as polyethylene glycol, dextran, and methyl cellulose, have been used for this purpose.

B. The Use of Additives to Create Isoelectric Spectra

If a mixture of ampholytes, e.g. proteins, is submitted to electrophoresis in a stable pH-gradient, each ampholyte will focus at a position where the pH is equal to the isoelectric point of the ampholyte. Svensson has developed an ingenious method utilizing this principle [96]. To suppress convection he performs the runs in a sucrose gradient. To use Svensson's technique for isoelectric fractionation in my free zone electrophoresis only a few simple modifications of the apparatus described in this monograph are required. One can proceed as follows.

The mixture of sample and carrier ampholytes [97] (without sucrose) is enclosed between two plugs of polyacrylamide gel which prevent the mixture from running out of the revolving electrophoresis tube. For the preparation of the gel, see section B, p. 51 ff. The gel plugs are placed a few centimeters from the ends of the revolving tube. The small compartments (volume ca. 200 μl) thus formed at the ends of the tube serve as electrode vessels. Phosphoric acid is used as anolyte and ethylene diamine as catholyte. Stationary platinum wires are inserted as electrodes.

As the cooling of the electrophoreis tube is very efficient, steep voltage gradients can be used. Besides decreasing the time for a run such gradients also increase the resolving power of the isoelectric fractionation method, as shown by Vesterberg and Svensson [97].

V. SUMMARY

The free zone electrophoresis method described in this monograph can be used for the fractionation of small molecules, large molecules, and particles. Its versatility is illustrated in runs with inorganic ions, organic ions, nucleic acid bases, nucleosides, nucleotides, proteins, nucleic acids, subcellular particles, viruses, and erythrocytes. The principles of the construction of the electrophoresis equipment are described in detail. The separation chamber is a horizontal tube which slowly rotates round its long axis. The rotation eliminates the need for a supporting medium. A mathematical treatment of this rotational stabilization is given. The equipment is fitted with a unique UV-scanning system and is automated so that it requires no attention after the introduction of the sample. Because the "boundary anomaly" effects cause the concentration of any ion inside a migrating zone to be different from that outside, the scanning system can also be used to detect substances which have no UV-absorption if the buffer contains appropriate UV-absorbing ions. Free zone electrophoresis is intended primarily for analytical purposes but can also be used for preparative experiments on a small scale. The amount of material required is about the same as in paper electrophoresis. The mobility values obtained by free zone electrophoresis agree well with those determined by the classical Tiselius moving boundary method. Free zone electrophoresis also permits determinations of electroendosmotic mobilities, and thereby ζ-potentials of the surface of the revolving electrophoresis chamber. The empirical relationship between recorder deflection and zone concentration fits the theoretically derived curve closely. Using these calibration curves an accuracy of about four per cent was obtained in quantitative determinations. Some sections also apply to electrophoresis methods other than free zone electrophoresis, e.g. the sections dealing with the electrophoretic migration velocity profile, the elimination of the electroendosmotic disturbances, and the detection of substances which have no UV-absorption.

Institute of Biochemistry, Uppsala, Sweden

VI. REFERENCES

1. A. Tiselius, The Moving Boundary Method of Studying the Electrophoresis of Proteins, inaugural dissertation, Almqvist & Wiksells Boktryckeri AB, Uppsala, 1930.
2. A. Tiselius, Koll. Z., *85* (1938) 129.
3. H. Svensson, Arkiv Kemi Mineral. Geol., *22A*, No. 10 (1946).
4. M. Bier, Electrophoresis, Theory, Methods, and Applications, Academic Press Inc., New York, 1959.
5. C. J. O. R. Morris and P. Morris, Separation Methods in Biochemistry, Sir Isaac Pitman & Sons Ltd., London, 1963.
6. R. J. Wieme, Agar Gel Electrophoresis, Elsevier, Amsterdam, 1965.
7. H. Haglund and A. Tiselius, Acta Chem. Scand., *4* (1950) 957.
8. A. Tiselius, Far. Soc. Disc., No. *13* (1953) 29.
9. J. Barrolier, E. Watzke and H. Gibian, Z. Naturforsch., *13b* (1958) 754.
10. K. Hannig, Z. anal. Chem., *181* (1961) 244.
11. A. Kolin, J. Appl. Physics, *25* (1954) 1442.
12. S. Hjertén, Arkiv Kemi, *13* (1958) 151.
13. J. L. Synge and B. A. Griffith, Principles of Mechanics, McGraw-Hill Book Company, Inc., New York, 1949, p. 142.
14. S. Hjertén, in H. Peeters, Protides Biol. Fluids, Proc. 7th Colloq. Bruges, 1959, Elsevier, Amsterdam, 1960, p. 28.
15. R. S. Sokolova and T. N. Krylova, Optika i Spektroskopiia, *6* (1959) 788.
16. M. Kasha, J. Opt. Soc. Am., *38* (1948) 929.
17. G. Schwarzenbach and K. Lutz, Helv. Chim. Acta, *23* (1940) 1139.
18. W. L. van Es and J. H. Wisse, Anal. Biochem. *6*, (1963) 135.
19. H. S. Anker, Electronics, *20*, June, 1947, p. 138.
20. S. Hjertén, Arch. Biochem. Biophys., Suppl. *1* (1962) 147.
21. S. Hjertén, S. Jerstedt and A. Tiselius, Anal. Biochem., *11* (1965) 211.
22. C. E. Schildknecht, Vinyl and Related Polymers, John Wiley & Sons, New York, 1952.
23. B. Vollmert, Grundriss der Makromolekularen Chemie, Springer-Verlag, Berlin, 1962.
24. D. L. Mould and R. L. M. Synge, Biochem. J., *58* (1954) 585.
25. C. C. Brinton, Jr., and M. A. Lauffer, in M. Bier, Electrophoresis, Theory, Methods, and Applications, Academic Press Inc., New York, 1959, p. 441.
26. A. Kolin, in H. Peeters, Protides Biol. Fluids, Proc. 12th Colloq., Bruges, 1964, Elsevier, Amsterdam, 1965, p. 410.
27. H. A. Abramson, L. S. Moyer and M. H. Gorin, Electrophoresis of Proteins, Reinhold Publishing Corp., New York, 1942.
28. J. Th. G. Overbeck and J. Lijklema, in M. Bier, Electrophoresis, Theory, Methods, and Applications, Academic Press Inc., New York, 1959, p. 1.
29. B. S. Magdoff, in P. Alexander and R. J. Block, A Laboratory Manual of Analytical Methods of Protein Chemistry, Vol. II, Pergamon Press, London, 1960, p. 170.

30. C. H. Hodgman, Handbook of Chemistry and Physics, Chemical Rubber Publ. Co., Cleveland, 1958.
30 b. I. Watanabe, N. Ui and M. Nakamura, J. Phys. Colloid Chem., 54 (1950) 1366.
31. A. Tiselius, Trans. Faraday Soc., *33* (1937) 524.
32. J. Porath, Arkiv Kemi, *11* (1957) 161.
33. A. P. Peniston, H. D. Agar and J. L. McCarthy, Anal. Chem., *23* (1951) 994.
34. R. G. Bates and V. E. Bower, Anal. Chem., *28* (1956) 1322.
35. A. Tiselius, Biochem. J., *31* (1937) 1464.
36. E. W. Gill, Biochim. Biophys. Acta, *102* (1965) 302.
37. L. G. Longsworth, in M. Bier, Electrophoresis, Theory, Methods, and, Applications, Academic Press, New York, 1959, p. 91.
38. G. V. Troitskii and G. V. Kobozev, Biokhimiia, *23* (1958) 869.
39. H. G. Kunkel and A. Tiselius, J. Gen. Physiol., *35* (1951) 89.
40. H. Waldmann-Meyer, Chromatographic Reviews, *5* (1963) 1.
41. J. R. Boyack and J. C. Giddings, Arch. Biochem. Biophys., *100* (1963) 16.
42. S. Hjertén, Biochim. Biophys. Acta, *53* (1961) 514.
43. S. Hjertén, J. Chromatog., *12* (1963) 510.
44. P. Roos, Biochim. Biophys. Acta, *93* (1964) 217.
45. J. Porath, Biochim. Biophys. Acta, *22* (1956) 151.
46. F. W. Küster, Logarithmische Rechentafeln für Chemiker, Walter de Gruyter und Co, Berlin und Leipzig, 1925, p. 78.
47. J. de Wael, Chemisch Weekblad, No. 14, 4 april (1953) 229.
48. J. Edward, Chem. Ind. (London), No. 10 (1958) 276.
49. S. Hjertén, in G. Milazzo, Electrochemistry, Elsevier, Amsterdam, 1963, p. 399.
50. A. Tiselius and F. L. Horsfall, Arkiv Kemi Mineral. Geol., *13A*, No. 18 (1939).
51. J. Monod, J. Wyman and J.-P. Changeux, J. Mol Biol., *6* (1963) 306.
52. J. Monod, J.-P. Changeux and F. Jacob, J. Mol. Biol., *12* (1965) 88.
53. J. R. Cann and W. B. Goad, J. Biol. Chem., *240* (1965) 1162.
54. J. W. Williams, K. E. van Holde and R. L. Baldwin, Chem. Revs., *58* (1958) 715.
55. J. Kendall, Nature, *150* (1942) 136.
56. T Wieland, in M. Bier, Electrophoresis, Theory, Methods, and Applications, Academic Press, New York, 1959, p. 514.
57. D. O. Jordan, The Chemistry of Nucleic Acids, Butterworths, London, 1960, p. 64.
58. R. Consden, A. H. Gordon and A. J. P. Martin, Biochem. J., *40* (1946) 33.
59. K. Dimroth, L. Jaenicke and I. Vollbrechtshausen, Hoppe-Seyl. Z., *289* (1952) 71.
60. D. P. Holdgate and T. W. Goodwin, Biochim. Biophys. Acta, *91* (1964) 328.
61. L. M. Weiner and B. Zak, Clin. Chim. Acta, *9* (1964) 407.
62. W. C. Werkheiser and R. J. Winzler, J. Biol. Chem., *204* (1953) 971.
63. L. Jaenicke and I. Vollbrechtshausen, Naturwissenschaften, *39* (1954) 86.
64. D. C. Burke, Chem. Ind. (London), No. 49 (1954) 1510.

65. H. Laurell, "Zone Electrophoresis of Human Sera at pH 4–6", Thesis, University of Uppsala, Almqvist & Wiksells Boktryckeri AB, Uppsala, 1958.
66. P. Roos, Biochim. Biophys. Acta, *82* (1964) 218.
67. P. Roos and C. Gemzell, in G. E. W. Wolstenholme and J. Knight, Gonadotropins: Physicochemical and Immunological Properties, Ciba Foundation, Stydy Group No. 22, J. & A. Churchill Ltd., 1965, p. 11.
68. G. Pettersson, to be published in Biochim. Biophys. Acta.
69. E. Karlsson, D. L. Eaker and J. Porath, Biochim. Biophys. Acta, *127* (1966) 505.
70. J.-C. Janson and J. Porath, in S. P. Colowick and N. O. Kaplan, Methods in Enzymology, Vol. VIII, Academic Press, New York, 1966, p. 615.
71. S. Brishammar and L. Philipson, Biochim. Biophys. Acta, *127* (1966) 140.
72. P. S. Squire, S. Delin, and J. Porath, Biochim. Biophys. Acta, *89* (1964) 409.
73. H. Bennich and G. Johansson, to be published in Biochem. J.
74. W. Björk, to be published in Arkiv Kemi.
75. B. v. Hofsten, H. v. Kley and D. Eaker, Biochim. Biophys. Acta, *110* (1965) 585.
76. J. J. Hermans, J. Polymer Sci., *18* (1955) 527.
77. P. D. Ross and R. L. Scruggs, Biopolymers, *2* (1964) 79.
78. P. D. Ross and R. L. Scruggs, Biopolymers, *2* (1964) 231.
79. L. Costantino, A. M. Liquori and V. Vitagliano, Biopolymers, *2* (1964) 1.
80. J. D. Mandell and A. D. Hershey, Anal. Biochem., *1* (1960) 66.
81. B. M. Olivera, P. Baine and N. Davidson, Biopolymers, *2* (1964) 245.
82. K. Fridborg, S. Hjertén, S. Höglund, A. Liljas, B. K. S. Lundberg, P. Oxelfelt, L. Philipson and B. Strandberg, Proc. Natl. Acad. Sci., *54* (1965) 513.
83. A. Tiselius, S. Hjertén and S. Jerstedt, Archiv für die gesamte Virusforschung, *17* (1965) 512.
84. S. Höglund, to be published in Virology.
85. A. Tiselius, Arkiv Kemi, *15* (1960) 171.
86. C. Hellerström and B. Hellman, Acta Endocrinolog., *42* (1963) 615.
87. C. Hellerström, Acta Endocrinolog., *45* (1964) 122.
88. S. Hjertén, S. Höglund and B. Hellman, in Brolin, Hellman, Knutson, The Structure and Metabolism of the Pancreatic Islets", Proc. 3rd Internat. Symp., Stockholm, 1963, Pergamon Press, London, 1964, p. 223.
89. M. Nomura and J. D. Watson, J. Mol. Biol., *1* (1959) 204.
90. K. Agarwal and S. Hjertén, Acta Endocrinolog., Suppl. *93* (1964) 53.
91. H. S. Jacobs and J. H. Jandl, J. Clin. Invest., *41* (1962) 779.
92. K. N. Agarwal and L. Garby, Acta Endocrinolog., Suppl. *93* (1964) 3.
93. H. Svensson, in P. Alexander and R. J. Block, A Laboratory Manual of Analytical Methods of Protein Chemistry, Vol. I, Pergamon Press, London, 1960, p. 193.
94. A. Kolin, in Glick, Methods of Biochemical Analysis, Interscience Publishers, Inc., New York, Vol. VI, p. 259.
95. F. Kohlrausch, Wied. Ann., *62* (1897) 209.
96. H. Svensson, Arch. Biochem. Biophys., Suppl. *1* (1962) 132.
97. O. Vesterberg and H. Svensson, Acta Chem. Scand., *20* (1966) 820.

ALMQVIST & WIKSELL 671158